The Journal of Gemmology

2015 / Volume 34 / No. 7

SSEF SCHWEIZERISCHES GEMMOLOGISCHES INSTITUT SWISS GEMMOLOGICAL INSTITUTE INSTITUT SUISSE DE GEMMOLOGIE

Gem-A THE GEMMOLOGICAL ASSOCIATION OF GREAT BRITAIN

The Gemmological Association of Great Britain

Gem-A

THE GEMMOLOGICAL ASSOCIATION
OF GREAT BRITAIN

Gem-A Conference

21–22 November 2015

The **2015 Gem-A Conference** will be held at the **Royal Institute of British Architects (RIBA)** in Marylebone, London. Incorporating the 18th Symposium of the Federation for European Education in Gemmology (FEEG), this year's Conference promises to be bigger and better than ever, with a host of world-class speakers delivering talks on a wide range of topics, as well as exclusive events and hands-on workshops.

Visit **www.gem-a.com** for the full programme or email the Events team at **events@gem-a.com** to book your place.

Understanding Gems

Join us.

The Gemmological Association of Great Britain, 21 Ely Place, London, EC1N 6TD, UK. T: +44 (0) 20 7404 3334 F: +44 (0) 20 7404 8843.
Registered charity no. 1109555. A company limited by guarantee and registered in England No. 1945780. Registered Office: 3rd Floor, 1-4 Argyll Street, London W1F 7LD.

The Journal of Gemmology
2015 / Volume 34 / No. 7

COLUMNS

Cover Photo: This jewellery suite features red tourmaline from Nigeria that was all cut from the same piece of rough (1.20–9.07 ct; 99.19 carats total weight); see Gem Note on p. 569. Courtesy of Barker & Co., Scottsdale, Arizona; photo by Jeff Scovil.

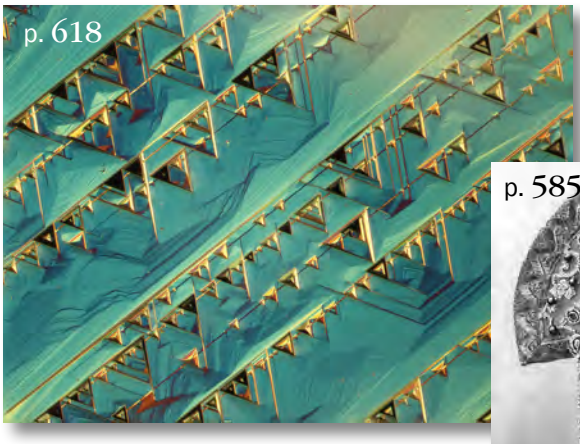
p. 618


p. 585

ARTICLES

Feature Articles

Gemmological Brief

The Journal is published by Gem-A in collaboration with SSEF and with the support of AGL and GIT.

ISSN: 1355-4565, http://dx.doi.org/10.15506/JoG.2015.34.7

The Journal of Gemmology

Content Submission

The Editor-in-Chief is glad to consider original articles, news items, conference/excursion reports, announcements and calendar entries on subjects of gemmological interest for publication in *The Journal of Gemmology*. A guide to the preparation of manuscripts is given at www.gem-a.com/publications/journal-of-gemmology.aspx, or contact the Production Editor.

Subscriptions

Gem-A members receive *The Journal* as part of their membership package, full details of which are given at www.gem-a.com/membership.aspx. Laboratories, libraries, museums and similar institutions may become Direct Subscribers to *The Journal* (see www.gem-a.com/publications/subscribe.aspx).

Advertising

Enquiries about advertising in *The Journal* should be directed to the Marketing Consultant. For more information, see www.gem-a.com/publications/journal-of-gemmology/advertising-in-the-journal.aspx.

Copyright and Reprint Permission

The Journal of Gemmology is published quarterly by Gem-A, The Gemmological Association of Great Britain. Any opinions expressed in *The Journal* are understood to be the views of the contributors and not necessarily of the publisher.

Printed by DG3 (Europe) Ltd.

ISSN: 1355-4565

Gem-A
THE GEMMOLOGICAL ASSOCIATION OF GREAT BRITAIN

21 Ely Place
London EC1N 6TD
UK

t: +44 (0)20 7404 3334
f: +44 (0)20 7404 8843
e: information@gem-a.com
w: www.gem-a.com

Registered Charity No. 1109555
Registered office: Palladium House, 1–4 Argyll Street, London W1F 7LD

Understanding Gems™

What's New

INSTRUMENTS AND TECHNIQUES

B&W Tek GemRam Mini

In mid-2015, B&W Tek launched the GemRam Mini handheld Raman spectrometer containing a spectral library of nearly 400 gem species that was assembled by Prof. Dr Henry A. Hänni (GemExpert, Basel, Switzerland). Measuring 19 × 10 × 5 cm and weighing 0.9 kg, the instrument utilizes a touch screen interface, a 785 nm diode laser and a high-resolution spectrometer. Raman data from the instrument can be synchronized to a PC-based database via Wi-Fi or Ethernet to perform additional data analysis. It may be powered by mains electricity or a rechargeable Li-ion battery for >5 hrs of continuous operation. For more information on handheld and portable Raman spectrometers from B&W Tek, visit http://bwtek.com/technology/raman.

OGI DiaPix

In January 2015, OGI Systems launched DiaPix, a technology for capturing high-definition images of diamonds, coloured stones and jewellery. Users can produce videos showing 360° views of an object, which can be uploaded to corporate websites, social networking sites and trade platforms. The instrument weighs 5 kg and measures 46 × 46 × 31.5 cm. Visit www.ogidiapix.com.

NEWS AND PUBLICATIONS

Bursztynisko Amber Newsletter and Baltic Amber Classification

The latest issue of *Bursztynisko* (No. 37, March 2015), the annual bilingual (English/Polish) newsletter of the International Amber Association (IAA), contains articles on the history, mining, certification, and people associated with amber, as well as reports on amber collections, shows, exhibitions and conferences. It also features several short technical articles on fossilized insects and mites in Baltic, Dominican and English amber.

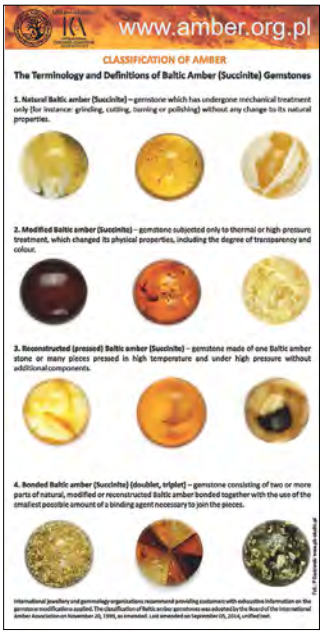

Download the issue at www.amber.org.pl/index.php/download_file/view/460.

In September 2014, the IAA updated their classification of Baltic amber, which provides definitions for Natural, Modified, Reconstructed (pressed) and Bonded (assembled) Baltic amber. Download the illustrated reference card at www.amber.org.pl/index.php/down load_file/view/452.

GTL Newsletter

The latest *Lab Information Circular* (Vol. 72, July 2015) from the Gem Testing Laboratory (Jaipur, India) is available at http://gtljaipur.info/circulars/LIC_Vol72_July2015_English.pdf. It describes resin-filled Cu-bearing tourmaline, fossilized dinosaur bone, banded serpentine, aquamarine with strong dichroism, 'neon' green synthetic sapphire, orthoclase feldspar with abundant hematite inclusions similar to those seen in 'sunstone' plagioclase, and glass with crystalline inclusions.

Gems & Gemology Cumulative PDF

In August 2015, Joseph Gill made available a single searchable PDF file containing all issues of *Gems & Gemology* from January 1934 to Summer 2015 (330 issues covering 81 years in 17,183 pages). Download the file at https://archive.org/details/GemsGemologyOrGGJan.1934Summer2015330Issues17.183Pages81YearsOfGemology.

GIT Lab Update

In July 2015, The Gem and Jewelry Institute of Thailand in Bangkok issued a Lab Update on a yellow lead-glass-filled sapphire. The 10.27 ct oval mixed cut contained fractures and cavities that were filled with lead glass that was coloured yellow by vanadium. Download the report at www.git.or.th/2014/eng/testing_center_en/lab_notes_en/glab_en/2015/07/16/Yellow_Lead-glass_filled_sapphire.pdf.

ICA Congress Presentations

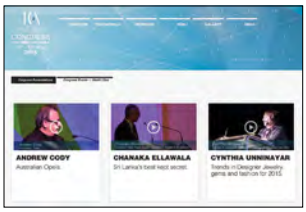

Videos of speaker presentations from the International Colored Gemstone Association Congress that took place in Colombo, Sri Lanka on 16–19 May 2015 are available at www.icacongress.com/videos/congress-presentations.html. There are 13 talks, one panel discussion, and a speech by Paolo Valentini on the history of the ICA.

Ivory Regulations Proposed by the U.S. Fish & Wildlife Service

In July 2015, the U.S. Fish & Wildlife Service proposed ivory regulations intended to curb poaching of African elephants and other species. The regulations would prohibit most U.S. interstate commerce in African elephant ivory and further restrict commercial exports, resulting in a near-total ban on the domestic commercial trade of African elephant ivory. The regulations include specific, limited exceptions for certain pre-existing manufactured items such as musical instruments, furniture pieces, and firearms that contain less than 200 grams of ivory, as well as antiques (as defined by the Endangered Species Act). For more information, visit www.fws.gov/international/pdf/african-elephant-4d-proposed-changes.pdf.

Margaritologia Pearl Newsletter No. 2/3

In June 2015, *Margaritologia* No. 2/3 was released by Elisabeth Strack of Gemmologisches Institut Hamburg, Germany. The issue features an informative 18.5 page report on freshwater

cultured pearls from China—the history of their farming (in 1962–1980, the 1980s, the 1990s and the 2000s, as well as the current situation), production methods and varieties. Details are given of recently developed grafting methods for mantle and gonad implantation using mother-of-pearl beads. The report also contains a short glossary of trade terms for Chinese bead-cultured freshwater pearls. To subscribe to the newsletter, visit www.gemmologisches-institut-hamburg.de.

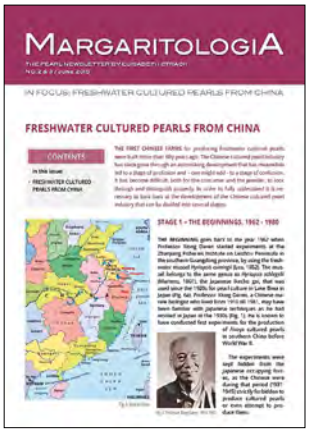

Perettiite-(Y), a New Mineral from Momeik, Myanmar

A new mineral has been discovered as an inclusion in gem-quality phenakite from Momeik, Myanmar. Perettiite-(Y) is named after Dr Adolf Peretti of GRS Gemresearch Swisslab AG. The mineral forms isolated yellow needles in gem-quality crystals of colourless phenakite that were purchased in the Mogok gem market in 2007 and 2014. Visit www.gemresearch.ch/news/2015-08-04_Perettiite/index.htm.

Rough Octahedral Synthetic Diamonds

In July 2015, HRD Antwerp announced encountering some small gem-quality near-colourless synthetic diamond crystals showing octahedral shapes, rather than the cubo-octahedral morphology that is typical of HPHT-grown synthetics. The crystals ranged from 0.01 to 0.04 ct and were produced by Taidiam Technology Co. Ltd., Zhengzhou, Henan, China. View the announcement at www.hrdantwerp.com/en/news/hrd-antwerp-in-focus-rough-octahedral-lab-grown-diamonds-ar.

Rubies from Madagascar

In September 2015, Lotus Gemology in Bangkok released a report describing the gemmological characteristics of a new production of rubies from Andilamena, Madagascar. The gems showed properties similar to those of rubies produced in 2005 from the nearby Moramanga area, except that the new stones were larger, with faceted gems ranging from 1.04 to 7.16 ct. Visit www.lotusgemology.com/index.php/library/articles/322-blood-red-rubies-from-madagascar-lotus-gemology.

Silver Institute Publications

In March 2015, the Silver Institute released its '2014 Silver Jewelry Sales Results', which compiles the results of surveying jewellery retailers about silver sales. Download the executive summary at www.silverinstitute.org/site/wp-content/uploads/2011/06/2014SilverJewelrySalesReport.pdf.

More recently, the Silver Institute released its 'World Silver Survey 2015—A Summary', which reported that silver jewellery fabrication rose to a new record level of 215.2 million ounces in 2014, helped by lower silver prices and a strong rebound in Indian demand. Download the report at www.silverinstitute.org/site/wp-content/uploads /2011/06/WSS2015Summary.pdf.

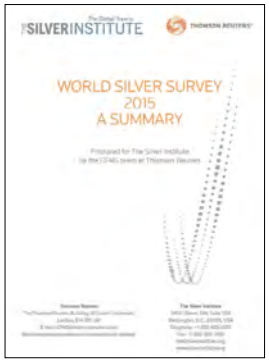

Synthetic Ruby Overgrowth on Corundum

In June 2015, the Gemological Institute of America released a report titled 'Analysis of Synthetic Ruby Overgrowth on Corundum' by S. Saeseaw et al. The paper describes the properties of 10 samples (1.40–2.17 ct) acquired in 2014 through a Bangkok-based supplier, which reportedly consisted of rejects from experiments performed by Duros Company (known for their synthetic rubies) during the early 2000s. The starting material probably consisted of colourless sapphire from Sri Lanka, and may have been provided to Duros after initial Cr-diffusion experiments proved unsuccessful. Download the report at www.gia.edu/gia-news-research/synthetic-ruby-overgrowth-corundum-analysis.

World Diamond Conference Presentations

Reports and videos of some of the presentations at the World Diamond Conference, held 11–12 December 2014 in New Delhi, India, are available at www.gjepc.org/wdc.php. Included is an address by the Prime Minister of India.

World Gold Council Publications

In July 2015, the World Gold Council released a report titled 'Developing Indian Hallmarking' that outlines the importance of quality assurance, assesses the current state of hallmarking in India, considers lessons learned from other countries and establishes a roadmap for the future. Download the report at www.gold.org/download/file/4025/Developing-Indian-hallmarking.pdf.

In August 2015, the World Gold Council issued its 'Gold Demand Trends Second Quarter 2015', which states that gold demand from the jewellery industry dropped 14% to a three-year low of 513.5 tons, mostly due to a downturn in consumer sentiment in India and China. Download the report at www.gold.org/download/file/4107/GDT_Q2_2015.pdf.

MISCELLANEOUS

Gem Museum in Singapore

In June 2015, the Gem Museum opened in Singapore. Founded by the directors of Far East Gem Institute, it is the first and most comprehensive gem and mineral museum in Singapore. The Museum's purpose is to educate

the public and foster an awareness of gemmology to hobbyists and collectors. Various displays focus on aspects ranging from crystals to organic gems, phenomenal stones and even imitation and synthetic gem materials. Workshops are occasionally provided, and the most popular one is the Gem Discovery Series. For more information, visit http://thegemmuseum.gallery or email contact@thegemmuseum.gallery.

Huiying Loke (huiying@gem.com.sg)
Far East Gem Institute, Singapore

What's New provides announcements of new instruments/technology, publications, online resources and more. Inclusion in What's New does not imply recommendation or endorsement by Gem-A. Entries are prepared by Brendan Laurs unless otherwise noted.

SSEF

SCHWEIZERISCHES GEMMOLOGISCHES INSTITUT
SWISS GEMMOLOGICAL INSTITUTE
INSTITUT SUISSE DE GEMMOLOGIE

ORIGIN DETERMINATION · TREATMENT DETECTION

DIAMOND GRADING · PEARL TESTING

EDUCATION · RESEARCH

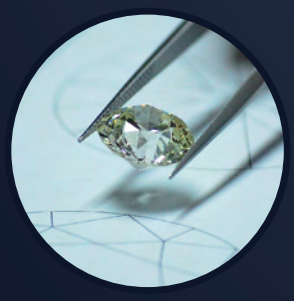

THE SCIENCE OF GEMSTONE TESTING©

Aeschengraben 26, CH-4051 Basel, Switzerland Tel. +41 61 262 06 40 Fax + 41 61 262 06 41 admin@ssef.ch www.ssef.ch

Gem Notes

COLOURED STONES

Buchite from the Eifel Mountains, Germany

The name *buchite* is used for a glassy pyrometamorphic volcanic rock (Callegari and Pertsev, 2007). It originates from the contact of basaltic melts with sandstone, and can be regarded as a glassy sandstone. The name traces back to the famous German geologist Leopold von Buch (1774–1853). Classic occurrences are found in Germany, especially Hohen Hagen near Göttingen, Blaue Kuppe near Eschwege (type locality) and Biebergemünd in the Spessart Mountains.

Recently a faceted transparent green buchite from the Eifel Mountains in Germany was investigated. The specimen (Figure 1) is in the collection of the German Gemmological Association and weighs 0.245 ct. The RI measured with a standard gemmological refractometer was 1.510 and the hydrostatic SG was 2.40. Microscopic examination revealed two types of solid inclusions

Figure 1: This 0.245 ct faceted natural glass (buchite) from the Eifel Mountains, Germany, was investigated for this report. Photo by S. Koch, DSEF.

Figure 2: The inclusions in the buchite consisted of mullite needles (top) and dark crystals of spinel. Photomicrograph by U. Henn, magnified 45×.

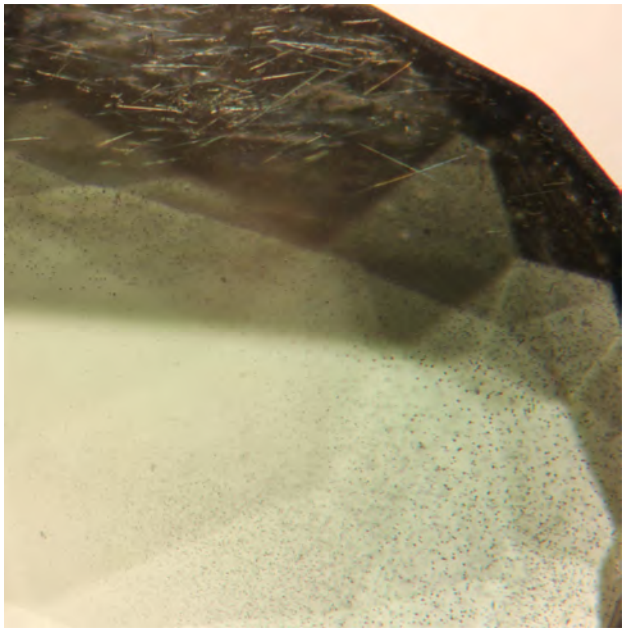

Figure 3: Tabby extinction was seen in the buchite between crossed polarizers. Photomicrograph by K. Schollenbruch, magnified 40×.

(Figure 2) and a distinct tabby extinction between crossed polarizing filters (Figure 3). The solid inclusions were identified as mullite and spinel using a Renishaw inVia Raman microscope.

The absorption spectrum measured with a Perkin Elmer Lambda 12 spectrometer was characterized by two broad absorption regions in the red and blue-violet range, with no distinct absorption maxima. Chemical analysis carried out by electron microprobe (Jeol JXA 8200 at the Institute for Geosciences, Johannes Gutenberg University of Mainz, Germany) yielded 73.47 wt.% SiO_2, 3.72 wt.% Al_2O_3, 6.68 wt.% Na_2O, 8.59 wt.% K_2O, 3.40 wt.% FeO and 0.64 wt.% MnO.

Dr Ulrich Henn (ulihenn@dgemg.com)
German Gemmological Association
Idar-Oberstein, Germany

Reference

Callegari E. and Pertsev N.N., 2007. 10. Contact metamorphic rocks. In *A Systematic Nomenclature for Metamorphic Rocks*, IUGS Subcommission on the Systematics of Metamorphic Rocks: Web version 01.02.07, www.bgs.ac.uk/scmr/docs/papers/paper_10.pdf.

Colour-zoned Fluorite from Shan and Kayah States, Myanmar

Fluorite in various colours (i.e. purple, violet, green and yellow) has been known from the Mogok Stone Tract in Myanmar for years (Kammerling et al., 1994). More recently, additional localities in east-central Myanmar have produced some multi-coloured fluorite that has been polished into cabochons.

In Shan State, fluorite is known from two localities: Langhko and Pinlaung townships. It was discovered at Langhko (113 km south-east of Taunggyi) in 2012 and mined in 2013 by Shan people during a peace agreement with the Myanmar government. From ~200 rough pieces, about 1,000 cabochons have been cut and polished in mostly oval shapes (average 4 × 3 × 2 mm). Some of these cabochons were worn in rings by top officials from the Shan group. At Pinlaung (80 km south of Taunggyi), fluorite was discovered in 2014 in a banana plantation. The material has been picked up from the surface by local villagers, and no mining has taken place yet. This author obtained a rough piece from the villagers, and a portion of it was subsequently cut into a cabochon of 3.0 × 2.5 × 0.5 mm. It is hoped that good-quality fluorite will be produced from this area in the future.

In Kayah State, fluorite was found in ~2011 in Bawlake township (182 km south of Taunggyi). Only a small quantity of this material has been cut so far, in various sizes and shapes, and it is typically oiled due to the presence of fractures.

Figure 4: From left to right, the Burmese fluorite samples studied for this report were from Langhko in southern Shan State (88.0 and 24.5 ct), Bawlake in Kayah State (35.5 ct) and Pinlaung in Shan State (47.25 ct cabochon and 15.8 g piece of rough). The cabochons appear rather dark in this reflected-light photo. Photo by U T. Hlaing.

Five samples of fluorite from these localities were studied for this report: four cabochons of 24.5–88.0 ct and one rough piece weighing 15.8 g (Figure 4). Viewed with reflected light, all of the cabochons appeared dark with bands or irregular zones of lighter colour. Transmitted light most commonly showed various shades of blue, greenish blue, violet and colourless; rarely present were green or black bands (Figure 5). Energy-dispersive X-ray fluorescence spectroscopy (EDXRF) of the rough piece from Pinlaung (light and dark violet bands) using an Innov-X portable instrument revealed traces of Al, Si, Cl, S, Fe, Cr and Mn (note that the instrument was not set up to detect heavy elements such as rare earths).

Colour-banded fluorite is common from various world localities, typically dominated by violet, yellow or green bands. The fluorite from

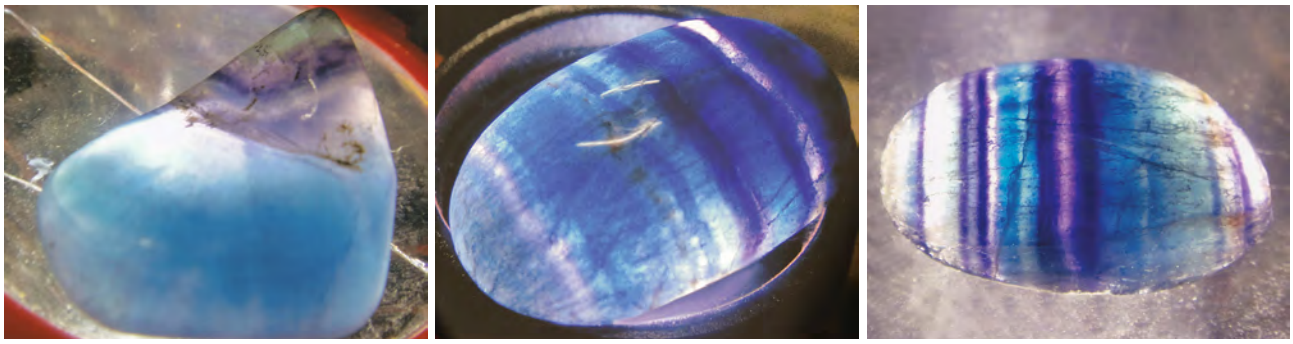

Figure 5: Seen here in transmitted light are the fluorite cabochons from Langhko, Shan State (88.0 ct on the left, and 24.5 ct in the centre) and Bawlake, Kayah State (right, 35.5 ct). Photos by U T. Hlaing.

east-central Myanmar is distinctive for its mostly blue coloration.

U Tin Hlaing (p.tinhlaing@gmail.com)
Dept. of Geology (retired)
Panglong University, Myanmar

Reference

Kammerling R.C., Scarratt K., Bosshart G., Jobbins E.A., Kane R.E., Gübelin E.J. and Levinson A.A., 1994. Myanmar and its gems—An update. *Journal of Gemmology*, **24**(1), 3–40, http://dx.doi.org/10.15506/jog.1994.24.1.3.

Malachite-Azurite from Peru

Malachite is a popular ornamental stone, but only rarely is it cut as a mixture with chemically similar azurite. An important exception is seen in rare bicoloured malachite-azurite cabochons from Morenci, Arizona, USA, which typically display a sharp border between the two minerals. A new occurrence of malachite-azurite was discovered in 2011 from Moquegua Department in southern Peru. The first specimens were mentioned by Hyršl (2012), but several dozen much better stones were offered for sale during the February 2014 Tucson gem shows.

The polished stones typically consist of rather large flat cabochons that measure up to ~8 cm long. The blue azurite typically forms irregular brecciated masses within the green malachite matrix. An unusual feature displayed by some specimens is a fine banding of both minerals, with regular bands of ~0.5–1 mm wide (e.g. Figure 6). Advanced testing of interstitial areas within the bands using both X-ray diffraction and Raman analysis proved them to be gypsum. In some specimens, white granular calcite is also present.

With standard gemmological testing, the material is easily recognizable by its strong carbonate birefringence blink on the refractometer. Also, the hydrostatic SG is 2.64–2.79, there is no fluorescence to UV radiation, and both malachite and azurite will effervesce when exposed to dilute hydrochloric acid.

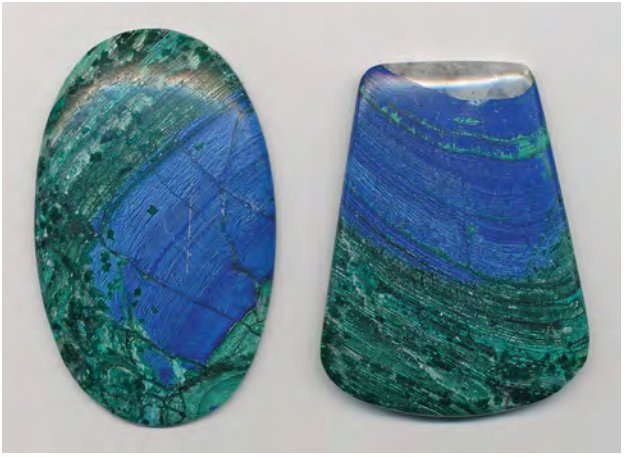

Figure 6: These cabochons of malachite-azurite from Peru (64 and 57 mm long) display an unusual fine banding. Photo by J. Hyršl.

The banded and/or brecciated structure of this material is unique for malachite-azurite, but the amount available on the market is unknown and it may remain a collector's curiosity.

Jaroslav Hyršl (hyrsl@hotmail.com)
Prague, Czech Republic

Reference

Hyršl J., 2012. *Gemstones of Peru*. Granit, Prague, Czech Republic, 104 pp.

Gem Mosandrite from Russia

Mosandrite is a rare-earth element (REE)-bearing silicate with the formula $(\square,Ca,Na)_3(Ca,REE)_4Ti(Si_2O_7)_2[H_2O,OH,F]_4 \bullet H_2O$, where □ = a vacancy (Sokolova and Hawthorne, 2013). It was named by Axel Joakim Erdmann in 1841 after the Swedish mineralogist Carl Gustav Mosander. Mosandrite has a Mohs hardness of 5, and for several years small quantities of facetable material have been produced only from the Kirovsky apatite mine, Khibiny Massif, Kola Peninsula, Russia. The Khibiny Massif is a famous and unique mineral locality that is composed of a nepheline syenite intrusion rich in a large number of rare minerals. Other locations for mosandrite are Norway and Canada, from which the authors are not aware of any gem-quality material.

A 0.38 ct faceted mosandrite (Figure 7) of brown-orange colour was investigated by standard gemmological methods. The gem was supplied by a colleague in 2014 as Russian mosandrite. The RI values were $n_x = 1.650$, $n_y = 1.653$ and $n_z = 1.658$, with a birefringence of 0.008 and a biaxial positive optic sign. The hydrostatic SG was 3.28. These values fall within reference data for mosandrite reported by Phillips and Griffen (1981): RIs of $n_x = 1.643–1.662$, $n_y = 1.645–1.667$ and $n_z = 1.651–1.681$; birefringence 0.008–0.019; and SG of 2.93–3.50. Examination with a gemmological microscope revealed numerous crystal inclusions

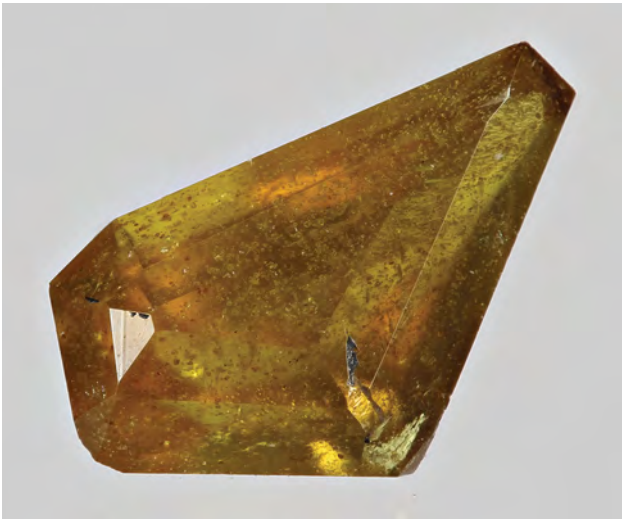

Figure 7: This faceted brown-orange mosandrite (0.38 ct) is from the Kola Peninsula, Russia. Photo by S. Koch, DSEF.

(Figure 8, left) and a noticeable roiled appearance (Figure 8, right). The inclusions partly showed an octahedral habit, and analysis with a Zeiss DSM 942 scanning electron microscope at the Institute for Gemstone Research, University of Mainz, Germany, identified them as pyrochlore, $(Ca,Na)_2Nb_2(O,OH,F)_7$.

A visible-near infrared absorption spectrum obtained with a Perkin Elmer Lambda 12 spectrometer showed a typical REE spectrum (Figure 9), with maxima at 512, 527, 585, 684,

Figure 8: The mosandrite contained crystal inclusions of partly octahedral habit that were identified as pyrochlore (left, magnified 50×). A roiled appearance was noticeable when the stone was viewed with crossed polarizers (right, magnified 30×). Photos by F. Schmitz.

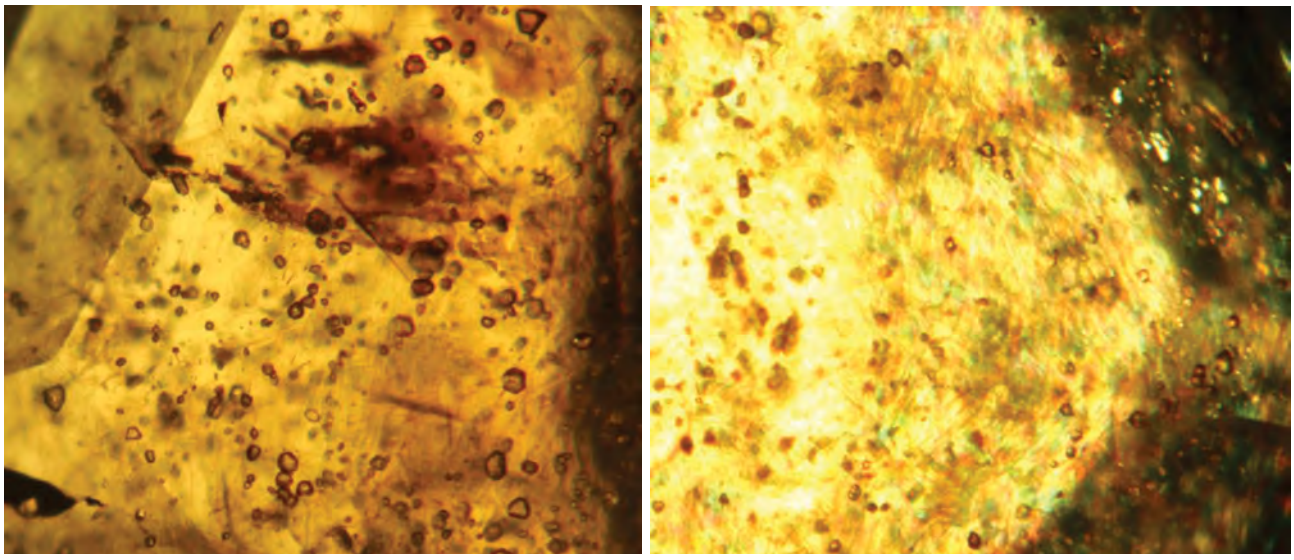

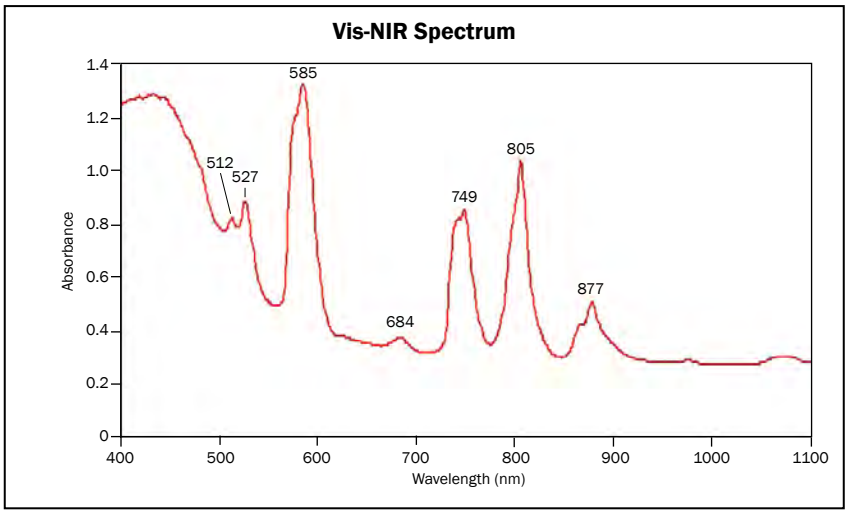

Figure 9: The absorption spectrum of the mosandrite showed several lines corresponding to Nd^{3+}. The path length of the beam was ~2.9 mm.

749, 805 and 877 nm that are due to Nd^{3+} (Wybourne, 1960).

Dr Ulrich Henn (ulihenn@dgemg.com) and Fabian Schmitz
German Gemmological Association
Idar-Oberstein, Germany

References

Phillips W.R. and Griffen D.T., 1981. *Optical Mineralogy: The Nonopaque Minerals*. Freeman, San Francisco, California, USA.

Sokolova E. and Hawthorne F.C., 2013. From structure topology to chemical composition. XIV. Titanium silicates: Refinement of the crystal structure and revision of the chemical formula of mosandrite, $(Ca_3REE)[(H_2O)_2Ca_{0.5}\square_{0.5}]Ti(Si_2O_7)_2(OH)_2(H_2O)_2$, a Group-I mineral from the Saga mine, Morje, Porsgrunn, Norway. *Mineralogical Magazine*, **77**(6), 2753–2771, http://dx.doi.org/10.1180/minmag.2013.077.6.05.

Wybourne B.G., 1960. Analysis of the solid-state spectra of trivalent neodymium and erbium. *Journal of Chemical Physics*, **32**(3), 639–642, http://dx.doi.org/10.1063/1.1730773.

A Shattuckite Briolette

Recently, the Gem Testing Laboratory, Jaipur, India, received for identification an 8.13 ct intense blue briolette measuring 14.69 × 10.90 × 6.29 mm (Figure 10). On initial observation, it appeared to be composed of azurite and chrysocolla because of its patchy blue coloration and the presence of some green areas (Figure 11, left).

The gemmological refractometer showed a vague shadow edge at ~1.76, while the hydrostatic SG was 3.94. With the desk-model spectroscope, a broad absorption band was visible from the green through red region. Magnification revealed a radiating fibrous pattern that is typical of spherulitic growth (Figure 11, right) and was associated with banding and uneven coloration in the specimen. The RI and SG values ruled out chrysocolla, and although the SG was somewhat higher than expected for azurite (cf. O'Donoghue, 2006), this possibility could not be discarded.

Figure 10: This 8.13 ct intense blue briolette was identified as shattuckite. Photo by G. Choudhary.

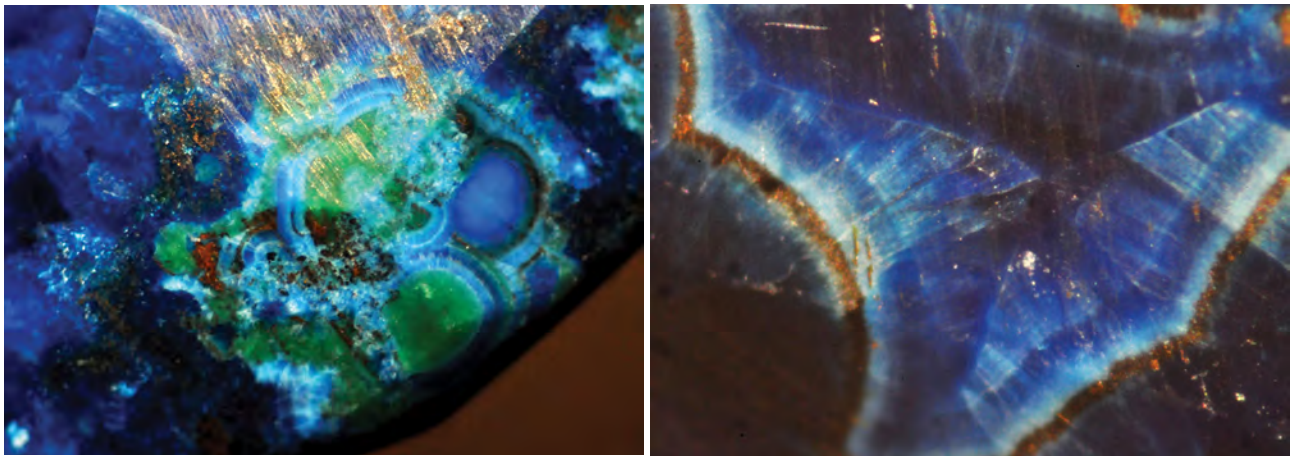

Figure 11: Some green patches of malachite also were present in the shattuckite specimen (left, image width 6.35 mm). The radiating fibrous pattern is typically associated with spherulitic growth (right, image width 5.08 mm). Photomicrographs by G. Choudhary.

Raman spectra in the region 200–2000 cm^{-1} identified the specimen as shattuckite, with characteristic peaks at ~259, 329, 395, 450, 508, 559, 661, 775, 847, 942 and 1069 cm^{-1} (see, e.g., www.rruff.info/doclib/hom/shattuckite.pdf), while the green areas displayed peaks for malachite.

Shattuckite is a hydrous copper silicate, $Cu_5(SiO_3)_4(OH)_2$, which occurs as a secondary mineral in oxidized copper deposits and is commonly associated with chrysocolla, ajoite, malachite and quartz (Anthony et al., 1995). It is known from Bisbee (Shattuck mine), Arizona, USA, as well as Namibia, Democratic Republic of Congo (Overlin, 2014), Chile and elsewhere (Anthony et al., 1995).

This specimen was identified as shattuckite on the basis of Raman spectroscopy, and without this technique it could have been mistaken for azurite. The client was not aware of the sample's identity or origin.

Gagan Choudhary (gagan@gjepcindia.com)
Gem Testing Laboratory, Jaipur, India

References

Anthony J.W., Bideaux R.A., Bladh K.W. and Nichols M.C., 1995. *Handbook of Mineralogy, Vol. II—Silica, Silicates*, Part 2. Mineral Data Publishing, Tucson, Arizona, USA, 726.

O'Donoghue M., Ed., 2006. *Gems*, 6th edn. Butterworth-Heinemann, Oxford.

Overlin S., 2014. Gem News International: Shattuckite from DRC. *Gems & Gemology*, **50**(2), 167–168.

Saguaro Stone, a New Ornamental Material from Arizona (USA)

During the 2014 Tucson gem shows in Arizona, USA, Warren Boyd FGA (Apache Gems, San Carlos, Arizona) donated to Gem-A a 39.60 ct oval cabochon marketed as *Saguaro Stone*. This new gem material had been recently surface-collected by Charles Vargas on the San Carlos Apache Reservation in Arizona. Boyd indicated that so far 700–800 kg of rough have been stockpiled, and that nearly 1,000 cabochons have been cut and polished in China and the USA, ranging from 10 × 8 mm to 20 × 10 mm, as well as a number of free forms. A few pieces have been sold to local designers, and in the future there are plans to market the material on a larger scale.

For this report, the authors investigated the 39.60 ct oval cabochon (Figure 12) and a few small rough fragments. Viewed with the unaided eye, and particularly with the microscope, it was evident that this new ornamental material consisted of multiple phases that differed in colour and lustre. Standard gemmological testing was inconclusive, so a thin section was cut from one of the rough fragments for detailed mineralogical study. Under the high magnification of a petrographic microscope

Figure 12: This attractive new ornamental material (39.60 ct), called Saguaro Stone *and found on Arizona's San Carlos Apache Reservation, consists mainly of brecciated green volcanic glass and veins of calcite. Gift to Gem-A from Apache Gems; photo © M. S. Krzemnicki, SSEF.*

and assisted by Raman microspectroscopy, it became evident that this material consisted of a volcanic rock, formed mainly by brecciated masses of green volcanic glass. In places it showed wavy flow structures, and also present were a few primary magmatic inclusions such as plagioclase (up to 1.3 mm) and altered greenish brown biotite platelets (0.5–1.6 mm; Figure 13a). Additionally, small vacuoles in the rock (Figure 13b) were filled with fibrous chalcedony and opal (amorphous), and also some zeolites. The greenish colour of the brecciated masses was possibly due to the secondary formation of submicroscopic chlorite.

The Raman analyses further revealed that the whitish veins between the brecciated volcanic glass masses consisted of calcite. Also present were small transparent grey grains (with a distinctly higher lustre) of alkali feldspar that contained tiny metallic hematite flakes and small orange patches, possibly iron hydroxide. When exposed to short-wave UV radiation, the calcite veins fluoresced weak reddish pink, whereas the volcanic glass remained inert (Figure 14). The entire stone was inert to long-wave UV radiation.

EDXRF chemical analysis (with a spot size of ~3 mm in diameter) revealed major amounts of Si, Ca and Al, minor Fe and Mn, and traces of alkalis and alkaline earths (including Sr and Ba). This composition is consistent with a silica-

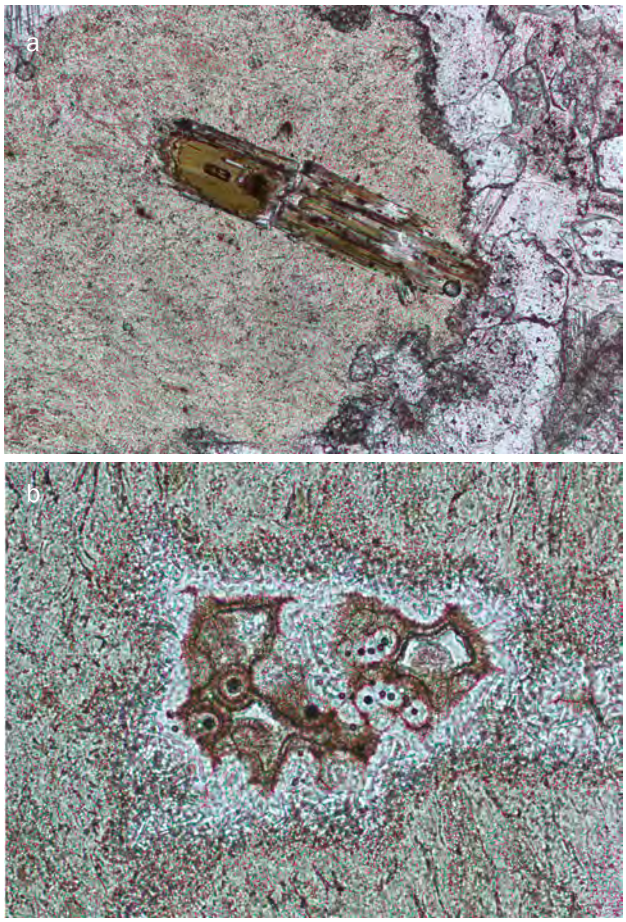

Figure 13: Thin-section examination of the green volcanic rock revealed interesting features. (a) A primary magmatic inclusion of biotite is hosted by a matrix of volcanic glass showing weak flow structures. The colourless grains on the right side correspond to a secondary calcite vein. (b) A small cavity in the rock is filled with acicular chalcedony and amorphous opal. Photos © L. Franz, MPI University of Basel; image width 1.25 mm (a) and 0.56 mm (b).

Figure 14: When the 39.60 ct cabochon is exposed to short-wave UV radiation, the calcite veins in the volcanic rock show a pinkish reaction, whereas the volcanic glass masses remain inert. Photo © M. S. Krzemnicki, SSEF.

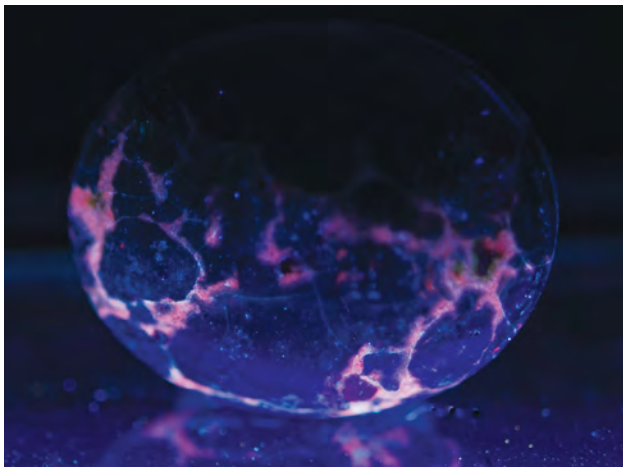

rich volcanic glass containing plagioclase and phyllosilicate inclusions, together with secondary calcite veins.

This ornamental rock makes an attractive addition to the gem market, especially as it is relatively tough and hard, and thus shows a high lustre combined with an attractive colourful brecciated texture.

Dr Michael S. Krzemnicki
(michael.krzemnicki@ssef.ch)
Swiss Gemmological Institute SSEF
Basel, Switzerland

Dr Leander Franz
Mineralogical and Petrographical Institute
University of Basel, Switzerland

'Ruby'-red Tourmaline from Nigeria

During the June 2015 JCK show in Las Vegas, Nevada, USA, Bill Barker (Barker & Co., Scottsdale, Arizona, USA) displayed some red tourmaline from a new discovery at the Oyo Valley deposits in Nigeria, which was notable for its ruby-like coloration. He obtained three large pieces of rough in April 2015 from his supplier in Lagos, Nigeria. Although the rough was dark, it was very red. Cutting of a piece that weighed 8.4 kg yielded 3,973 carats of faceted stones (not including melee from the offcuts) ranging from ~1 to 16 ct each. The final yield of 9.5% was far below the typical yield (13–16%) that Barker has obtained in the past from Oyo Valley Nigerian rubellite, and resulted from his choice to cut smaller stones (especially Portuguese-style rounds) so they would not appear overly dark. Also, only clean faceted stones and no cabochons were cut from the rough.

Barker assembled seven jewellery suites from this material (see, e.g., the cover of this issue), and also offered individual cut stones (Figure 15). They displayed an attractive red colour similar to Thai ruby—so much so that he displayed the rubellite next to Thai ruby at the JCK show (e.g. Figure 16). This coloration is rather distinct from the lighter pink to purplish pink hues that are typically shown by Nigerian tourmaline.

Brendan M. Laurs

Figure 15: These 'ruby'-red tourmalines from Nigeria weigh 4.25–7.25 ct. Photo by Rich Barker.

Figure 16: The Nigerian rubellite on the left (2.71 ct) shows a similar coloration to the Thai ruby on the right (3.14 ct). Both gems were faceted by the same cutter as Portuguese-style rounds. Photo by Rich Barker.

Tremolite from Mwajanga, Tanzania

During the 2015 Tucson Gem shows, gem dealer Werner Radl of Mawingu Gems (Niederwörresbach, Germany) displayed a prismatic gem-quality crystal (Figure 17) that he obtained in Tanzania. It was sold to him as tourmaline, and reportedly came from a new find in the Mwajanga area (Manyara region of north-central Tanzania).

Figure 17: This prismatic crystal is gem-quality tremolite, an amphibole-group mineral. It measures 69.5 mm long and weighs 8.05 g. Photo by J. C. Zwaan.

The elongate crystal was transparent and had a light, slightly greyish, green colour. It weighed 8.05 g and measured approximately 69.5 × 9.37 × 5.48 mm. Both ends of the crystal were broken, and one end also displayed an area with a parallel fibrous structure. The surface of the crystal displayed fine striations along its length, and an incipient cleavage fracture was present in the same orientation. Another fracture positioned in the middle of the crystal was oriented almost perpendicular to the longitudinal direction. Inclusions consisted of parallel growth tubes and partially healed fissures.

One side of the crystal had been polished, but no clear readings could be obtained with the refractometer due to the poor quality of the polish. The hydrostatic SG was 2.99. With the dichroscope, weak trichroism could be observed: colourless, light yellowish green and light green. No fluorescence was observed to long- or short-wave UV radiation. Compared to amphiboles in the tremolite-actinolite-ferroactinolite series (Deer et al., 1997), the overall pale colour, relatively low SG and weak pleochroism corresponded to a member with a low iron content, and therefore suggested tremolite, rather than actinolite, as the identity of this crystal.

Raman analysis taken with 532 nm laser excitation revealed a spectrum that had closest matches to several reference spectra for tremolite in the RRUFF database (www.rruff.info). However, the Raman spectra of actinolite may be very similar, and therefore caution must be exercised when interpreting the spectra (Figure 18). The best match was to a tremolite spectrum that also showed a peak at 120 cm^{-1}. For most of the tremolite and actinolite spectra in the database, spectral features below 150 cm^{-1} were not recorded, and some of those tremolite and actinolite spectra were virtually indistinguishable.

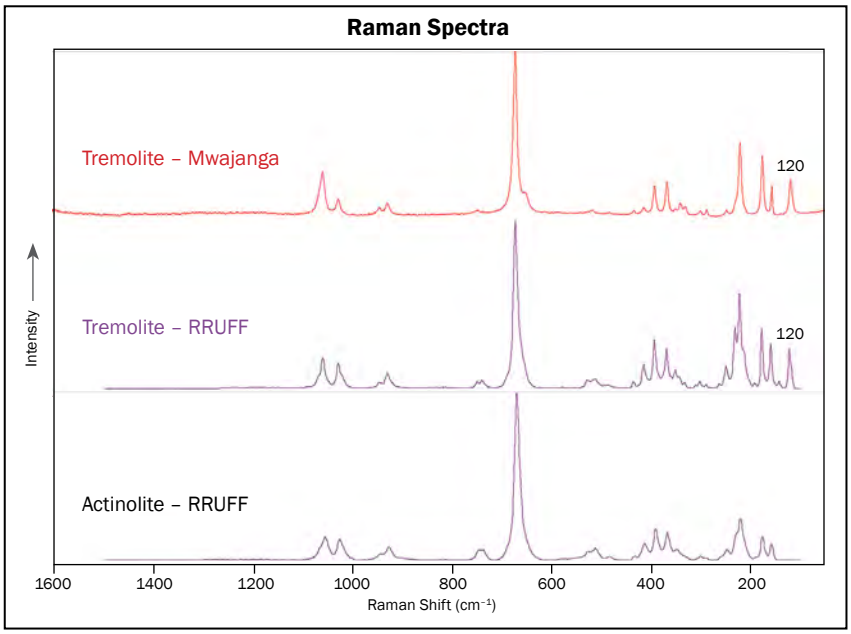

Figure 18: The Raman spectrum of the crystal showed the best match with a tremolite spectrum in the RRUFF database, containing a distinct peak at 120 cm^{-1}. The crystal's spectrum also showed a good match with reference spectra for actinolite (e.g. bottom spectrum). Raman spectra of tremolite and actinolite may be very similar and therefore indistinguishable.

The compositional range of tremolite extends from $\square Ca_2Mg_5Si_8O_{22}(OH)_2$ (where $\square$ = a vacancy) to $\square Ca_2Mg_{4.5}Fe^{2+}_{0.5}Si_8O_{22}(OH)_2$, whereas actinolite extends from $\square Ca_2Mg_{\leq 4.5}Fe^{2+}_{\geq 0.5}Si_8O_{22}(OH)_2$ to $\square Ca_2Mg_{2.5}Fe^{2+}_{2.5}Si_8O_{22}(OH)_2$ (Leake et al., 1997; Hawthorne et al., 2012). Electron microprobe analysis of the crystal by one of the authors (FCH) confirmed that it was indeed tremolite: $(Na_{0.05}K_{0.03})(Ca_{1.94}Na_{0.06})_2(Mg_{4.85}Fe_{0.10}Mn_{0.01}Al_{0.03})_{4.99}Si_{7.99}O_{22}(OH)_{1.92}F_{0.08}$. This formula, with $Mg/(Mg+Fe^{2+}) = 0.98$ (cf. Leake et al., 1997) and with $^{A}(Na+K+2Ca) = 0.08$ and $^{C}(Al+Fe^{3+}+2Ti) = 0.03$ (cf. Hawthorne et al., 2012), shows that the crystal has a composition that is very close to the pure end-member composition of tremolite.

In July 2015, Radl reported that he obtained three more crystals of this tremolite from the same find. Also, his supplier indicated that a few kilograms of the rough tremolite were sold into the market as tourmaline. This is not surprising, given the similar appearance of this tremolite to some of the tourmaline that was recently mined from the Mwajanga area (e.g. www.minrec.org/pdfs/Toms%20Online%20report%2039.pdf).

Radl indicated that he encountered significant amounts of tremolite of the same pale green colour (associated with quartz and purple scapolite) during his first trip to Tanzania in 1995. The only other occurrences of gem-quality tremolite known to these authors are yellowish green material from Merelani, Tanzania (Fritz et al., 2007) and greyish green crystals from Bancroft, Ontario, Canada (www.youtube.com/watch?v=od4OfHsGQbg).

Dr J. C. (Hanco) Zwaan (hanco.zwaan@naturalis.nl)
Netherlands Gemmological Laboratory
National Museum of Natural History 'Naturalis'
Leiden, The Netherlands

Dr Frank C. Hawthorne
University of Manitoba, Winnipeg, Canada

References

Deer W.A., Howie R.A. and Zussman J., 1997. *Rock Forming Minerals—Double-chain Silicates*, Vol. 2B, 2nd edn. Geological Society of London, 763 pp.

Fritz E.A., Laurs B.M., Downs R.T. and Costin G., 2007. Yellowish green diopside and tremolite from Merelani, Tanzania. *Gems & Gemology,* **43**(2), 146–148, http://dx.doi.org/10.5741/gems.43.2.146.

Hawthorne F.C., Oberti R., Harlow G.E., Maresch W.V., Martin R.F., Schumacher J.C. and Welch M.D., 2012. IMA report—Nomenclature of the amphibole super group. *American Mineralogist*, **97**, 2031–2048, http://dx.doi.org/10.2138/am.2012.4276.

Leake B.E., Woolley A.R., Arps C.E.S., Birch W.D., Gilbert M.C., Grice J.D., Hawthorne F.C., Kato A., Kisch H.J., Krivovichev V.G., Linthout K., Laird J. and Mandarino J., 1997. Nomenclature of amphiboles: Report of the subcommittee on amphiboles of the International Mineralogical Association Commission on New Minerals and Mineral Names. *Mineralogical Magazine*, **61**, 295–321, http://dx.doi.org/10.1180/minmag.1997.061.405.13.

DIAMONDS

Diamond Horse-head Carving

Sculpting and carving are very intricate and patience-consuming art forms. Numerous examples of sculptures and carvings created from stone and various gem materials are known worldwide, but hand sculpting of diamond is virtually unheard of (e.g. Fryer, 1983; Du Toit, 2009).

In January 2015, this author examined a unique two-headed horse sculpted from natural diamond (Figure 19). It was accompanied by GIA report no. 1209011703, certifying it as a carving weighing 4.07 ct that was made from near-colourless natural diamond. It measured 13.72 × 7.02 × 4.34 mm, and the two horse heads formed a perfect mirror image of one another. The carving was well proportioned with precise symmetry when viewed from any direction. Although designed to stand upright on its base, it was balanced with such precision that it would stand upside-down on the ears without toppling over (see Figure 19, centre). When the sculpture was observed in detail, the illusion of harness straps going across the faces of the horses could be seen.

The sculptor reportedly required more than a full year to plan and execute the carving. A paper

Figure 19: A 4.07 ct diamond horse-head carving is shown in these three views. Photos by Sameer Doshi.

sketch was made first, followed by a wooden prototype, and then the design was marked on the actual diamond rough, which weighed 8.38 ct (Figure 20). Since only a diamond can scratch diamond, to actually carve and sculpt an entire three-dimensional figurine without making use of laser technology required a great amount skill and patience that only a master craftsman would have. The piece was sculpted using subtractive carving techniques, in which material was gradually removed from the diamond rough. Any slight negligence while working could either cleave the diamond or create a misproportioned carving.

One has to give credit to the initiative of the sculptor, as there is no school or institute that provides training in diamond carving. This carving is indeed an extremely rare creation and an amazing piece of art to be treasured.

Dr Jayshree Panjikar FGA
(jayshreepanjikar@gmail.com)
Pangem Testing Laboratory, Pune, India

References

Du Toit G., 2009. Lab Notes: Carved diamond crucifix. *Gems & Gemology*, **45**(2), 135–136.

Fryer C., Ed., 1983. Gem Trade Lab Notes: Carved diamond. *Gems & Gemology*, **19**(1), 43.

Figure 20: The diamond carving started with a paper sketch (left) that was followed by a wooden prototype (centre) before the design was marked on the actual piece of diamond rough, which weighed 8.38 ct (right). Photos by Sameer Doshi.

SYNTHETICS AND SIMULANTS

Gastropod Shell Beads Disguised in a Coral Necklace

The GGTL Laboratories – Gemtechlab in Geneva recently received a coral necklace (e.g. Figure 21) for identification that weighed 100.55 g and consisted of eight round white freshwater cultured pearls and 107 'salmon'-coloured beads (3.3–10.2 mm in diameter). Microscopic examination showed that most of the coloured beads consisted of coral (i.e. *Corallium elatius*: Ridley, 1882). However, the beads present on either side of each freshwater cultured pearl had a distinctly different origin: they were cut from the shell of a gastropod (i.e. *Strombus gigas*:

Figure 21: A portion of a 'coral' necklace containing 'salmon'-coloured beads (3.3–10.2 mm in diameter) and white freshwater cultured pearls is shown here. The two beads adjacent to each cultured pearl in the necklace proved to have been cut from Strombus gigas *shell. Photo by E. Disner.*

Linnaeus, 1758). *Strombus gigas* is the host mollusc for conch pearls, and indeed pink and orange coral beads are occasionally mistaken for conch pearls (Farn, 1986, cited by Fritsch and Misiorowski, 1987).

The discrimination of *Strombus gigas* shell from coral is made by structural observations and may be aided by hydrostatic SG measurements. A diagnostic flame-like structure (Figure 22, left), is exhibited by non-nacreous pearls (and shell material, to a lesser extent) of various gastropods (*Strombus gigas*, *Voluta melo*, etc.). This pattern is caused by domains of stacked aragonite tablets in alternating orientations (Hänni, 2010). In the best specimens, the 'flames' can be seen by microscopic observation as thin lamellae that are almost parallel to one another and are sometimes perpendicular to the axis of pearl, thereby giving rise to a rough chatoyancy (Fritsch and Misiorowski, 1987). By contrast, polished coral beads display banded striations that are much more regular than the flame structures seen in conch pearls and shells. These parallel lines have a spacing of 0.25–0.5 mm, and in cross-section they appear as radiating shapes with very faint concentric lines joining them, in a pattern somewhat resembling a spider web (Figure 22, right), also called a 'tree-ring' structure (Campbell Pedersen, 2004).

Note that the characteristic flame-like and spider-web patterns are not always present or directly seen in these materials. If the flame structure is not visible in a conch pearl with the unaided eye, it is called porcelaneous (Fritsch and Misiorowski, 1987). Also, depending on the location of the drill hole, the spider-web pattern in coral may be invisible. Lack of the radial lines may indicate the presence of shell material. Striations should be easily visible in red coral, but may be harder to discern in lighter coloured coral; a complete lack of structure always raises suspicion (Campbell Pedersen, 2004).

SG measurements may also be effective for differentiating coral from shell material. The SG of 'precious' coral is between 2.6 and 2.7 (Webster, 1994) and is dependent on the porosity of the sample (Karampelas et al., 2009), whereas that of a pink conch pearl is around 2.85 (Webster, 1975). This SG value corresponds to a mixture of about 40% calcite (SG = 2.71) and 60% aragonite (SG = 2.95; Webster, 1975, cited by Fritsch and Misiorowski, 1987). It must be emphasized that

Figure 22: These photos show the flame-like structure in a Strombus gigas *pearl (left) and the typical spider-web structure in coral (right). Photomicrographs by F. Notari.*

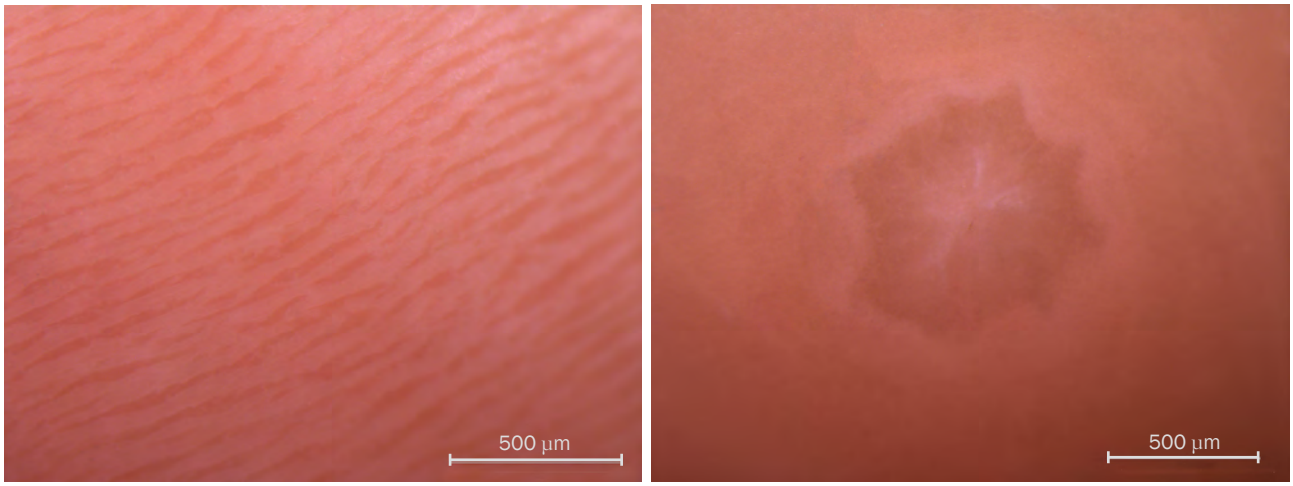

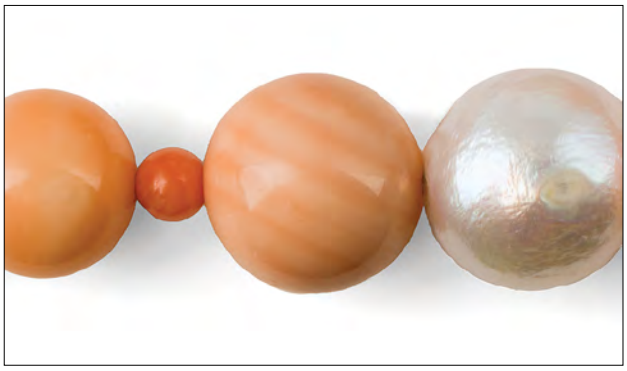

Figure 23: Within the 'coral' necklace, this bead cut from Strombus gigas *shell (10 mm in diameter) displays a layered structure. Photo by E. Disner.*

SG measurements should only be used as an indication, due to the approximate results given by the hydrostatic balance and because coral and conch pearl may have overlapping values.

In general, beads cut from shell material can be distinguished from non-nacreous pearls using only a microscope: Shell beads display a layered structure with an uneven distribution of the flame-like pattern, if any (e.g. Figure 23). This is in contrast to the uniform flame structure that is visible from all directions in those pearls that show this effect (Figure 22, left). In the authors' experience, the distribution of the flame pattern in shell beads is even more irregular than in pearls that have been reshaped.

As demonstrated by the necklace reported here, careful microscopic examination should be systematically done on every sample found within a piece of purportedly coral jewellery.

Emilie Disner (emilie.disner@ggtl-lab.org)
and Franck Notari
GGTL Laboratories – Gemtechlab
Geneva, Switzerland

References

Campbell Pedersen M., 2004. *Gem and Ornamental Materials of Organic Origin*. Butterworth-Heinemann, London, pp. 151, 211–212.

Farn A.E., 1986. *Pearls: Natural, Cultured and Imitation*. Butterworths, London.

Fritsch E. and Misiorowski E., 1987. The history and gemology of queen conch "pearls". *Gems & Gemology*, **23**(4), 208–221, http://dx.doi.org/10.5741/gems.23.4.208.

Hänni H.A., 2010. Explaining the flame structure of non-nacreous pearls. *Australian Gemmologist*, **24**(4), 85–88.

Karampelas S., Fritsch E., Rondeau B., Andouche A. and Métivier B., 2009. Identification of endangered pink-to-red *Stylaster* corals by Raman spectroscopy. *Gems & Gemology*, **45**(1), 48–52, http://dx.doi.org/10.5741/gems.45.1.48.

Webster R., 1975. *Gems: Their Sources, Descriptions and Identification*, 3rd edn. Archon Books, Hamden, Connecticut, USA.

Webster R., 1994. *Gems: Their Sources, Descriptions and Identification*, 5th edn., revised by P.G. Read. Butterworth-Heinemann, Oxford, 562.

TREATMENTS

A Barium-Glass-Filled Ruby

In June 2015, a 3.71 ct oval cabochon-cut ruby (Figure 24) was sent to the Liechtenstein branch of GGTL Laboratories for treatment analysis. Microscopic observation revealed rather obvious glassy residues within fissures, and also some noticeable filled cavities that showed gas bubbles mostly from the shrinking of the glass upon cooling (Figure 25).

To determine the nature of the filler—that is, to separate high-density glass from silica glass residues resulting from flux-assisted heating (typically involving a borax flux that is sometimes combined with quartz during heat treatment)—a high-definition three-dimensional radiograph was recorded, of which one position can be seen in Figure 26 (left). The radiograph showed that the density of the glass filling (white to very light grey portions) is considerably higher than the density of the host ruby. This made us suspect that lead glass was present, although the similarities of the fillings to glassy residues from flux-assisted heating raised suspicion that the stone may have been treated by a combination of these two techniques.

We then analysed the sample with the DFI fluorescence imaging and spectroscopy system,

Figure 24: This 3.71 ct ruby proved to contain fissures and cavities filled with barium glass. Photo by C. Nacht, GGTL Laboratories.

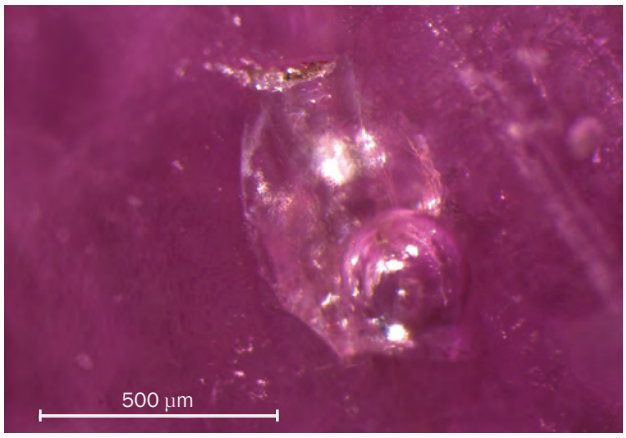

Figure 25: This filled surface-reaching cavity in the ruby contains a large round gas bubble. Photomicrograph by T. Hainschwang.

and all the fissures exhibited blue fluorescence under the deep-UV short-wave excitation (Figure 26, right). The typical reaction of lead glass to the short-wave UV generated by the DFI instrument is a dull and very chalky blue to 'olive' green luminescence that is much fainter than observed for this sample. Glassy residues from flux-assisted heating are generally inert to any type of UV excitation.

Infrared spectroscopy revealed a small 3309 cm^{-1} absorption that is generally a good indicator of heat treatment in ruby, plus a broad band centred at 2640 cm^{-1}. This broad absorption is typically observed in stones that contain significant quantities of glass filling, and is caused by the absorption spectrum of glass overlaying the corundum spectrum. While such a band is seen in most lead-glass-filled rubies, it only very rarely appears in the spectra of flux-assisted heat-treated stones.

To determine the chemical composition of the glass, the stone was analysed by EDXRF spectroscopy. The first spectrum (Figure 27, left) was recorded with an accelerating voltage of 24 kV, typical for the detection of chromophoric elements in corundum (i.e. *K*-lines of lighter elements and *L*-lines of heavier elements). Nothing obviously unusual was detected, only Cr, V, Ga, Fe and Ti appeared to be present, but no Pb or other heavy element; the only curiosities were unusually high Ti and somewhat enriched V. Therefore a second EDXRF analysis was performed with the X-ray tube set to 50 kV to specifically detect heavy elements. This revealed strong barium *K*-lines (Figure 27, right); since these lines are present at energies greater than 24 keV, Ba could not be easily detected with the X-ray tube set at 24 kV. Although the *L*-lines of Ba can be detected at 24 kV, they coincide almost

Figure 26: The light-coloured areas in the radiograph on the left show that the glass-filled fissures and cavities contain far heavier elements than the host ruby. When exposed to the deep-UV short-wave excitation of the DFI fluorescence microscopy and imaging system (right), the glass in the 3.71 ct ruby fluoresces a distinct blue. Images by T. Hainschwang.

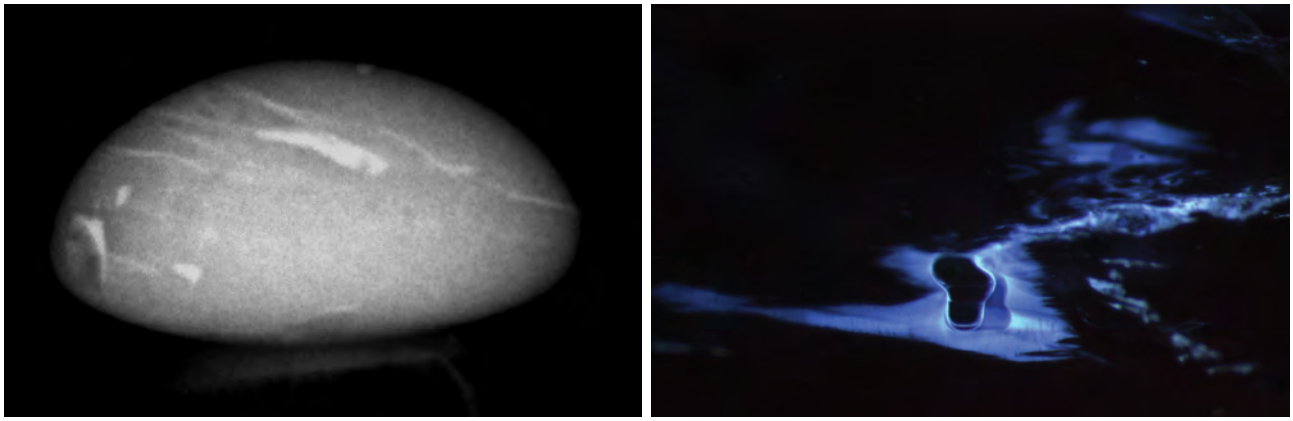

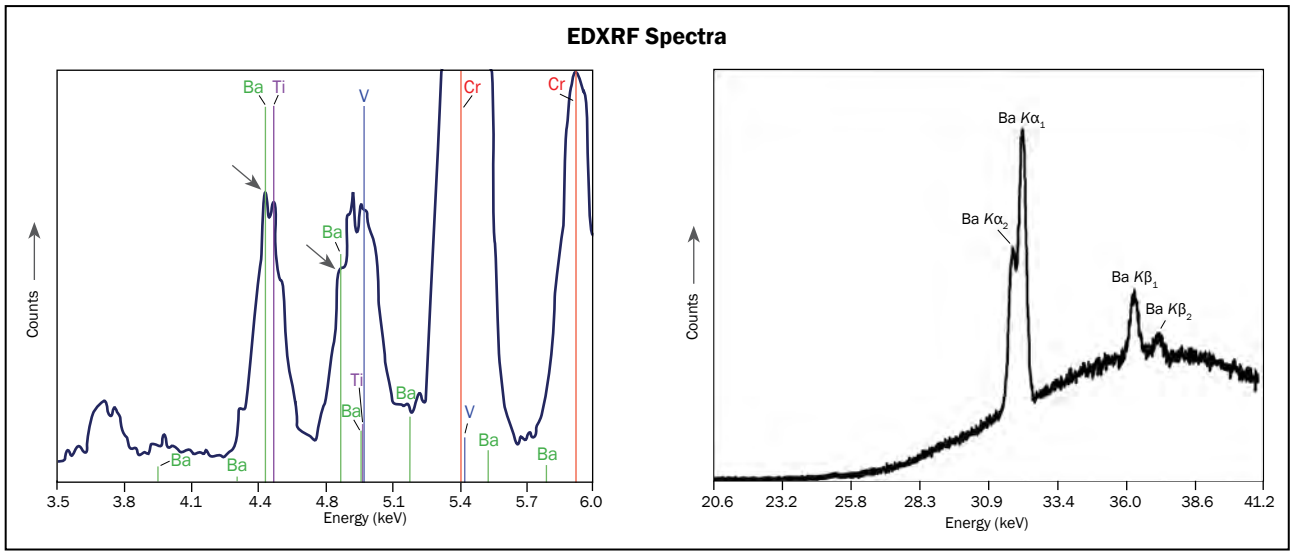

Figure 27: EDXRF spectra of the filled ruby are shown using a voltage of 24 kV (with an Al filter), a setting typically used to see the chromophoric elements in corundum (left), and at 50 kV (with a Pd filter), a setting that revealed the presence of Ba (right). The Ba peaks are difficult to distinguish at the lower energy setting; they are suggested only by an increase in the intensity of the Ti Kα-line by the Ba Lα-line, and a widening of the V Kα-line by the Ba Lβ-line. The Ba Lλ- and Lγ-lines, as well as the small Ba Lα-line, do not substantially modify the spectral appearance at the lower-energy setting of the instrument. Note that in rubies lacking V, the Ba Lβ-line should be detectable and could not be confused with the V Kα-line.

exactly with the Ti and V lines (Figure 27, left). This explains the apparently elevated Ti and V that were shown by the first analysis.

This is the first ruby we have seen in our laboratories that has been filled with a high-refractive-index barium glass. Depending on the Ba content, such glass can have a refractive index above 1.7 (the RI of the glass in this sample could not be determined since the cavities were not large enough to measure it). To identify barium glass with EDXRF spectroscopy, caution is required since Ba may not be detected using standard analytical conditions for lead glass; a higher-energy setting is necessary to properly identify Ba.

According to the client, this stone had been in stock for more than 10 years, which may indicate that it was possibly an experimental treatment product before the more efficient fissure filling procedure was developed using lead glass, starting in 2004.

Dr Thomas Hainschwang (thomas.hainschwang@ggtl-lab.org) and Franck Notari
GGTL Laboratories, Balzers, Liechtenstein, and Geneva, Switzerland

Diffusion-induced Blue Colour and Asterism in Sapphire

In April 2015, a client submitted a bright blue star sapphire weighing 13.69 ct and measuring 13.85 × 11.89 × 10.28 mm (Figure 28). The crown was polished into a typical domed cabochon, while the pavilion was faceted so that it reflected light like a faceted stone. This cutting arrangement is only rarely seen in natural star sapphires. The six-rayed star had straight 'arms' that were sharp and bright under a point light source, and the stone exhibited a double star when photographed from an angle.

The crown gave a spot RI reading of 1.76, and the faceted pavilion yielded RIs of 1.760–1.770 (birefringence 0.010). The gem was inert to UV radiation. Viewed with magnification, the stone had small 'fingerprint' inclusions (e.g. Figure 29) that indicated a natural (not synthetic) origin. However, there were no prismatic needle-like inclusions that are typically associated with asterism in sapphire. Instead, at higher magnification (20×–30×), the asterism was seen to be caused by wispy 'silk'

Figure 28: Both the asterism and blue colour of this 13.69 ct sapphire are the result of diffusion treatment. Photo by Tay Thye Sun.

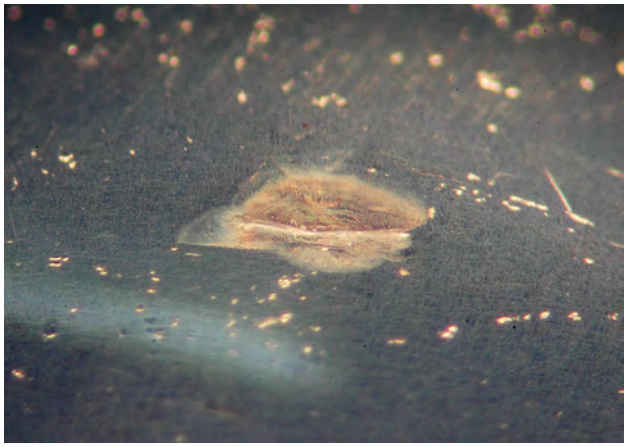

Figure 29: This 'fingerprint' inclusion found under the dome of the star sapphire displays subtle interference colours. Note the hazy appearance of the stone's surface and minute pits that resulted from the diffusion process. Photo by Tay Thye Sun; magnified 35×.

or fine fur-like inclusions that were present just under the surface (Figure 30). Such inclusions have been ascribed to diffusion treatment in synthetic star sapphires (e.g. 'AIGS finds more stars', 1994; Kammerling and Fritsch, 1995; Singbamroong et al., 2015). When the stone was immersed in eucalyptus oil and viewed with diffused lighting, the pavilion showed inconsistent coloration between various facets and colour concentrations along facet junctions (Figure 31), proving that the gem was repolished after diffusion treatment (e.g. Kane et al., 1990).

We concluded that this was a natural sapphire that had been diffused-treated to induce its colour and asterism. Although some previously documented diffusion-induced star sapphires were synthetic in origin ('AIGS finds more stars', 1994; Kammerling and Fritsch, 1995; Singbamroong et al., 2015), gemmologists should remember that natural as well as synthetic starting materials may be used for this type of treatment.

Acknowledgement: The authors thank Mr Yu Xiong for bringing this sapphire to their attention.

Tay Thye Sun (tay@gem.com.sg)
and Loke Hui Ying
Far East Gemological Laboratory, Singapore

References

AIGS finds more stars, 1994. *Jewellery News Asia*, June, **118**, 74.

Kammerling R.C. and Fritsch E., 1995. Gem Trade Lab Notes: Synthetic star sapphire with an unusual color. *Gems & Gemology*, **31**(1), 57–58.

Figure 30: Wispy 'silk' is responsible for the asterism in the sapphire. Photomicrograph by Tay Thye Sun; magnified 30×.

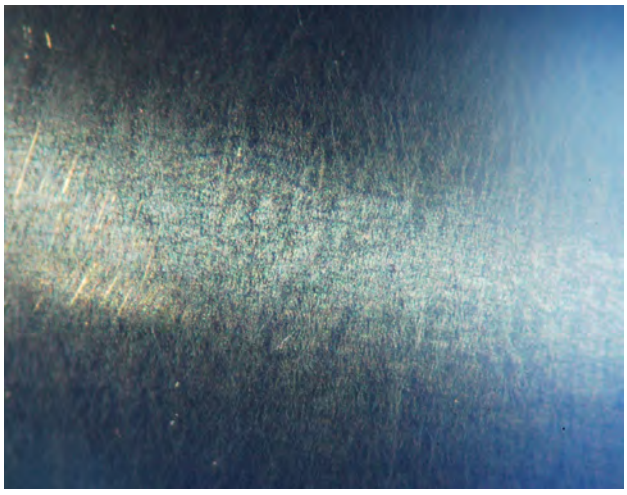

Figure 31: Inconsistent coloration between various facets and colour concentrations along facet junctions of the pavilion prove that the sapphire underwent diffusion treatment and was then repolished. Photo by Tay Thye Sun; magnified 20×.

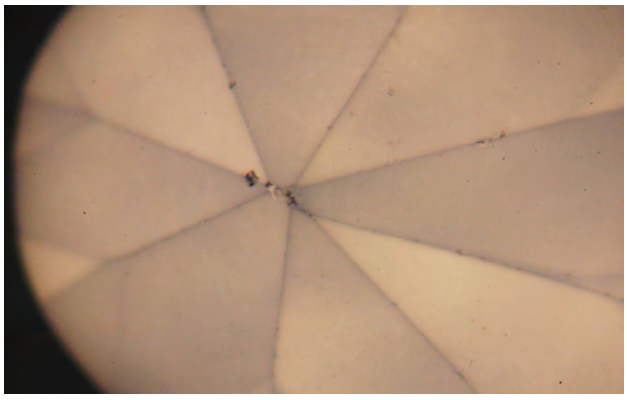

Kane R.E., Kammerling R.C., Koivula J.I., Shigley J.E. and Fritsch E., 1990. The identification of blue diffusion-treated sapphires. *Gems & Gemology*, **26**(2), 115–133, http://dx.doi.org/10.5741/gems.26.2.115.

Singbamroong S., Ahmed N. and Al Muhairi N., 2015. Gem News International: Synthetic sapphire with diffusion-induced color and star. *Gems & Gemology*, **51**(2), 203–205.

MISCELLANEOUS

Highlights of the 52nd Gems Emporium in Myanmar

The 52nd Gems Emporium took place in Naypyitaw, Myanmar, on 24 June–6 July 2015. There were 8,943 jadeite lots offered, and 5,843 of them were sold for €938.58 million. Of the 316 gem lots offered, 126 were sold for €5.59 million. The best-quality rubies were supplied by Ruby Dragon Co., and consisted of two rough pieces weighing a total of 79 ct that sold for €801,000. There were 18 lots of rough ruby from Mong Hsu that sold at relatively low prices due to their quality. The highest-quality rough sapphires came from Bawma Mining Co., and consisted of 98 pieces weighing 138 ct that sold for €200,999. In addition, Bawma Mining Co. supplied four lots of cut sapphires, all of which were sold.

Various non-jade materials also were popular, with 18 lots sold. A 6.0 kg piece of green fluorite sold for €23,800 (e.g. Figure 32). Yellow-to-orange quartzite was offered as cabochons (220 pieces weighing 1.5 kg that sold for €1,917; Figure 33, left), and also as discs left over from cutting bangles (not sold; Figure 33, right).

Figure 32: This 6.0 kg piece of green fluorite sold for €23,800 at the 52nd Gems Emporium. Photo by Kaung Naing.

U Tin Hlaing (p.tinhlaing@gmail.com)
Dept. of Geology (retired)
Panglong University, Myanmar

Figure 33: Yellow-to-orange quartzite was offered at the 52nd Gems Emporium as cabochons (left side, 1.5 kg), and as discs that remained from cutting bangles (right). Photos by Kaung Naing.

The Fire Within

"For in them you shall see the living fire of the ruby, the glorious purple of the amethyst, the sea-green of the emerald, all glittering together in an incredible mixture of light."

– Roman Elder Pliny, 1st Century AD

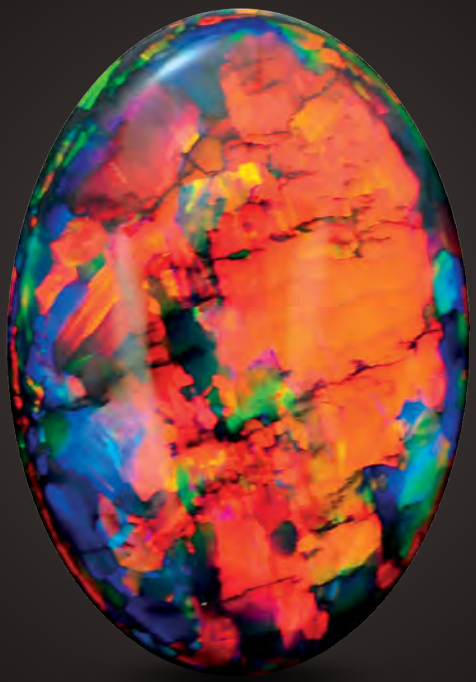

Black Opal 15.7 Carats

Suppliers of Australia's finest opals to the world's gem trade.

CODY OPAL

Level 1 - 119 Swanston Street Melbourne Australia

T. +61 3 9654 5533 E. INFO@CODYOPAL.COM

WWW.CODYOPAL.COM

INTERNATIONAL COLORED GEMSTONE ASSOCIATION MEMBER

JOG

European Freshwater Pearls: Part 1—Russia

Elisabeth Strack

Freshwater pearls from *Margaritifera margaritifera* (L., 1758), also called the 'European pearl mussel', are part of European cultural history. The mussels live in cool, clean, oxygenated waters, and formerly ranged from the north-western Iberian Peninsula to north-western Russia. During the last century, populations have largely diminished due to environmental influences, and the species is listed as endangered in the International Union for the Conservation of Nature (IUCN) Red List; harvesting them for pearls is prohibited. In north-western Russia, particularly from the 18th and 19th centuries until 1917, the pearls were commonly incorporated into embroideries, traditional headdresses, jewellery and various objects of religious significance. Interest in pearls waned after the Russian Revolution, and interviews conducted during the 2000s with people in former pearling centres showed an almost complete lack of awareness of pearls.

The Journal of Gemmology, 34(7), 2015, pp. 580–592, http://dx.doi.org/10.15506/JoG.2015.34.7.580

Introduction

The freshwater mussel *Margaritifera margaritifera* (L., 1758) has been reported as a source of pearls since antiquity, and eventually became known as the 'European pearl mussel' in popular language. Significant pearl production has occurred in only a few countries, such as parts of Germany (especially Bavaria and Saxony) and Great Britain (especially Scotland). The mussel's population levels have fallen by more than 90% (with few exceptions) during the last century, mainly due to environmental reasons. The species has been listed on the IUCN Red List as endangered since 1996 (www.iucnredlist.org/details/12799/0).

Over the centuries, freshwater pearls from *Margaritifera margaritifera* became part of European cultural history, and this article is the first part of a series that will cover their past and present importance. The focus of this article is Russia, where freshwater pearls were used abundantly for both secular and ecclesiastical purposes, particularly from the 18th and 19th centuries up to the 1917 Revolution. Some secular examples include embroidered dresses, traditional headdresses for women called *kokoshniks* (e.g. Figure 1) and jewellery (e.g. Figure 2). However, visits by the author to north-western Russia in 2001, 2006 and 2008 have shown that local knowledge about pearls has nearly disappeared, and only a few such items were seen at museums in the former pearling centres of Kem in Karelia and Umba on the Kola Peninsula.

The purpose of this article is to describe the history, taxonomy and biology of the *Margaritifera margaritifera* mussel, and then to trace the origins of Russian freshwater pearls, followed by a brief

Figure 1: Russian freshwater pearls (2–4 mm in diameter) are featured in this late-19th-century kokoshnik *(traditional headdress). Courtesy of The Russian Museum of Ethnography, St Petersburg. Photo by E. Strack.*

characterization of their properties. Much of the information in this article is based on what the author observed and was told during her visits to Russia. In addition, general information was taken from Strack (2006).

Historical Context

The pearl mussel was first described by Carl von Linné (or Carolus Linnaeus) as *Mya margaritifera* in the 10th edition of his *Systema Naturae* in 1758. He most probably took the word *Mya* from Pliny the Elder (Gaius Plinius Secundus, AD 24–79), who used it in his *Historia Naturalis* for a small freshwater mussel. In 1816, the Danish scientist Heinrich Christian Friedrich Schumacher recognized the genus *Margaritifera*, which he named *Margaritana* in 1817. In the course of the 19th or early 20th century, the name was changed back to *Margaritifera*; the exact date and reason for this are unknown. *Margaritifera*, taken from *margarita*, the Latin word of Greek origin for *pearl*, indicates 'the pearl-bearing one'.

Pearls from *Margaritifera margaritifera* had been known and worked into jewellery long before von Linné described the mussel in 1758. One of the oldest written testimonies to European pearls is from Gaius Suetonius Tranquillus (AD 75–150), when he refers, in his history of Roman emperors, to the pearls that had made "the divine Julius undertake his conquest of Britain". Before him, both Pliny the Elder and Cornelius Tacitus (AD 55 and AD 116/120) had expressed their disappointment with the lack of beauty shown by British freshwater pearls (Strack, 2006).

From the Middle Ages until about 100–150 years ago, the European freshwater pearl undoubtedly was important as a valuable decorative object. Fine-quality individual pearls or necklaces were extremely rare, and most of them probably were sold into the natural pearl market as being from classical localities such as the Persian Gulf. The majority of European freshwater pearls were used for the decoration of objects of both secular and ecclesiastical use. Some of these items are kept today in churches, monasteries and museums where they serve as a unique witness to the existence of pearls in European cultural history.

Figure 2: These earrings containing Russian freshwater pearls (5–6 mm in diameter) are dated to the late 19th century. Courtesy of The Russian Museum of Ethnography, St Petersburg. Photo by E. Strack.

Freshwater Pearl Mussels

Taxonomy

Freshwater mussels occur worldwide and, along with marine bivalve molluscs, belong to the class Bivalvia. They have two shells, or valves, that are connected by a hinge and a ligament. Their inner soft body has a slightly different, more delicate organization than marine molluscs, and the reproductive cycle of some species is distinctly more complicated (see below).

Pearl production occurs from those mussels within the suborder Schizodonta belonging to the superfamily Unionoidea. Such mussels have been called *najades* in scientific colloquial language. This name dates back to the 18th century, and alludes to the nymphs in Greek mythology that protected rivers and lakes. The superfamily Unionoidea is divided into two families, Unionidae and Margaritiferidae. Both families probably originated from a common freshwater lineage that developed from marine molluscs migrating into freshwater during the Mesozoic Era (Strack, 2006).

The Unionidae family has ~140 genera with more than 1,000 species that occur worldwide. Significant pearl production from Unionidae mussels is known from the eastern half of the United States, specifically the Mississippi River and its tributaries where huge quantities of pearls were fished during the so-called pearl rush in the second half of the 19th and early 20th centuries. Pearl production concentrated on 50–60 species.

The occurrence of the Margaritiferidae family is confined to the northern hemisphere, situated between approximately 40° and 70° north latitude, with the Arctic Circle representing the northern boundary. The Margaritiferidae family was classified in 1929, and until that year the genus *Margaritifera* was seen as belonging to the Unionidae family. Also, some old texts still attribute it to the 'Najade' family. Today's taxonomic classification of the genus is not clearly structured and shows overlaps; it is not described in further detail here. Pearls that were to become known on the world market as 'European freshwater pearls' come from only one species, *Margaritifera margaritifera*. This is considered the youngest species, probably originating about 8 million years ago during the Late Miocene Epoch (Strack, 2006).

Figure 3: Each of these three Margaritifera margaritifera *mussels measures ~8.5 cm long. They typically bury about half of their shell into the ground, while the other half protrudes into the water and is positioned at an oblique angle toward the current. The mussels are usually found growing close to one another with their shells pointing in the same direction. Courtesy of R. Altmüller; photo by E. Strack.*

Biology

Margaritifera margaritifera (e.g. Figure 3) is native to an area comprising parts of the Iberian Peninsula (Portugal and Spain); southern, central and eastern France; Belgium; Luxembourg; northern and central Germany; and eastern Austria and the Czech Republic. It stretches in the north-west to Great Britain and in the north and north-east to Scandinavia and north-western Russia (Figure 4; see also Reis, 2003; Strack, 2006).

Margaritiferidae have the highest life expectancy of all known invertebrates, and may live up to 200+ years (R. Altmüller, pers. comm., 2007). This extraordinary life span is due to the extremely low metabolism that goes hand-in-hand with a slow growth rate of 1.0–1.5 mm per year, dependent on water temperature.

The pearl mussel needs clean, summer-cool waters with temperatures between 4° and 23°C with high oxygen and low nutrient and Ca contents. As the Ca content should not exceed 0.0045–0.0153 grams per litre, the species is regarded as a so-called calcium hater (Strack, 2006). This seems contradictory, since the mussel needs Ca to grow its relatively thick shells. It

apparently compensates for the low amount of available Ca with its slow growth rate.

The pearl mussel prefers a substrate of coarse sand or pebbles consisting of quartz, granite or gneiss. It responds to muddy or fine-grained sandy substrates by becoming smaller and thinner. It generally avoids both stagnant waters and strong currents, and prefers streams but also inhabits rivers and occasionally lakes (Strack, 2006). Mountainous sites are preferred and lowlands are the exception. The ideal water depth is 0.5–2 m, but up to 8 m has been recorded (Strack, 2006).

The shells are made up of two symmetric, oval-shaped convex halves (Figure 3). They can attain a maximum size of ~16 × 6 × 6 cm, while the average length is 10 cm (Strack, 2006). Various localities may show slight morphological differences with regard to shape, size and thickness of the shells.

Margaritifera margaritifera is unique compared to freshwater mussels from the Unionidae family, which have far less demanding life cycles and shorter life expectancies. In particular, this mussel requires for its parasitic glochidial (larval) stage a host fish that is exclusively of the genus *Salmo*; in central Europe the salmonid is the brown trout (*Salmo trutta fario*) and in western and northern Europe it is the Atlantic salmon (*Salmo salar*). The reliance on salmonids goes back to the earliest stages of the pearl mussel's development, when these fish carried the mussel larvae from the Mediterranean area to northern Europe (Strack, 2006).

Margaritifera margaritifera reaches sexual maturity at 15 years and remains fertile for the next 50–70 years. The breeding season starts in early summer, when female mussels transport their eggs from the gonads to special breeding chambers within their gills called marsupia. Fertilization takes place within the marsupia after male mussels from further upstream have released their sperm into the water. Tiny glochidia (larvae) form within four to six weeks. They are kept in the marsupia until July–August when water temperatures rise, and then are released into the water. Each female mussel can hold about 4 million larvae during one breeding season, and can produce about 200 million glochidia during her long active life. Although this is considered one of the highest fertility rates, survival is difficult, and of one million glochidia only about five survive (Strack, 2006).

The glochidia are only 0.07 mm when they are released into the water, but their bivalve shell is already fully developed. It has a hook on the shell rim and a larval thread, which enables several of them to connect into small balls and attach themselves into the gills of a host fish using their strong contractor muscles. New juvenile host fish are required each season, as the fish become immune once they have carried the glochidia. The host fish reacts to the glochidia by secreting a cover around them, and for the next six months the enclosed larvae transform into juvenile mussels. (The relationship between glochidia and host fish can be seen as a type of non-simultaneous symbiosis, in which the host fishes will later benefit from the filtering capacity of adult mussels in keeping the water clean.) In early summer of the following year, the mussels break through the cover secreted by the host fish and fall to the ground. At this time they measure 0.5 mm long and will dig themselves into the substrate where they will spend the next five years. Having attained a size of 1 cm, those that survive this period (about 5%) return above ground where they will spend the rest of their lives (Strack, 2006).

Transportation of glochidia by a host fish enables them to reach the upper regions of a river or stream, and an even wider distribution may occur if birds or other animals feed on the host fish. The complicated growth history of the larvae may also be designed to prevent them from moving downriver and eventually reaching the sea (as saltwater is toxic to freshwater mussels). It is only during the past 50 years that *Margaritifera margaritifera*'s life cycle has been fully understood, thus enabling an appreciation of the mortality factors that are faced by juvenile and adult mussels.

Russian Freshwater Pearls

Pearl Mussel Distribution

Originally, *Margaritifera margaritifera* occurred in a wide area of north-western Russia that stretched from Lithuania in the west to the slopes of the Ural Mountains in the east, and from the tributaries of the Don and Volga Rivers in the south to the White Sea in the north. The mussels formerly were especially abundant in rivers and streams flowing into the White Sea, where the Atlantic salmon served as a host fish (Korago,

Figure 4: The former range of Margaritifera margaritifera *mussels (shown in yellow) extended from the Iberian Peninsula in south-eastern Europe to Finland and north-western Russia. The outlined area refers to the view shown in Figure 5. Modified from http://maps.iucnredlist.org/map.html?id=12799.*

1981; Kaliuzhin, 2004). Today, large Russian populations of *Margaritifera margaritifera* remain only in the Keret River in Karelia and the Varzuga River on the Kola Peninsula (~6 and ~140 million mussels, respectively; see Figure 5; S. P. Kitaev, pers. comm., 2001; Makhrov et al., 2014; Popov and Ostrovsky, 2014). The Varzuga River hosts the largest uninterrupted population in Europe, with mussels living along an approximately 220 km stretch of river within an undisturbed, post-glacial ecosystem that provides adequate nourishment and space for breeding and survival (Ziuganov, 1994; Strack, 2006). Significant stocks have largely disappeared from most other rivers.

Pearl mussels also occurred in various rivers that spilled into Lake Ladoga and Lake Onega (particularly the terminus of the Kumsa, Oster and Vodla Rivers; see Ivanter and Kuznetsov, 1995; S. P. Kitaev, pers. comm., 2001).

In some areas, pearls were also produced from *Anodonta*, the common pond mussel belonging to the Unionidae family. They seem to have come particularly regularly from a lake near the city of Werh-Newinsk, 100 km north of Yekaterinburg in the Ural Mountains (Strack, 2006, p. 206).

Pearl Usage

The use of freshwater pearls for decoration and adornment in north-western Russia goes back to the Middle Ages. Pearls became more generally used towards the end of the 18th century. One might even say that they came into fashion during that time, and this lasted until the end of the Russian empire under the Romanoff dynasty in 1917 (Korago, 1981). Traditional festive linen or silk dresses were embroidered with pearls, which also were used to embellish kokoshniks, the tiara-like headdresses worn in traditional costume

Figure 5: The map shows the main rivers and former pearling centres in Karelia and on the Kola Peninsula in north-western Russia. After Strack (2006).

(Figure 6). Kokoshniks were not only embroidered with pearls, but were decorated in the forehead area with pearl strings in net-like, interwoven and tasselled patterns. Earrings were often made of fine pearl strings that were similarly arranged in a garland or flower pattern (e.g. Figure 2).

Pearling centres developed along the Dvina River and its tributaries near the city of Arkhangelsk, on the Keret and Kem Rivers in Karelia and on the Kola Peninsula (particularly near the Umba and Varzuga Rivers; Figure 5). Apart from the villages, where talented local women did the craftwork, professional workshops for pearl embroideries also opened up in some cities. The city of Kem, founded in 1783 and situated on the White Sea at the mouth of the Kem River, was particularly important, and the string of pearls that is shown on the city's coat of arms (Figure 7) bears witness to this. Another Karelian centre for working with pearls was the small city of Olonez, capital of a governorate with the same name, situated near Lake Ladoga. Olonez was an important and wealthy city in the past, but has fallen into obscurity since then and therefore was not included in the field research described below.

Figure 6: A pearl-bearing kokoshnik is worn by Princess Olga Konstantinovna Orlova as part of a masquerade costume for a ball in 1903. The original photograph measures 50.5 × 36.5 cm and was taken by Elena Mrozovskaya.

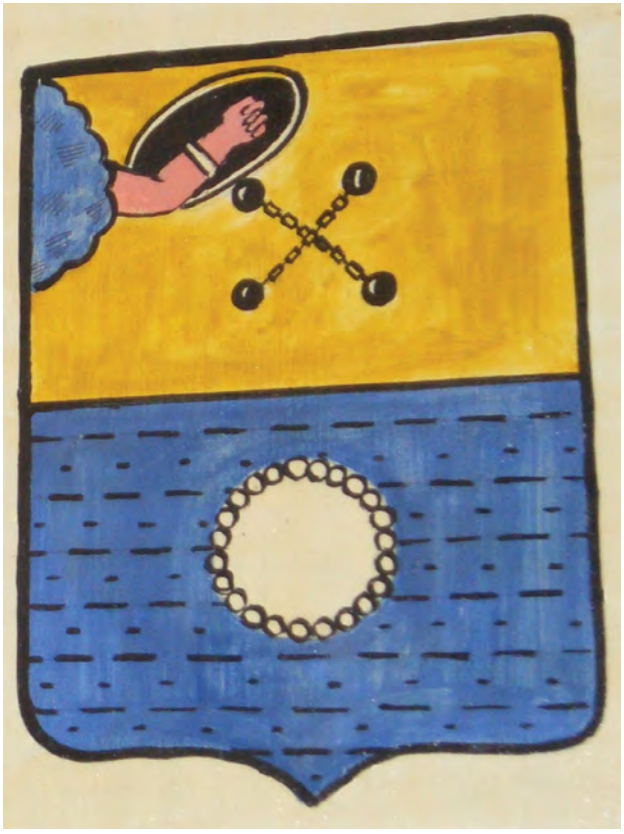

Figure 7: The coat of arms of the city of Kem, a 18th–19th century pearling centre at the mouth of the Kem River on the White Sea, includes a string of pearls in the form of a round necklace. The upper part depicts an arm emerging from a cloud that holds a shield which, together with the cannon balls underneath, alludes to the importance of Kem as a military base in the border region of the Olonez governorate. Courtesy of the Museum of the Coast, Kem, Russia; Photo by E. Strack.

In rural areas, the mussel shells themselves also were worked into buttons or other objects, and a number of small workshops existed along some of the northern rivers until the early Soviet era.

The Russian Museum of Ethnography in St Petersburg houses one of the most exquisite collections of Russian pearl works. The museum not only displays good examples of the quality and status of preservation of pearl-bearing objects prior to the Russian Revolution in 1917, but it also provides an image of traditional village life that has disappeared in modern times. Additional pearl holdings are present in the Armoury Chamber of the Kremlin in Moscow, which focuses on ecclesiastical treasures. The Russian Orthodox Church secured a considerable portion of the pearl riches in north-Russian rivers where it often held fishing rights. Chasubles for priests and antependia (altar-front decorations) were embroidered with pearls since the 10th century, and pearls also were used for devotional works such as chalices, book covers, crosses (so-called *panagia*), mitres and icons. The goldsmiths and silversmiths who created these objects often made lavish use of both pearls and floral designs.

Since 1721, by a decree of Peter the Great, all pearl rights belonged to the czar. This was revised in 1731, although large pearls still had to go to the imperial crown. It is questionable whether this rule was strictly followed by people in the villages. During the 18th and 19th centuries, young lads and women in villages that did laundry in the streams often searched for pearls, mainly using their toes to look for the mussels.

The first two decades of the Soviet era (1922–1991) saw a continuous decline in both the populations of pearl mussels (mostly as a result of pollution by various industries) and pearl production. Even more significant was an increasing lack of interest in pearls that went hand-in-hand with the establishment of the new political system. By this time, those who had used and appreciated pearls in the past—such as the local nobility, well-to-do citizens or the *kulaks* (wealthy village families)—no longer existed. In the aftermath of the revolution, they had left the country, been killed or gone into hiding by integrating themselves into early Soviet society. Also, when religious practices were forbidden after the Russian Revolution, devotional objects that used pearls were no longer produced.

Almost certainly, pearls continued to be found during the first decades after the Russian Revolution, but they are difficult or impossible to trace today. Interest in pearls decreased further in the decades after World War II. In 1966, the Soviet Ministry of Fisheries forbade the harvesting of pearl mussels in a number of rivers, and in 1985 it was completely prohibited (Makhrov et al., 2014). In 1995, *Margaritifera margaritifera* was listed as endangered in the *Red Data Book of Karelia* (Ivanter and Kuznetsov, 1995). In addition, all species of *Margaritifera* are listed as endangered in the *Red Data Book of the Russian Federation* (S. P. Kitaev, pers. comm., 2001).

Today Russian pearls are no longer significant within the country or on the world market, and since they are no longer harvested, they have practically been forgotten.

Field Research

To obtain updated information on Russian freshwater pearls, the author travelled to Karelia and the Kola Peninsula in 2001, 2006 and 2008. Visits were made to the towns of Umba, Kuzomen and Varzuga on the White Sea coast of the Kola Peninsula; the village of Keret and the city of Kem in Karelia; as well as the cities of Arkhangelsk on the coast of the White Sea and Petrozavodsk, the capital of Karelia, situated at Lake Onega. Interviews were conducted with local authorities, scientists and village citizens (approximately 13 people in total). The citizen interviews concentrated on elderly people (between 70 and 80 years old) who had grown up in the 1930s and 1940s. None of those interviewed remembered ever seeing pearls or having searched for them (or knew people who did). All persons agreed that pearls were never spoken about, although there seemed to be some vague collective knowledge among the elderly people interviewed that pearls had been found locally in the past. Not one family in the villages was known to possess local pearls. A retired fisheries inspector in Keret village reported that in 1974 an expedition from Moscow found 415 pearls in the area, but he could not give details, as at the time he was not allowed to ask questions.

Government authorities at the Fisheries Office in Umba and at the Fisheries Cooperative in Varzuga were well informed of the importance of the pearl mussel's symbiosis with local salmon populations (see also Kaliuzhin, 2004). However, all those interviewed agreed that pearls were an item of the past (and they did not seem interested in following up on the matter). Albeit, the head of the salmon cooperative in Varzuga was aware that a considerable number of pearls probably exists among the ~140 million pearl mussels that are thought to inhabit the Varzuga River. It is estimated that about four or five pearls can be harvested from every 1,000 mussels (V. Ziuganov, pers. comm., 1999; Strack, 2006).

Varzuga village, situated about 30 km inland from the mouth of Varzuga River, is an important religious centre for the White Sea coast. A monastery was established there in the second half of the 15th century by monks from the Solovetsky Islands. The monastery no longer exists, but Varzuga still has the oldest wooden church on the Kola Peninsula (built in 1674) and remains a place of religious pilgrimage. The local priest, Mitrofan Badanin, who has been Bishop of the Severomorsk and Umba regions of the Kola Peninsula since 2013, was a highly respected authority in Varzuga. A former high-ranking navy officer and a learned man, he stated that all old treasures and written records on the southern coast of the Kola Peninsula disappeared during the Soviet era when the churches were partially destroyed or used for other purposes. Only a few icons remain in the churches today, and these were made in recent times and decorated with inexpensive Chinese freshwater cultured pearls that seem to find their way to even the remotest corners of the world. Unfortunately, these recent icons have no artistic value.

Varzuga has no museum that traces the area's history, but due to its position as a centre for salmon fishing it is a busy village. Some families rent houses to the few visitors, mainly Russian scientists on summer excursions and a few Scandinavian tourists who come for the fishing. The author was told by her hosts in Varzuga that so far no foreigners have asked questions about pearls or pearl mussels.

Kuzomen village, situated at the mouth of Varzuga River on the White Sea, was once also a local salmon fishing centre (and consequently a source of pearls). The village is now nearly deserted, and is characterized by extreme poverty and desolation. It is connected with Umba by a bus that travels only once a week. An elderly lady, one of the perhaps 100 people still living in Kuzomen and a retired school teacher, indicated that there was no longer any knowledge of pearls in the village. The same opinion was encountered in Keret village, where the few elderly people still living there in partly broken-down houses hardly knew that pearls came from the area in the past. One of the better-kept wooden houses in Keret village belonged to the local fisheries inspector. He was in charge of a government programme for sustaining and restoring mussel populations in the Keret River, which was undertaken for environmental reasons and to secure the salmon population. Timber floating, hydro-engineering construction and industrial pollution have over the decades taken a toll on the salmon population, and thus of the pearl mussel's host fish (Makhrov et al., 2014). The restoration programme has so-far been successful, as the river still hosts about 6 million pearl mussels. Pearls do not seem to be on the governmental agenda.

Figure 8: This late-19th-century kokoshnik is embroidered with small imitation pearls (which also form the tassels) together with larger Russian freshwater pearls. The natural pearls range up to 7 mm, have off-round shapes and are strikingly white. Courtesy of the Museum of History, Culture and Life of Tersky Pomors, Umba, Russia; photo by E. Strack.

The busy town of Umba is situated in the western Tersky coast (i.e. the southern coast of Kola Peninsula) and is connected to Kirov-Apatity by a well-maintained system of roads. The city was once a pearling centre for the Umba River and continues to be a base for salmon fishing. The local fisheries office houses breeding facilities for both pearl mussels and salmon. The most extensive collection of artefacts and objects relating to Russian pearl fishing is found in Umba's Museum of History, Culture and Life of Tersky Pomors. On display are photographs of local pearl fishermen, as well as samples of the equipment (e.g. knives and collecting bags) that they used. Photographs include local village women in their festive dresses, and the museum also owns one kokoshnik that is abundantly decorated with pearls (Figure 8). They were incorporated into the flat top of the kokoshnik, as well as in the ear flaps and within tassel-like rows overhanging the forehead; these features are characteristic of kokoshniks from the Olonez area (Srebrodolski, 1985; Bespalaya et al., 2012).

A similar kokoshnik is owned by the Museum of the Coast in Kem. In addition, the collection includes village costumes and paintings/photographs that show wealthy village women wearing pearl-embroidered kokoshniks and pearl necklaces.

Materials and Methods

Due to the historical and present situation in Russia described above, only a few pearl-bearing items could be located that were available for characterization.

During the author's visit to the museum in Umba, the museum's director kindly allowed the kokoshnik (Figure 8) to be removed from its glass case for closer examination with a loupe and UV lamp equipped with long-wave (366 nm) and short-wave (254 nm) bulbs.

In June 1998, the author had the opportunity to examine a number of pearl objects at The Russian Museum of Ethnography in St Petersburg: several pairs of earrings from around 1800 (e.g. Figure 2), a kokoshnik (Figure 1) and a red velvet belt from the 19th century, and various necklaces from the late 19th century. These pieces were examined with an optical microscope (up to 80× magnification) and the UV lamp mentioned above.

Also in 2008, the author examined a necklace that was taken out of Russia by a Russian family in the 1920s (Figure 9). The pearls may have been harvested in the years before World War I or in

Figure 9: This necklace of Russian freshwater pearls has been owned by a family of Russian origin since the 1920s. The pearls range from 5.0 × 4.5 mm to 8.2 × 7.0 mm and have baroque shapes, are white to light grey and light to dark 'cream', and show distinct growth characteristics. The clasp is a modern addition. Photo by E. Strack.

the 19th century. The necklace was available for a limited amount of time, and only visual observation was possible.

Three additional pearls (Figures 10–12), harvested in the 1990s, were examined in 1999. They were made available by Russian fisheries biologist Valeriy Ziuganov, who obtained them during his studies of the Varzuga River. The pearls were examined using a gemmological microscope and the UV lamp mentioned above, and radiographs were taken with a Kodak 2200 digital X-ray system (60–70 kV, 49 W).

Results

Pearls from the 18th and 19th Centuries

Kokoshnik from the Umba Museum: Examination with a loupe and a UV lamp revealed that the small 'pearls' in this kokoshnik were imitations, and only the larger ones (up to 7 mm) were natural freshwater pearls, present both individually and arranged into rosettes.

Samples from The Russian Museum of Ethnography: The earrings consisted of small pearl strings that were arranged to form drops and rosettes. The kokoshnik and the red velvet belt were decorated with strings of pearls in tulip and rose patterns. The necklaces consisted of multiple strings; the most notable were a four-strand necklace originally attached to a kokoshnik and worn under the chin, and a necklace consisting of 14 rows that were about 40 cm long.

The pearls in these objects averaged 1–4 mm, while the largest measured 7 mm and 9 mm and were present at the centre of the necklaces. Their colours ranged from white and light 'cream' to light grey. A few pearls were greyish brown, brownish orange and brownish purple. Several showed a distinct dividing line in the centre that separated white and brownish grey halves. There were no overtones observed. Lustre was generally dull, with the darker colours showing no lustre at all. Shapes included off-round, flat, barrel, button and baroque. Most of the pearls

Figure 10: A barrel-shaped pearl from Varzuga River, measuring 7.08 × 6.77 × 6.72 mm (2.68 ct), is shown in these three views. This grey pearl has a brown dividing line in the middle (a), a brown spot at one end (b) and an indented area on the other end that is surrounded by cracks (c). Photos by E. Strack.

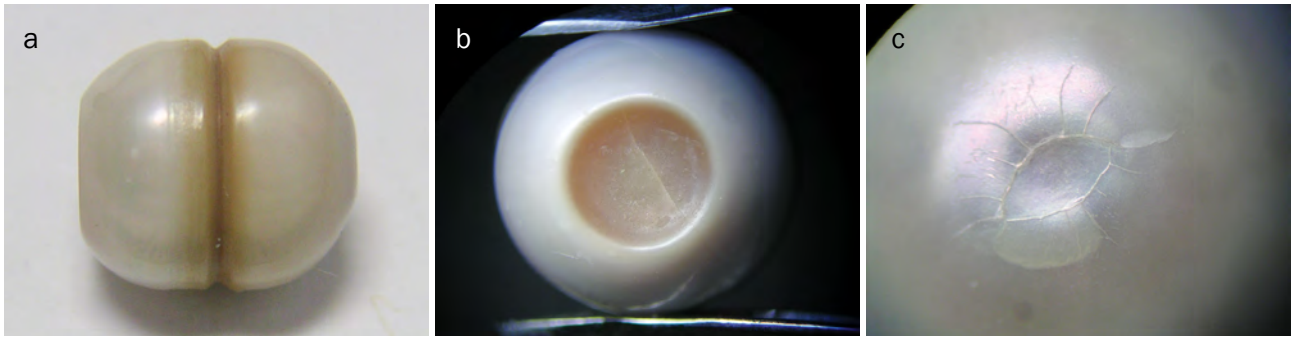

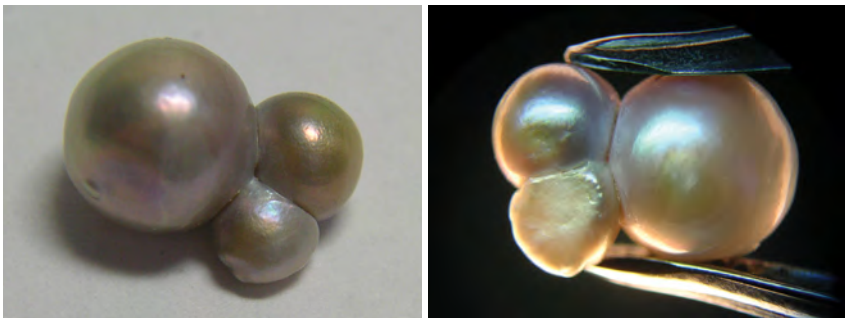

Figure 11: This intergrowth of three Varzuga River pearls measuring 3.18, 3.77 and 5.62 mm each is shown from the front (left photo) and back (right photo). It is greyish purple with 'bronze'-coloured areas and shows good lustre. The flat face on the back of the smallest pearl shows surface wrinkling that is characteristic for pearls of freshwater origin. Photos by E. Strack.

had flat areas with a wrinkled growth pattern on their surfaces.

Microscopic examination of a few of the light grey pearls showed tiny fractures below the surface that may be interpreted as signs of dehydration of originally white pearls. All of the pearls showed an evenly distributed faint blue to whitish blue fluorescence to long-wave UV radiation that was distinctly weaker to short-wave UV.

Nearly all of the items from The Russian Museum of Ethnography consisted entirely of natural freshwater pearls, and only a few small imitation pearls or small mother-of-pearl beads were noted.

Pearls from the 19th/20th Century

Necklace Owned by a Russian Family: This necklace consisted of baroque pearls ranging from 5.0 × 4.5 mm to 8.2 × 7.0 mm. The colours were white to light grey and light to dark 'cream'. Most of the pearls showed distinct growth characteristics, including a characteristic wrinkling on their flat surfaces.

Loose Pearls: The three loose pearls obtained from Valeriy Ziuganov are described as follows:

- A barrel-shaped pearl measured 7.08 × 6.77 × 6.72 mm (2.68 ct), and was grey with a brown dividing line in the middle (Figure 10a, similar to that observed in some pearls from The Russian Museum of Ethnography). One end of the pearl showed a brown spot (Figure 10b), while the other end was indented with associated cracks (Figure 10c). The lustre was dull.
- A sample consisting of three intergrown pearls with diameters of 3.18, 3.77 and 5.62 mm (1.83 ct total) was greyish purple with 'bronze'-coloured areas (Figure 11). The lustre was good. Microscopic examination revealed surface wrinkling on flat areas that is characteristically observed with pearls of freshwater origin.
- A drop-shaped pearl that measured 10.96 × 4.82 × 4.40 mm (1.27 ct) showed a greyish purple coloration similar to that of the triple pearl described above, with a bluish pink overtone and light brown portions (Figure 12a). Surface cracks were present on one side of the pearl (Figure 12b), and an opening on the other side showed a white colour and a surface micro-structure that appeared to consist of tiny rounded points that resembled nail heads (Figure 12c). Lustre was good.

Figure 12: These photos show a drop-shaped pearl from Varzuga River that measures 10.96 × 4.82 × 4.40 mm. It displays a greyish purple colour with a bluish pink overtone and light brown areas (a). (b) The 'bulb' of the pearl shows surface cracks on the front side (b) and a white opening on the underside with a structure made up of tiny rounded points that were visible at higher magnification (c). Photos by E. Strack.

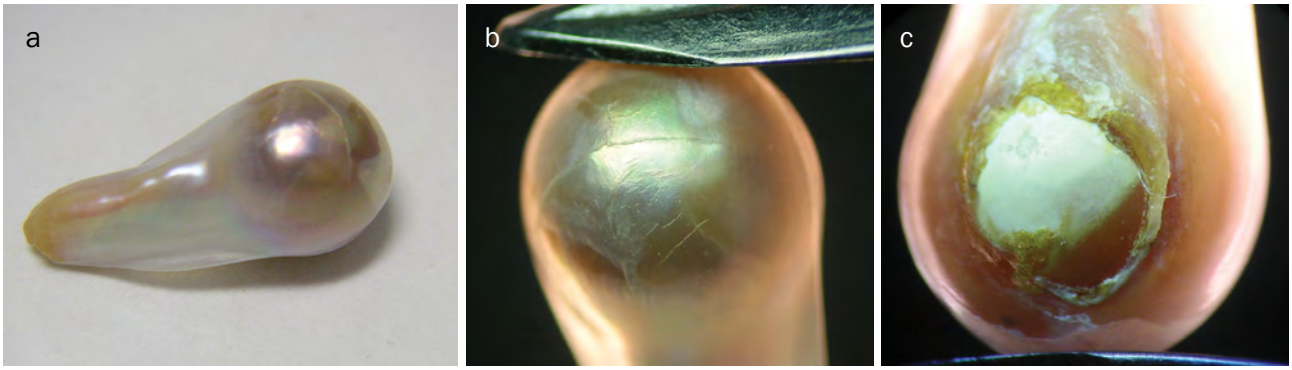

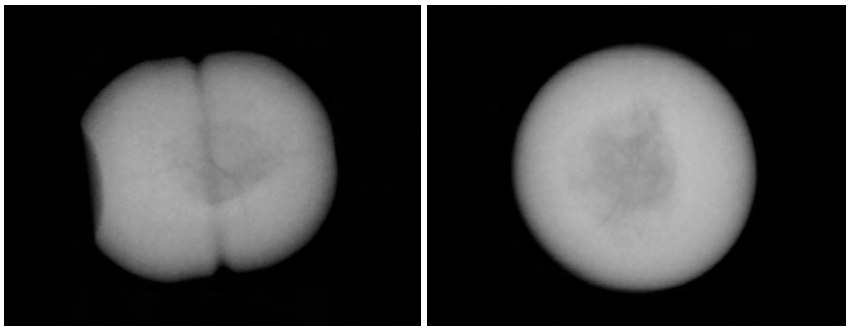

Figure 13: These radiographs of the barrel-shaped pearl in Figure 10 (~7.1 mm long and 6.7 mm in diameter) were taken at orientations parallel to and at right angles to its long axis. They reveal an irregular area of organic substance in the centre of the pearl, which appears dark in the radiographs. Radiographs by E. Strack.

All three pearl specimens showed a weak blue UV fluorescence that was weaker in short-wave than in long-wave UV radiation. Radiographs of the pearls showed irregular and linear deposits of organic substance (Figures 13–15).

Conclusion

The European freshwater pearl mussel *Margaritifera margaritifera* has largely disappeared from its original distribution area in rivers and streams flowing into the White Sea in north-western Russia. Apart from a number of small populations in several rivers, only the Varzuga and Keret Rivers still hold large stocks. The species has been listed as endangered in the IUCN Red List since 1996, and pearl fishing has been prohibited in Russia since 1985, so there has been no significant recent production of these pearls. Moreover, in the decades since the Russian Revolution in 1917, there has been a general lack of local interest and knowledge of pearls.

A limited number of Russian freshwater pearl samples was available for study, including several 18th–19th century objects from museums in St Petersburg and Umba, a necklace from the 1920s and three loose pearls collected from the Varzuga River in the 1990s. The pearls ranged from ~1 to 11 mm and their colours were predominantly white, light 'cream' and light grey; some brownish hues also were present. Their lustre varied from dull to good, and shapes included off-round, flat, barrel, button and baroque. Most of the pearls showed a wrinkled growth pattern on flat surfaces. Varying numbers of imitation pearls (all of small size) were found in the objects studied from the museum collections. X-radiography of the three loose pearls revealed irregular and linear deposits of organic substance.

Figure 14: The radiograph of the pearl intergrowth in Figure 11 shows a circle-shaped, thin linear deposit of organic material that is located just underneath the outer rim of the two larger pearls (~3.9 and 5.6 mm in diameter) and follows their outline. These circular features could initially be interpreted as beads, which obviously is not the case for this natural pearl specimen. In a cultured pearl, the demarcation line of a round bead would not necessarily follow the pearl's outline. Radiograph by E. Strack.

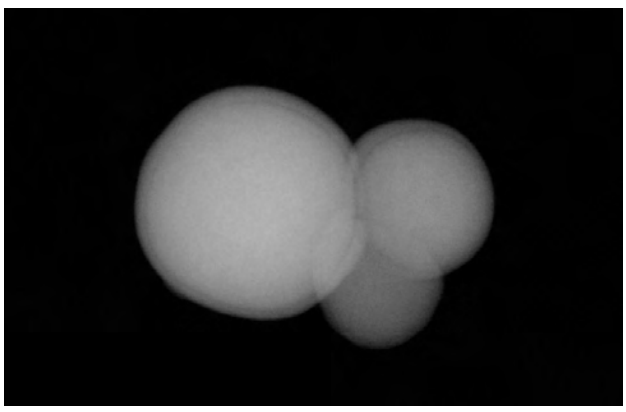

Figure 15: The radiograph of the drop-shaped pearl in Figure 12 (~11 mm long) shows a feature similar to that observed in the triple pearl. Within the 'bulb' is a circle-shaped, thin linear deposit of organic material slightly underneath the outer rim. At the centre of the bulb is a slightly darker core of organic substance. The 'tail' of the pearl has at its centre wavy branch-like extensions of organic material that are arranged parallel to one another along a common line. Radiograph by E. Strack.

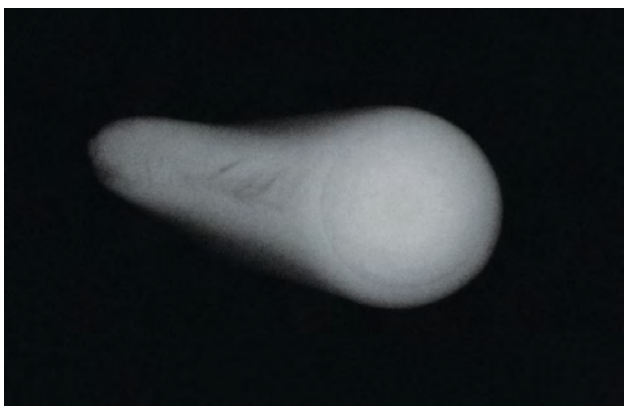

Although Russian freshwater pearls are no longer known or encountered on the pearl market, they form an interesting part of European cultural history.

References

Bespalaya Yu.V., Bolotov I.N., Makhrov A.A. and Vikhrev I.V., 2012. Historical geography of pearl fishing in rivers of the southern White Sea region (Arkhangelsk Oblast). *Regional Research of Russia*, **2**(2), 172–181, http://dx.doi.org/10.1134/s2079970512020025.

Ivanter E.V. and Kuznetsov O.L., Eds., 1995. *Red Data Book of Karelia*. Ministry of Ecology and Natural Resources of the Republic of Karelia, Karelian Scientific Centre of the Russian Academy of Sciences, Petrozavodsk State University, 286 pp. (in Russian).

Kaliuzhin S.M., 2004. *Atlantitscheskii Losos Belewo Moria* [*The Atlantic Salmon of the White Sea Basin: Problems of Reproduction and Fisheries*]. Petropress, Petrozavodsk, Russia, 263 pp.

Korago A.A., 1981. *Retschnoi Tschemtschug* [*Freshwater Pearls*]. Nedra Publishing House, St Petersburg, Russia, 120 pp.

Makhrov A., Bespalaya J., Bolotov I., Vikhrev I., Gofarov M., Alekseeva Y. and Zotin A., 2014. Historical geography of pearl harvesting and current status of populations of freshwater pearl mussel *Margaritifera margaritifera* (L.) in the western part of northern European Russia. *Hydrobiologia,* **735**(1), 149–159, http://dx.doi.org/10.1007/s10750-013-1546-1.

Popov I.Yu. and Ostrovsky A.N., 2014. Survival and extinction of the southern populations of freshwater pearl mussel *Margaritifera margaritifera* in Russia (Leningradskaya and Novgorodskaya oblast). *Hydrobiologia*, **735**(1), 161–177, http://dx.doi.org/10.1007/s10750-013-1640-4.

Reis J., 2003. The freshwater pearl mussel [*Margaritifera margaritifera* (L.)] (Bivalvia: Unionoida) rediscovered in Portugal and threats to its survival. *Biological Conservation*, **114**(3), 447-452, http://dx.doi.org/10.1016/s0006-3207(03)00086-7.

Srebrodolski B.I., 1985. *Tschemtschug* [*Pearls*]. Nauka, Moscow, Russia, 136 pp.

Strack E., 2006. *Pearls*. Rühle-Diebener-Verlag, Stuttgart, Germany, 707 pp.

Ziuganov V., 1994. *The Freshwater Pearl Mussels and Their Relationship with Salmonid Fish*. VNIRO Publishing House, Moscow, Russia, 104 pp.

The Author

Elisabeth Strack
Gemmologisches Institut Hamburg
Poststr. 33, Business Center
20354 Hamburg, Germany
E-mail: info@strack-gih.de

Acknowledgements

The author thanks Dr Reinhard Altmüller (Lachendorf, Germany) for information on the biology of *Margaritifera margaritifera* mussels; Dr Valeriy Ziuganov (Institute of Biology, Russian Academy of Sciences, Moscow, Russia) for lending pearls for examination and providing information on the occurrence of pearls in *Margaritifera margaritifera* mussels; Sviatoslav M. Kaliuzhin (Varzuga Fisheries Cooperative, Varzuga, Russia) for providing information about salmon fishing in Varzuga; Stanislav P. Kitaev (Institute of Biology, Karelian Research Centre, Russian Academy of Sciences, Petrozavodsk, Russia) for information on the status of *Margaritifera margaritifera* in Karelia and Russia; Mitrofan Badanin (currently Bishop of Severomorsk and Umba, Russia) for providing information on the history of the Twersky Coast in the Soviet era; and Anna Ratnikova and Dr Dimitri Baranov (The Russian Museum of Ethnography, St Petersburg) for allowing the examination and photography of pearl objects and respectively for participating in the trip to Karelia and the Kola Peninsula in 2006. The author is also grateful for the information supplied by the people interviewed in Keret, Kuzomen, Umba and Varzuga.

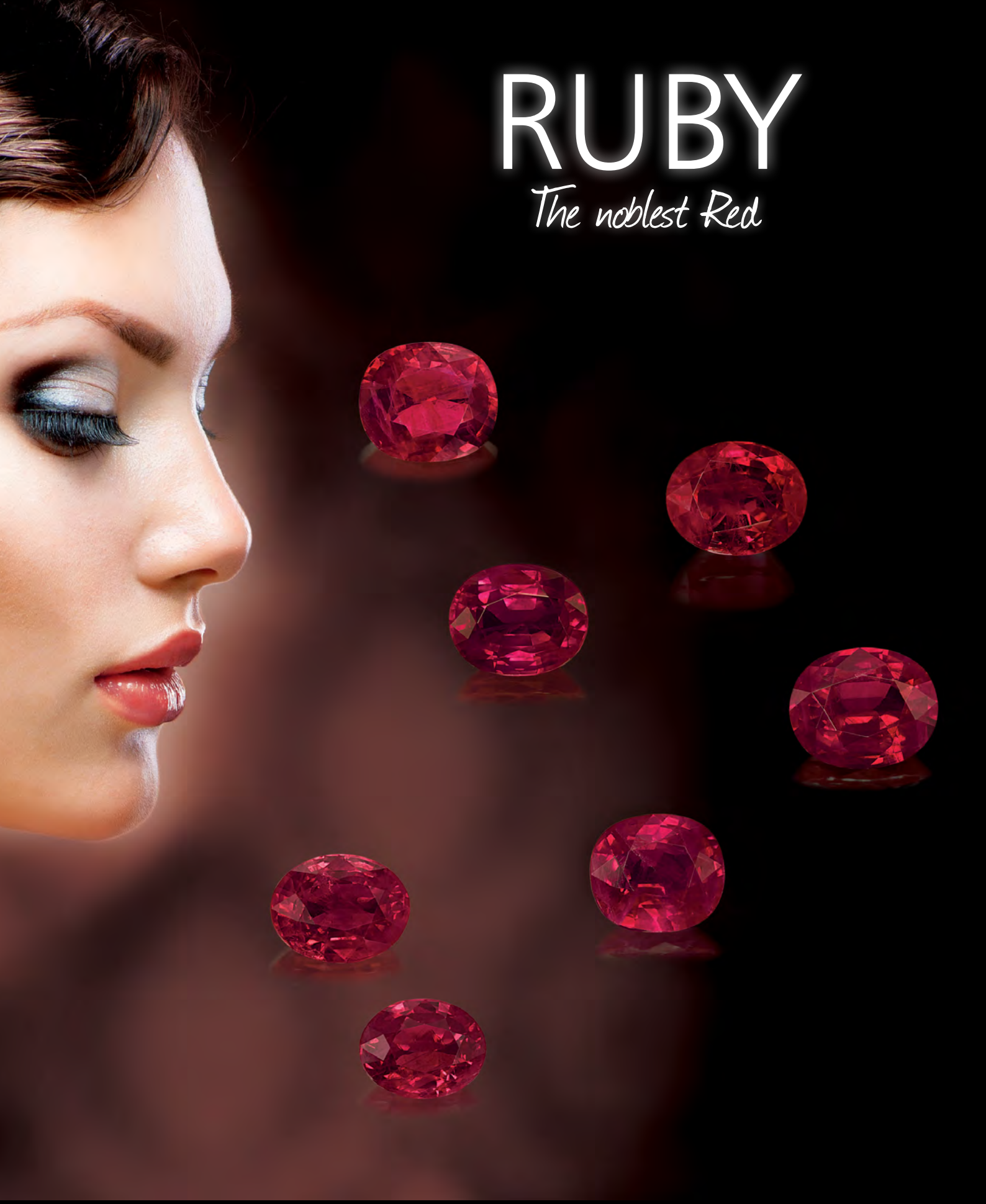

Paul Wild OHG
Auf der Lay 2 · D-55743 Kirschweiler (Germany)
Tel.: +49 (0) 6781 / 9343-0
Fax: +49 (0) 6781 / 9343-43
info@paul-wild.de

PAUL WILD OHG
Edelsteine · Lapidaries
PWK

www.paul-wild.de

Type Ib Yellow to Brownish Yellow CVD Synthetic Diamonds Seen at CGL

Hiroshi Kitawaki, Mio Hisanaga, Masahiro Yamamoto and Kentaro Emori

Fifteen yellow type Ib CVD synthetic diamonds were submitted to the Central Gem Laboratory (Tokyo, Japan) without disclosure in October 2014. They weighed between 0.18 and 0.40 ct and were cut as round brilliants. Their colour ranged between very light yellow and light yellow (some with a brownish tint), and they could not be distinguished visually from natural counterparts of similar colour. Infrared spectroscopy revealed isolated substitutional nitrogen in all the samples, which may be the main cause of their yellow colour. In addition, absorptions were recorded at 3032, 2948, ~2905 and ~2873 cm^{-1}, which are due to C-H-related defects and generally are not observed in natural diamonds. These features, together with optical centres such as H3, NV or N3 detected by photoluminescence spectroscopy, indicate that they underwent post-growth HPHT treatment at ~1,900–2,300+°C. The CVD synthetic origin of such gemstones can be identified by detecting the Si-related feature at 737 nm (when present) in low-temperature photoluminescence spectra, and by observing lamellar growth striations in the DiamondView.

The Journal of Gemmology, 34(7), 2015, pp. 594–604, http://dx.doi.org/10.15506/JoG.2015.34.7.594

Background

Submission for grading of a large parcel of synthetic diamonds grown by chemical vapour deposition (CVD) was reported by the International Gemological Institute in Antwerp in 2012, and this caused turmoil in the diamond industry (Even-Zohar, 2012). Since then, reports of undisclosed CVD synthetics have emerged from gem testing laboratories in India and China (e.g. Song et al., 2012; D'Haenens-Johansson et al., 2013). The Central Gem Laboratory (CGL) also reported on an undisclosed 1+ ct CVD synthetic diamond (Kitawaki et al., 2013). Gem-quality CVD products have been improving in size and quality year after year, and their range of colours has widened to include pink and blue in addition to (near-) colourless (e.g. Kitawaki et al., 2010; Wang et al., 2010; Peretti et al., 2013). Most of those previously reported were type II. However, recently some yellow CVD synthetic diamonds containing isolated substitutional nitrogen were found in the market (Hainschwang, 2014; Moe et al., 2014). So far, published descriptions of such gemstones have been based only on single samples.

This report provides a comprehensive description of 15 yellow to brownish yellow type Ib CVD synthetic diamonds submitted to CGL without disclosure in October 2014, and diagnostic features to distinguish them from natural diamonds are discussed in detail for the first time.

Figure 1: These type Ib yellow CVD synthetic diamonds (0.18–0.40 ct) were submitted to the Central Gem Laboratory for grading without disclosure. Photo by H. Kitawaki.

Materials and Methods

The 15 samples were submitted to CGL as natural diamonds for standard grading (see Table I). All the samples were loose and faceted as round brilliants; they weighed 0.18–0.40 ct (Figures 1 and 2). Their colour and clarity were graded by experienced diamond graders at CGL in accordance with the GIA grading system. The samples were examined with a Motic GM168 stereo microscope, and Manaslu standard 4-watt long-wave (365 nm) and short-wave (254 nm) UV lamps were used to observe fluorescence reactions in a completely

Figure 2: Twelve of the 15 CVD synthetic diamonds fell in the colour range of very light yellow (below N colour) to light yellow (below S colour), and three were graded as light brownish yellow (below S colour). The samples weigh 0.18–0.40 ct and are shown consecutively from DAG0119 to DAG0133 (left to right). Photo by H. Kitawaki.

Table I: The 15 type Ib yellow CVD synthetic diamonds examined in this study.

Sample no.	Weight (ct)	Colour	Clarity	Fluorescence colour* (DiamondView)	N_s^0 (ppm)	H3/NV^0	IR bands in C-H stretching region (cm^{-1})
DAG0119	0.180	Light yellow	SI_2	Bluish green	4.77	1.65	2907, 2878
DAG0120	0.187	Light yellow	SI_2	Bluish green	5.37	1.03	2903, 2873
DAG0121	0.194	Very light yellow	SI_2	Yellowish green	7.24	1.36	2906, 2874
DAG0122	0.198	Light brownish yellow	SI_1	Str. yellowish green	3.90	0.89	2902, 2872
DAG0123	0.200	Light yellow	SI_1	Yellowish green	4.78	2.36	2908, 2875
DAG0124	0.201	Light yellow	SI_1	Yellowish green	4.12	2.23	2907, 2876,
DAG0125	0.210	Very light yellow	SI_1	Bluish green	1.11	1.77	2908, 2875
DAG0126	0.232	Light yellow	SI_2	Yellowish green	1.47	1.41	2905, 2873
DAG0127	0.237	Light yellow	SI_1	Bluish green	5.68	0.95	2905, 2873
DAG0128	0.268	Light yellow	VS_2	Yellowish green	1.78	0.74	2905, 2873
DAG0129	0.279	Light yellow	SI_1	Yellowish green	3.49	1.54	2905, 2873
DAG0130	0.305	Very light yellow	SI_1	Yellowish green	2.92	1.05	2905, 2874
DAG0131	0.316	Light yellow	VS_2	Yellowish green	3.73	1.01	2905, 2874
DAG0132	0.365	Light brownish yellow	SI_1	Str. yellowish green	2.70	0.64	2902, 2871
DAG0133	0.402	Light brownish yellow	SI_1	Str. yellowish green	1.12	0.93	2902, 2872

* Abbreviation: Str. = strongly.

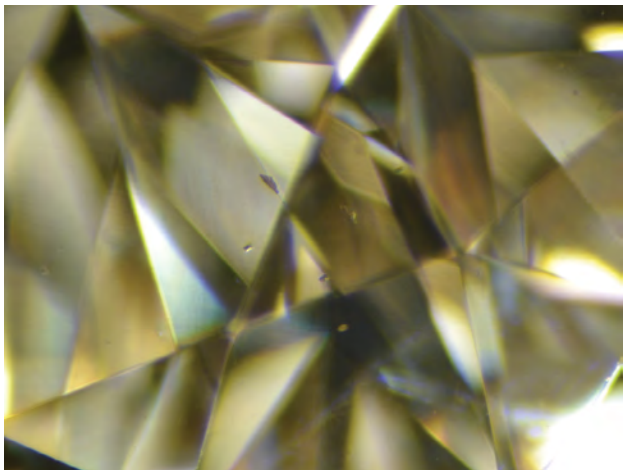

Figure 3: Each of the CVD synthetic diamonds contained irregular-shaped dark brown inclusions, presumably composed of non-diamond carbon. Photo by H. Kitawaki.

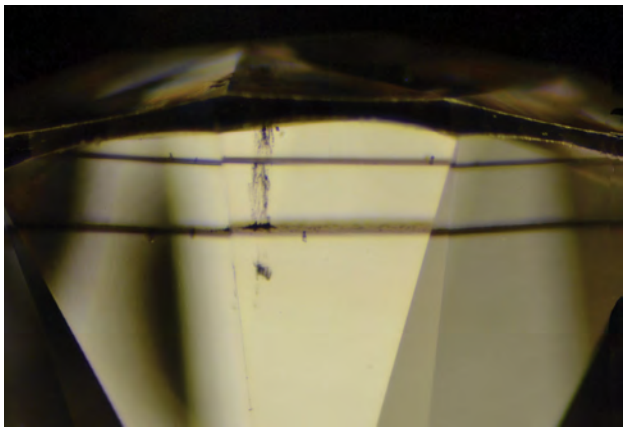

Figure 4: CVD sample DAG0133 shows two subparallel narrow straight bands of colour zoning. Photomicrograph by H. Kitawaki; image width 3.2 mm.

dark room. Ultraviolet-visible-near infrared (UV-Vis-NIR) absorption spectroscopy of all samples was performed at room temperature using a JASCO V-570 spectrometer between 220 and 1100 nm, with a bandwidth of 2.0 nm, resolution of 0.5 nm and scan speed of 400 nm/min. Infrared spectroscopy of all samples was carried out with a JASCO FT/IR-4200 spectrometer in the range 7000–400 cm^{-1} with a resolution of 4.0 cm^{-1} and 20 scans. Photoluminescence (PL) spectroscopy was performed on all samples while they were immersed in liquid nitrogen using a Renishaw Raman System 1000 instrument with several lasers (633, 514, 488 and 325 nm) in conjunction with a Renishaw inVia Raman microscope. All the samples also were tested with a DiamondPlus instrument, and their ultra-short-wave UV luminescence was observed with a DiamondView (both instruments developed by the Diamond Trading Company [DTC]).

Results and Discussion

Colour and Clarity

Of the 15 samples, 12 were in the colour range from very light yellow (below N colour) to light yellow (below S colour), and three were graded as light brownish yellow (below S colour). Two samples were clarity graded as VS_2, nine as SI_1 and four as SI_2. (Note that these are equivalent colour and clarity grades, since in Japan regulations of the Association of Gemmological Laboratories prohibit grading of synthetic diamonds.)

Figure 5: CVD sample DAG0126 contains many pinpoint inclusions arranged in a plane (left, image width 3.4 mm), which individually displayed a quadrilateral shape at higher magnification (right). Photomicrographs by H. Kitawaki.

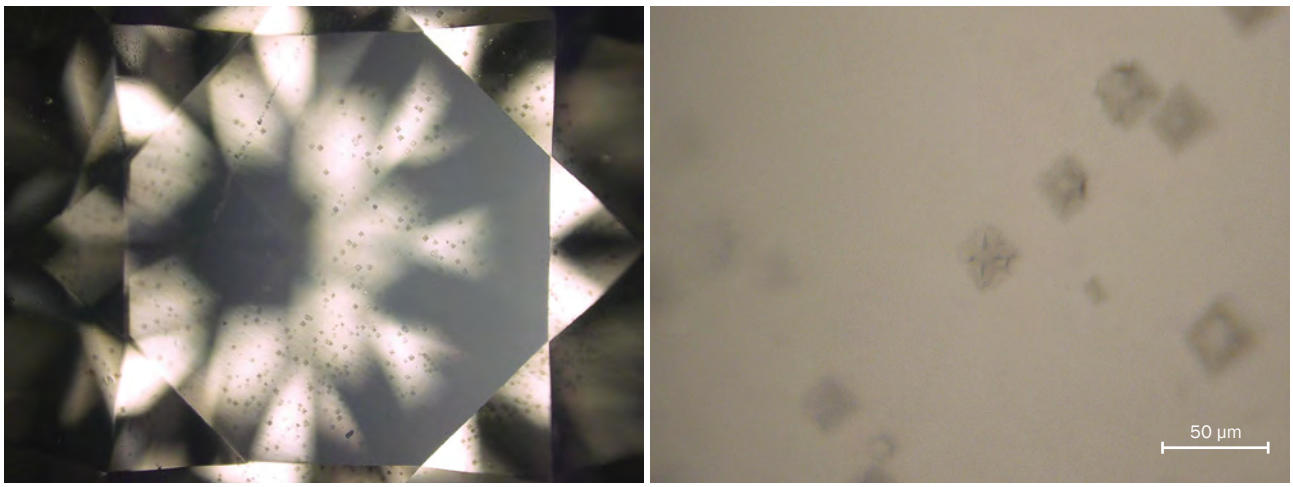

Microscopic Examination

Each sample contained a few pinpoint inclusions that were visible with a 10× loupe, which limited their clarity grade to VS or SI. When further magnified to several dozen times with the microscope, these inclusions appeared irregular shaped with a dark brown colour (Figure 3), and presumably consisted of non-diamond carbon. One sample (DAG0133) showed two narrow, subparallel, straight bands of colour zoning (Figure 4) that probably formed in response to growth from a seed crystal (which was not present). Another sample (DAG0126) contained many pinpoint inclusions arranged in a plane that displayed a quadrilateral shape under magnification (Figure 5). These were probably non-diamond carbon that were arranged in a {100} direction. Some of the samples showed dark areas of graphitization on their girdles (Figure 6). Similar features are seen in diamonds treated by high-pressure, high-temperature (HPHT) conditions (e.g. Moses et al., 1999), which strongly suggests that those samples underwent post-growth HPHT treatment.

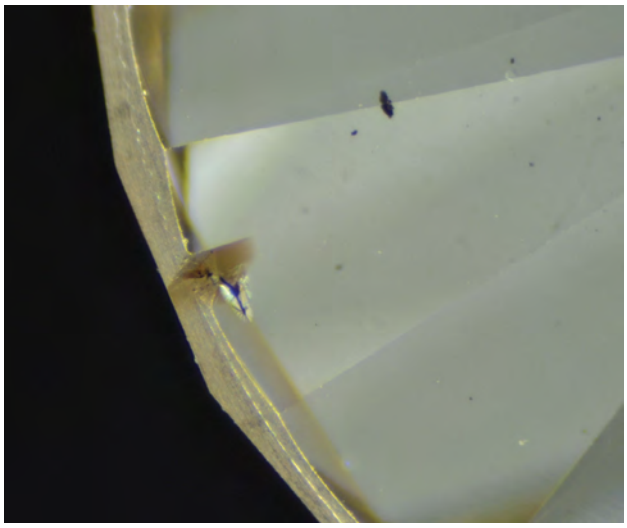

Figure 6: Some of the CVD synthetic diamonds showed dark areas of graphitization on their girdles. Photomicrograph by H. Kitawaki; image width 1.2 mm.

Birefringence

Microscopic examination with crossed polarizers revealed in all the samples a streaked pattern of anomalous double refraction due to strain (low-order black and white interference colours; Figure 7, bottom left). The streaks are interpreted to run parallel to the growth direction of the crystal, and were presumably caused by growth along screw dislocations derived from the interface between the seed crystal and the CVD overgrowth (Figure 7, right; cf. Gaukroger et al., 2008). This type of linear anomalous double refraction pattern is characteristic of CVD synthetic diamond (Martineau et al., 2004).

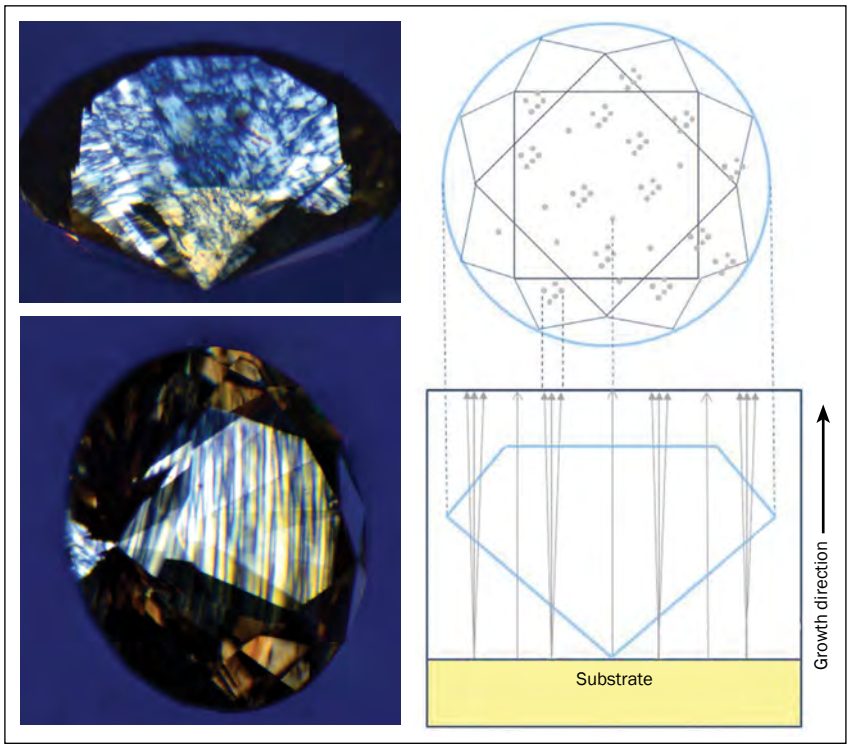

Figure 7: Microscopic observation of the CVD synthetic diamonds with crossed polarizers showed the characteristic streaked pattern of anomalous double refraction due to strain (bottom left). Viewed in certain orientations (top left), it may resemble the 'tatami' structure observed in natural type II diamonds. The schematic diagram shows the orientation of strain in a CVD synthetic diamond. Photos by H. Kitawaki; the diameter of the round brilliant is 4.66 mm.

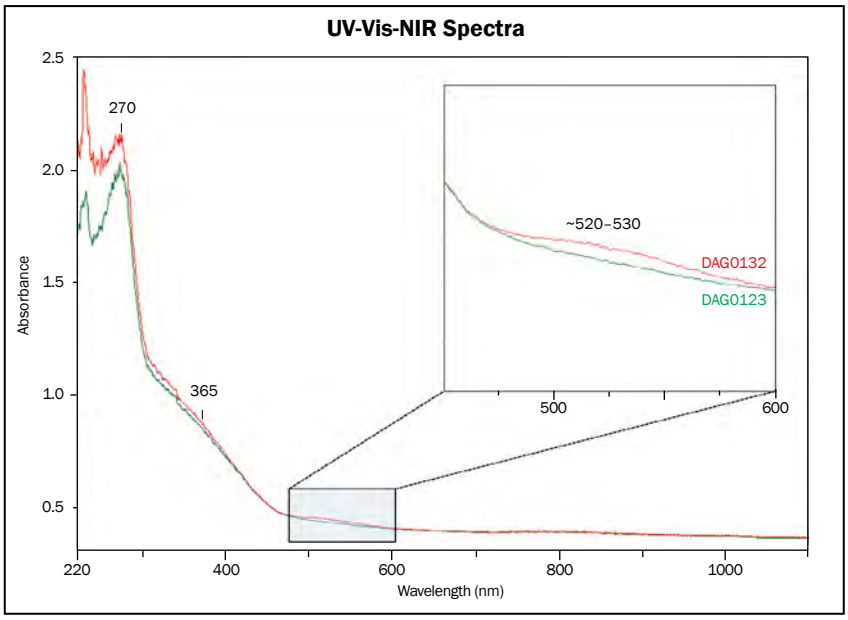

Figure 8: Representative room-temperature UV-Vis-NIR absorption spectra are shown for the light yellow (e.g. DAG0123) and light brownish yellow (e.g. DAG0132) CVD synthetic diamonds. A broad absorption band centred at 270 nm due to isolated nitrogen was observed in all the samples, and a broad band centred at ~520–530 nm was additionally present in only the brownish yellow gemstones.

However, when viewed perpendicular to the growth direction, the birefringence exhibited a fine intersecting mesh pattern (Figure 7, top left), which may resemble the 'tatami' structure observed in natural type II diamonds. Therefore, care should be taken to avoid confusion when observing such birefringence patterns.

UV Fluorescence

All the samples fluoresced yellow-green to both the long- and short-wave UV lamps. Similar-coloured phosphorescence lasting several seconds also was observed. The fluorescence intensity was weak to moderate, with a stronger reaction to short-wave UV.

UV-Vis-NIR Spectroscopy

All the samples showed gradually increasing absorption from the infrared region to near 600 nm in the visible spectrum, and the absorption rapidly increased beyond ~470–480 nm (Figure 8). A broad absorption centred at 270 nm also was observed in all the samples. These features are due to isolated substitutional nitrogen (Dyer et al., 1965). The three samples that had a brownish tint also showed a broad absorption band centred at ~520–530 nm (Figure 8). Martineau et al. (2004) reported that CVD synthetic diamonds synthesized at a high growth rate by doping with nitrogen showed absorptions at 270, 365 and 520 nm, and the latter two features vanished after HPHT treatment. Also, Khan et al. (2010) reported that as-grown brown CVD synthetic diamonds showed absorption bands at 270, 360 and 515 nm, and the band at 515 nm reportedly originated from a neutral complex consisting of nitrogen, a vacancy and hydrogen (NVH^0).

Infrared Spectroscopy

Absorption bands due to isolated substitutional nitrogen were detected at 1344, 1332 and 1130 cm^{-1} in all samples (Figure 9). The bands at 1344 and 1130 cm^{-1} are due to a neutral substitutional nitrogen centre (N_s^0; Collins et al., 1987), and the 1332 cm^{-1} band is associated with a positively charged state (N_s^+; Lawson et al., 1998). From the intensities of these peaks, concentrations of isolated nitrogen were estimated at 1.1–7.2 ppm (see Table I) by the method of Woods et al. (1990). Also, several features between ~3200 and 2800 cm^{-1} that are attributed to C-H-related defects were detected in all the samples. These absorptions were located at 3107, 3032, 2948, ~2905 (varied from 2908 to 2903 in different samples) and ~2873 (varied from 2878 to 2873) cm^{-1} in the 12 samples of yellow colour, while the latter two absorptions were shifted to slightly lower wavelengths (2902 and 2872–2871 cm^{-1}) in the three gemstones showing a brownish tinge (see Table I and Figure 9). Wang et al. (2010) and Kitawaki et al. (2010) reported similar absorption features in pink CVD synthetic diamonds.

PL Spectroscopy

PL spectra obtained with the 633 nm laser are shown in Figure 10. The Si-related feature at 737

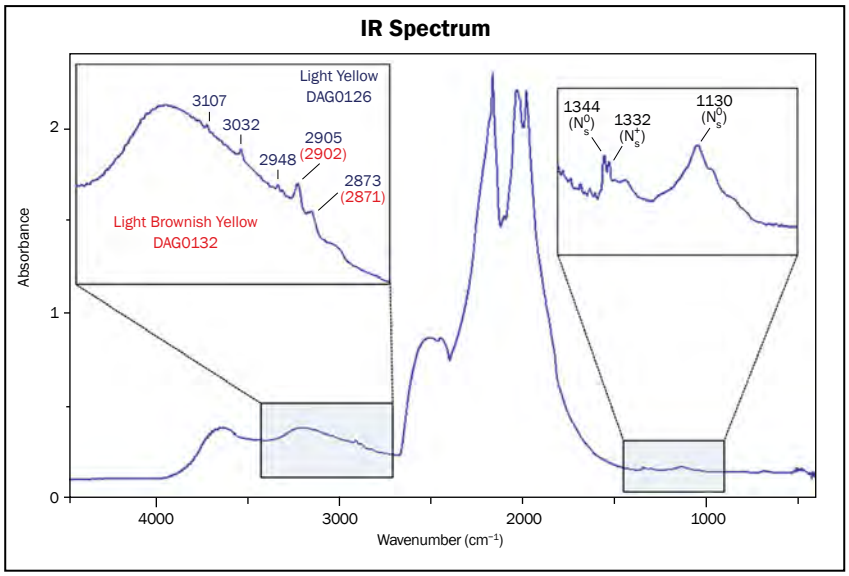

Figure 9: Infrared absorption spectra of the CVD synthetic diamonds (here, for yellow sample DAG0126) show bands due to isolated substitutional nitrogen at 1344, 1332 and 1130 cm^{-1}. In addition, C-H-related features are seen at ~2905 and ~2873 cm^{-1}; these are shifted to 2902 and ~2871 cm^{-1}, respectively, in the brownish yellow gemstones (e.g. DAG0132).

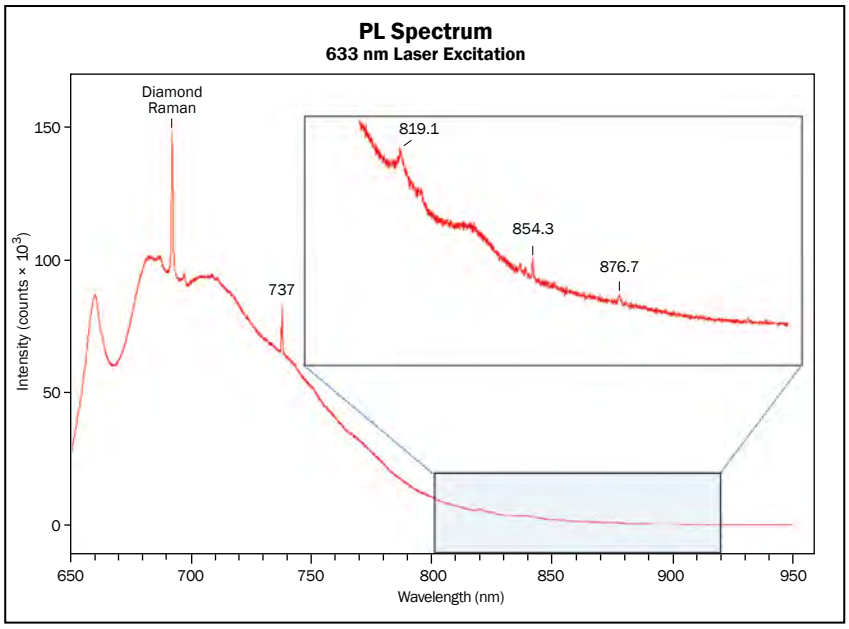

Figure 10: PL spectroscopy using 633 nm laser excitation detected the Si-related feature at 737 nm (actually a 736.4/736.8 doublet) in 13 of the 15 CVD samples, as shown here for sample DAG0120.

nm (actually a 736.4/736.8 doublet, seen when recorded at low temperature) was detected in 13 of the 15 samples (absent from DAG0122 and DAG0125), and this peak was very weak in five of them. Detection of the 737 nm feature in natural diamond is highly unusual, and where present it is accompanied by a series of peaks at 649.4, 651.1 and 714.7 nm (Breeding et al., 2008). The 737 nm feature has been detected in most gem-quality CVD synthetic diamonds previously reported. It is thought to originate from Si that is derived from the growth apparatus, and is regarded as a characteristic feature of CVD synthetic diamonds (e.g. Martineau et al., 2004; Wang et al., 2012). Therefore, although the 737 nm Si-related PL emission was only detected in 13 of the 15 samples studied, when present it is the most important indicator of CVD synthesis. Most of the samples showed small unattributed peaks at 795.8, 819.1, 824.6, 850.2, 851.6, 853.4, 854.3, 876.7 and 908.9 nm (not all of these are shown in Figure 10).

The PL spectra obtained with the 514 nm laser are shown in Figure 11. Very strong peaks at 575 nm (NV^0) and 637 nm (NV^-) were detected in all the samples. However, the 737 nm peak seen with the 633 nm laser was not evident in any of the samples using 514 nm excitation. A pair of peaks at 628.6 and 630.4 nm was detected in nine of the 15 samples. Most of the samples showed small unattributed peaks at 521.4, 524.1, 528.0, 529.1, 532.0, 533.0, 534.9, 536.5, 544.4, 554.0, 555.6 and 565.6 nm (not all of these are shown in Figure 11).

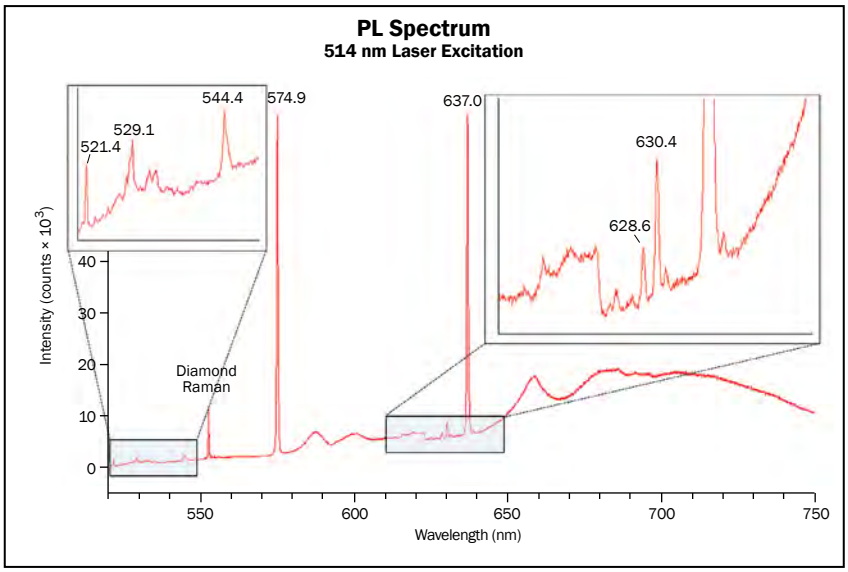

Figure 11: PL spectra obtained with the 514 nm laser show very strong peaks at 575 nm (NV^0) and 637 nm (NV^-). These peaks were seen in all the CVD samples, and are shown here for sample DAG0131.

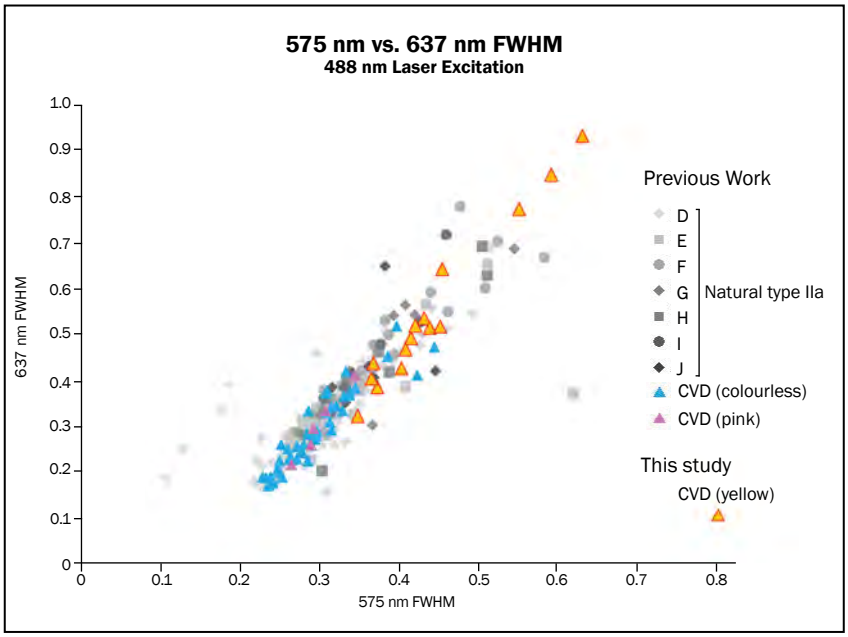

Figure 12: This diagram plots the full width at half maximum (FWHM) for PL data obtained with the 514 nm laser that are due to the 575 nm (NV^0) and 637 nm (NV^-) centres. The CVD synthetic diamonds examined in this study overlap the lower colour grades of natural type IIa diamonds from the authors' unpublished research (colourless and pink CVD synthetic diamonds are also shown for comparison).

The width of the zero-phonon line (ZPL) is known to increase in proportion to localized strain in diamond (Fisher et al., 2006). The full width at half maximum (FWHM) of the peaks at 575 and 637 nm obtained with the 514 nm laser are plotted in Figure 12 for all the samples, together with data for 167 natural type IIa diamonds and 44 CVD synthetic diamonds (of unknown manufacturer). The CVD samples consisted of 39 colourless to near-colourless and five pink samples that were previously analysed by CGL (unpublished data). Among the natural type IIa diamonds, stones with lower colour grades tend to show broader FWHM. Although the yellow CVD synthetic diamonds examined in this study overlap the lower colour grades of natural type IIa diamonds in the diagram, the colourless to near-colourless and pink CVD synthetic diamonds plot in the area of higher colour grades of natural type IIa diamonds.

Representative PL spectra obtained with the 488 nm laser are shown in Figure 13. Strong peaks at 503.2 nm (H3) and 574.9 nm (NV^0) were detected in all the samples. The intensity ratio of H3/NV^0 was between 0.74 and 2.36 for the 12 yellow samples, and was 0.64–0.93 for the three brownish yellow gemstones.

A typical PL spectrum from the 325 nm laser is shown in Figure 14. Other than a series of N3 peaks (ZPL at 415.2 nm, with smaller, relatively

broad peaks at 428.2, 438.8 nm, etc.), several features not seen in natural diamonds were detected (425, 428, 439, 441, 451, 453, 457, 462, 486, 492 and 499 nm; not shown in Figure 14). Martineau et al. (2004) and Wang et al. (2012) reported peaks at ~451–459 nm of unknown origin in CVD synthetic diamonds that had been HPHT treated after synthesis with intentionally doped nitrogen.

DiamondPlus Testing

The DiamondPlus is a compact device developed by DTC to detect HPHT-treated type II diamonds that have been commercially available since 2009. The testing takes 15 seconds per stone, and a 'Pass' result means the diamond is natural and untreated, whereas 'Refer' indicates that the sample requires further laboratory testing. The DiamondPlus is also designed to detect CVD synthetic diamond, and the presence of a 737 nm feature will give the result 'Refer (CVD Synthetic?)' along with its normalized peak intensity.

All 15 samples resulted in 'Refer (CVD Synthetic?)'. However, when re-tested on the device, some samples showed 'Refer' and some of those again produced 'Refer (CVD Synthetic?)' after further re-testing. Such samples had normalized intensities of only 0.057–0.179, and the inconsistent results are presumably due to the weak intensity of the 737 nm feature.

DiamondView Observations

The high-intensity ultra-short-wave UV (<225 nm) radiation of the DiamondView revealed that all the samples had an essentially green luminescence (due to the H3 centre), together with lamellar striations that are characteristic of CVD synthetic diamond (Figure 15). Similar-coloured phosphorescence also was observed in all samples. Three of the gemstones (DAG0122, DAG0132 and DAG0133) showed more yellowish luminescence (Figure 16, left), and four samples (DAG0119, DAG0120, DAG0125 and DAG0127) showed areas with a bluish overtone (Figure 16, right). The former three gemstones correspond to those that were colour graded as light brownish yellow, and their H3/NV^0 intensity ratios were lower than those of most of the other samples (Table I). In the four samples with the bluish overtone, N3 centres were detected by PL analysis.

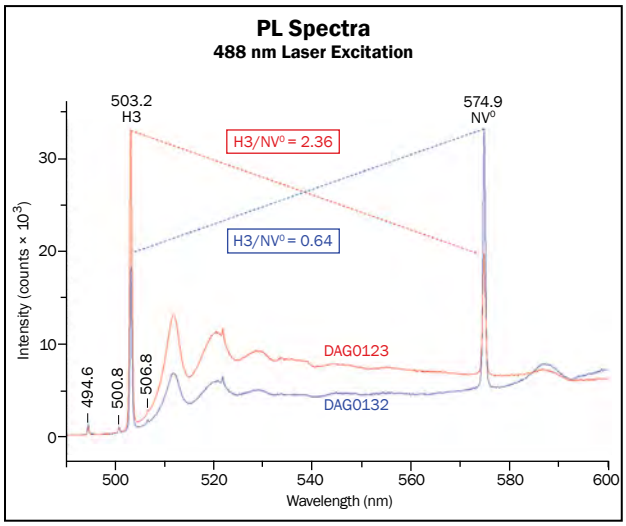

Figure 13: The PL spectra of all the CVD samples obtained with the 488 nm laser showed strong peaks due to H3 and NV centres. In general, the intensity ratio of H3/NV^0 from the yellow samples (here, DAG0123) was much higher than for the brownish yellow gemstones (here, DAG0132).

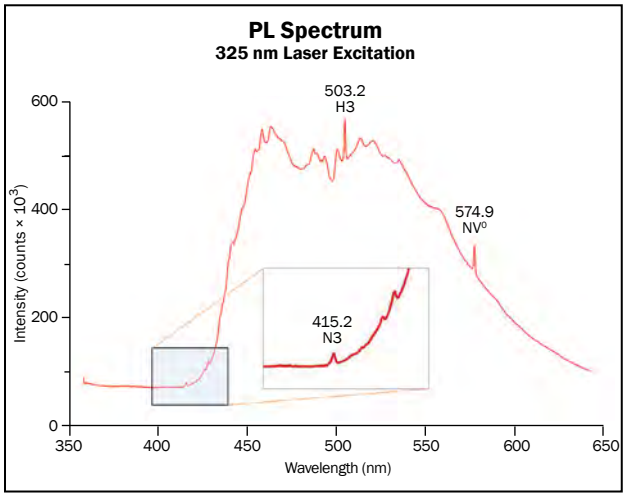

Figure 14: This representative PL spectrum obtained with the 325 nm laser shows weak emission at 415.2 nm from the N3 centre, which was detected in all the CVD samples.

Evidence for Post-growth HPHT Treatment

Most of the colourless to near-colourless CVD synthetic diamonds currently on the market have been intentionally doped with nitrogen to increase the growth rate (Theije et al., 2000). This results in a less attractive brown tint, so the material commonly undergoes post-growth HPHT treatment (Wang et al., 2012). The concentrations of isolated substitutional nitrogen in all the samples in this study confirmed that nitrogen was intentionally added during their growth.

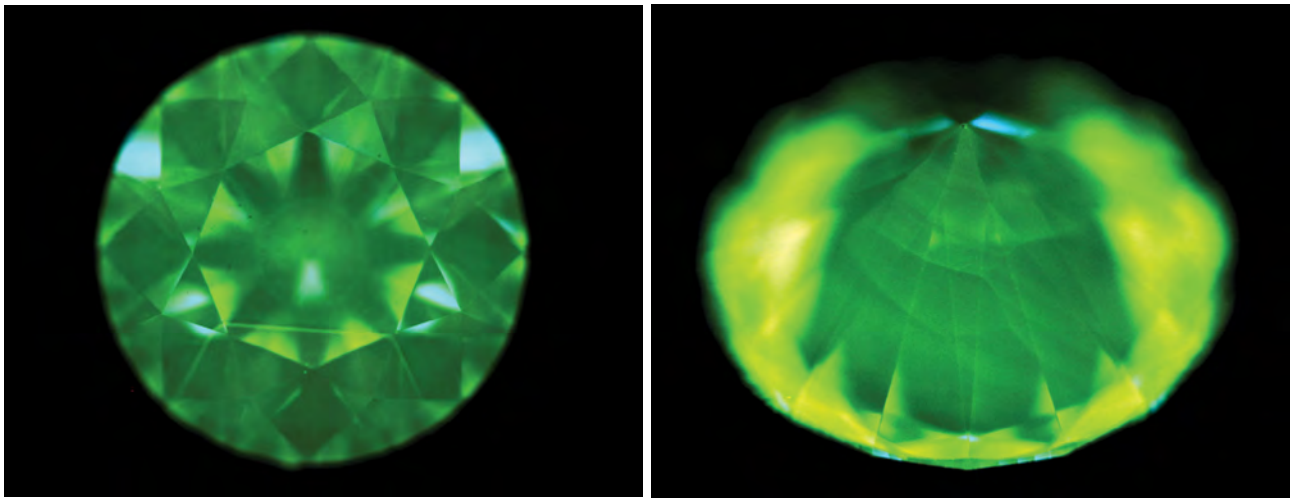

Figure 15: The DiamondView excited green luminescence in all the samples due to the H3 centre (left), together with a lamellar pattern of striations that is characteristic of CVD synthetic diamonds (right). Both images are of sample DAG0131 (0.32 ct). Photos by M. Yamamoto.

UV-Vis-NIR spectroscopy of all the samples showed a broad absorption around 270 nm related to isolated substitutional nitrogen, and a broad absorption centred at ~520–530 nm was present for the three brownish yellow stones. The ~520–530 nm absorption is seen in nitrogen-doped CVD synthetic diamonds, and it is known to be removed by HPHT treatment (Martineau et al., 2004; Meng et al., 2008; Khan et al., 2010). Meng et al. (2008) reported that this absorption is related to NV centres, while Khan et al. (2010) attributed it to NVH^0 centres.

Infrared spectroscopy revealed several bands related to C-H absorptions between 3200 and 2800 cm^{-1} in all samples. These are seen in nitrogen-doped CVD synthetic diamonds that are then HPHT treated (Charles et al., 2004; Meng et al., 2008). According to Charles et al. (2004), bands at 2902 and 2872 cm^{-1} that were detected after HPHT treatment at 1,900°C shifted to 2905 and 2873 cm^{-1}, respectively, after HPHT treatment at 2,200°C. Our unpublished studies of CVD synthetic diamonds before and after HPHT treatment also confirmed that bands at 2902 and 2871 cm^{-1} detected after treatment at 1,600°C shifted to 2907 and 2873 cm^{-1}, respectively, after treatment at 2,300°C. The bands at ~2905 and ~2873 cm^{-1} that were detected in the yellow samples in this study indicate that they may have been HPHT treated at temperatures exceeding 2,300°C. These bands in the three brownish yellow

Figure 16: Three of the CVD synthetic diamonds showed more yellowish luminescence (e.g. left: sample DAG0122; 0.20 ct), and four samples had areas of luminescence with a bluish overtone (e.g. right: DAG0119; 0.18 ct). Photos by M. Yamamoto.

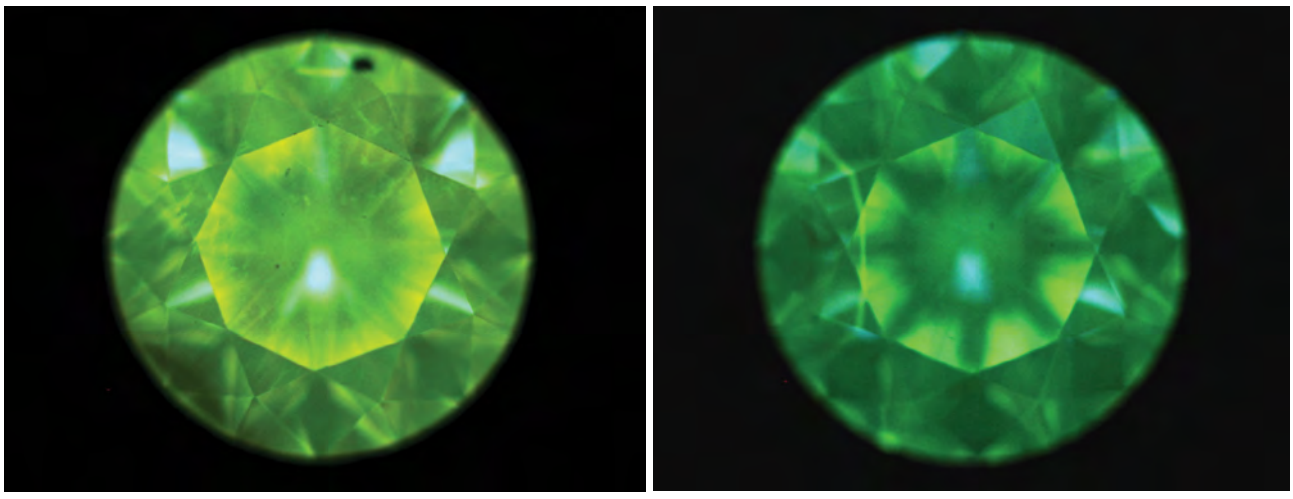

samples were shifted towards lower wavelengths (2902 and 2872–2871 cm^{-1}), and are presumed to have been treated at ~1,900°C.

The H3 centre is not seen in as-grown CVD synthetic diamond, but it can be detected after HPHT treatment (Charles et al., 2004; Meng et al., 2008). Meng et al. (2008) found that the ratio NV^0>H3 after low-pressure, high-temperature treatment at 1,970°C inverted to NV^0<H3 after HPHT treatment at 2,030°C. In our study, only two of the 12 yellow samples and all three brownish yellow samples showed the ratio NV^0>H3, which may indicate they were treated at a lower temperature than the other yellow samples.

The N3 centre has not been detected in as-grown CVD synthetic diamonds; thus it is known that this peak at 415.2 nm is formed by post-growth HPHT treatment (Charles et al., 2004; Martineau et al., 2004). During treatment, the peak intensity becomes stronger with prolonged heating at 2,200°C. In the PL data from this study, the N3 centre in three brownish yellow samples was weaker than in the yellow gemstones. This result also suggests that the brownish yellow samples were HPHT treated at lower temperature than the others.

Conclusion

Fifteen CVD synthetic diamonds in yellow hues were submitted to CGL for grading without disclosure. They proved to be type Ib, containing 1.1–7.2 ppm of isolated substitutional nitrogen. From the presence of the H3 and N3 centres, as well as the H3/NV^0 intensity ratio and the infrared absorption bands due to C-H-related defects, these samples appear to have undergone post-growth HPHT treatment at ~1,900–2,300+°C. The presence of the Si-related feature at 737 nm in the PL spectra (when present) and the lamellar pattern of growth striations observed with the DiamondView are the two most important characteristics for the identification of these CVD synthetic diamonds.

References

Breeding C.M. and Wang W., 2008. Occurrence of the Si-V defect center in natural colourless gem diamonds. *Diamond and Related Materials*, **17**, 1335–1344, http://dx.doi.org/10.1016/j.diamond.2008.01.075.

Charles S.J., Butler J.E., Feygelson B.N., Newton M.E., Carroll D.L., Steeds J.W., Darwish H., Yan C.-S., Mao H.K and Hemley R.J., 2004. Characterization of nitrogen doped chemical vapour deposited single crystal diamond before and after high pressure, high temperature annealing. *Physica Status Solidi (a)*, **201**(11), 2473–2485, http://dx.doi.org/10.1002/pssa.200405175.

Collins A.T., 1987. Migration of nitrogen in electron-irradiated type Ib diamond. *Journal of Physics C: Solid State Physics*, **11**(10), L417–L422, http://dx.doi.org/10.1088/0022-3719/11/10/002.

D'Haenens-Johansson U., Eaton-Magaña S., Bhoir M. and Shinde Y., 2013. Lab Notes: Three CVD synthetic diamonds submitted to Mumbai laboratory. *Gems & Gemology*, **49**(1), 49–50.

Dyer H.B., Raal F.A., Du Preez L. and Loubser J.H.N., 1965. Optical absorption features associated with paramagnetic nitrogen in diamond. *Philosophical Magazine*, **11**(112), 763–774, http://dx.doi.org/10.1080/14786436508230081.

Even-Zohar C., 2012. Synthetics specifically 'made to defraud'. *Diamond Intelligence Briefs*, **27**(709), 7281–7290.

Fisher D., Evans D.J.F., Glover C., Kelly C.J., Sheehy M.J. and Summerton G.C., 2006. The vacancy as a probe of the strain in type IIa diamonds. *Diamond and Related Materials*, **15**(10), 1636–1642, http://dx.doi.org/10.1016/j.diamond.2006.01.020.

Gaukroger M.P., Martineau P.M., Crowder M.J., Friel I., Williams S.D. and Twitchen D.J., 2008. X-ray topography studies of dislocations in single crystal CVD diamond. *Diamond and Related Materials*, **17**(3), 262–269, http://dx.doi.org/10.1016/j.diamond.2007.12.036.

Hainschwang T., 2014. Gem Notes: First CVD synthetic diamond discovered in a parcel of natural melee-sized diamonds. *Journal of Gemmology*, **34**(4), 300–302.

Khan R.U.A., Martineau P.M., Cann B.I., Newton M.E., Dhillon H.K. and Twitchen D.J., 2010. Color alterations in CVD synthetic diamond with heat and UV exposure: Implications for color grading and identification. *Gems & Gemology*, **46**(1), 18–26, http://dx.doi.org/10.5741/gems.46.1.18.

Kitawaki H., Abduriyim A., Kawano J. and Okano M., 2010. Identification of CVD-grown synthetic melee pink diamond. *Journal of Gemmology*, **32**(1–4), 23–30, http://dx.doi.org/10.15506/jog.2010.32.1-4.23.

Kitawaki H., Yamamoto M., Hisanaga M., Okano M. and Emori K., 2013. Gem News International: Undisclosed samples of large CVD synthetic diamond. *Gems & Gemology*, **49**(1), 60–61.

Lawson S.C., Fisher D., Hunt D.C. and Newton M.E., 1998. On the existence of positively charged

single-substitutional nitrogen in diamond. *Journal of Physics: Condensed Matter*, **10**(27), 6171–6180, http://dx.doi.org/10.1088/0953-8984/10/27/016.

Martineau P.M., Lawson S.C., Taylor A.J., Quinn S.J., Evans D.J.F. and Crowder M.J., 2004. Identification of synthetic diamond grown using chemical vapor deposition (CVD). *Gems & Gemology*, **40**(1), 2–25, http://dx.doi.org/10.5741/gems.40.1.2.

Meng Y.F., Yan C.S., Lai J., Krasnicki S., Shu H., Yu T., Ling Q., Mao H.K. and Hemley R.J., 2008. Enhanced optical properties of chemical vapour deposited single crystal diamond by low-pressure/high-temperature annealing. *Proceedings of the National Academy of Sciences*, **105**(46), 17620–17625, http://dx.doi.org/10.1073/pnas.0808230105.

Moe K.S., Wang W. and D'Haenens-Johansson U., 2014. Lab Notes: Yellow CVD synthetic diamond. *Gems & Gemology*, **50**(2), 154–155.

Moses T.M., Shigley J.E., McClure S.F., Koivula J.I. and Van Daele M., 1999. Observations on GE-processed diamonds: A photographic record. *Gems & Gemology*, **35**(3), 14–22.

Peretti A., Herzog F., Bieri W., Alessandri M., Günther D., Frick D.A., Cleveland E., Zaitsev A.M. and Deljanin B., 2013. New generation of synthetic diamonds reaches the market (part A): CVD-grown blue diamonds. *Contributions to Gemology*, **14**, 1–14.

Song Z., Lu T., Lan Y., Shen M., Ke J., Liu J. and Zhang Y., 2012. The identification features of undisclosed loose and mounted CVD synthetic diamonds which have appeared recently in the NGTC laboratory. *Journal of Gemmology*, **33**(1-4), 45–48, http://dx.doi.org/10.15506/jog.2012.33.1.45.

Theije F.K., Schermer J.J. and Enckevort W.J.P., 2000. Effect of nitrogen impurities on the CVD growth of diamond: Step bunching in theory and experiment. *Diamond and Related Materials*, **9**(8), 1439–1449, http://dx.doi.org/10.1016/s0925-9635(00)00261-2.

Wang W., Doering P., Tower J., Lu R., Eaton-Magaña S., Johnson P., Emerson E. and Moses T., 2010. Strongly colored pink CVD lab-grown diamonds. *Gems & Gemology*, **46**(1), 4–17, http://dx.doi.org/10.5741/gems.46.1.4.

Wang W., D'Haenens-Johansson U.F.S., Johnson P., Moe K.S., Emerson E., Newton M.E. and Moses T.M., 2012. CVD synthetic diamonds from Gemesis Corp. *Gems & Gemology*, **48**(2), 80–97, http://dx.doi.org/10.5741/gems.48.2.80.

Woods G.S., Van Wyk J.A. and Collins A.T., 1990. The nitrogen content of type Ib synthetic diamond. *Philosophical Magazine B*, **62**(6), 589–595, http://dx.doi.org/10.1080/13642819008215257.

The Authors

Hiroshi Kitawaki, Mio Hisanaga, Masahiro Yamamoto and Kentaro Emori
Central Gem Laboratory
Miyagi Building, 5-15-14, Ueno Taito-ku
Tokyo 110-0005 Japan
Email: kitawaki@cgl.co.jp

Acknowledgements

We express our gratitude to Dr Kenji Watanabe of the National Institute for Material Science (Tsukuba, Japan) for his assistance with the PL analyses with the UV laser, and to Dr Hisao Kanda of the Tsukuba Expo Center (Tsukuba, Japan) for discussions regarding optical centres.

Letter

Quartz Imitation of Star Sapphire

The Gem Notes section of *The Journal* Vol. 34, No. 6, 2015, pp. 485–486 documented a quartz imitation of star sapphire. Such imitations were manufactured in large quantities in Wembley in the 1940s and sold under the trade name 'Starstones'. They were made by a cousin of my husband, Hermann Stern. The starting material was always rose quartz that was carefully selected to show good asterism. The gems were cut as cabochons and the blue base was affixed under vacuum. Such imitations were mostly set in silver.

Evelyne Stern (evelynestern@btinternet.com)
Harrow, Middlesex

An innovator in gemstone reporting

• Identification of colored gemstones • Country of origin determination • Full quality and color grading analysis

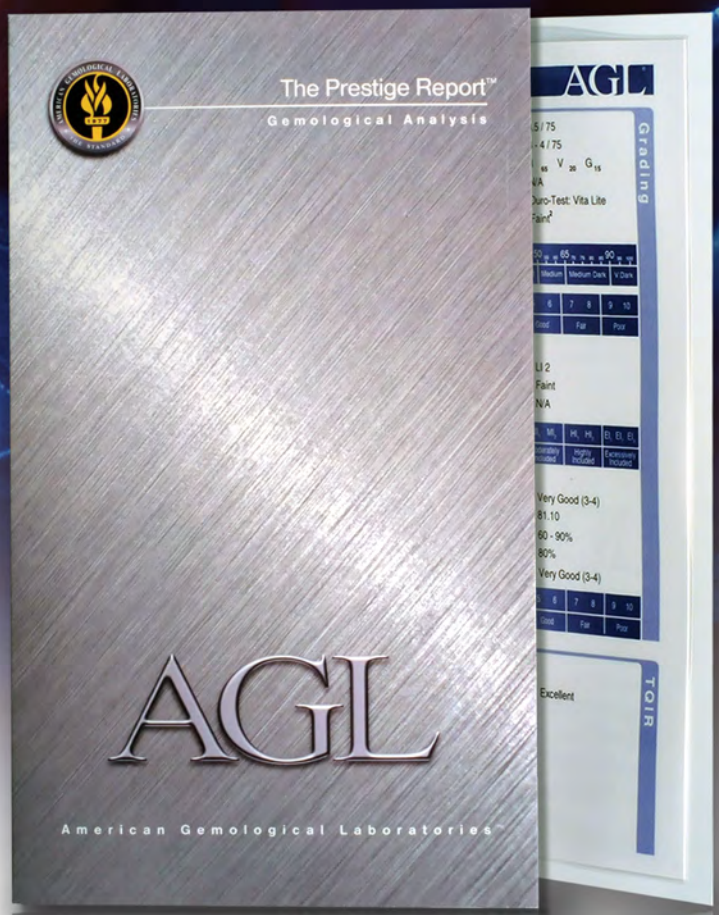

AMERICAN GEMOLOGICAL LABORATORIES AGL

580 5th Ave • Suite 706 • New York, NY 10036, USA
www.aglgemlab.com • +1 (212) 704 - 0727

Burmese Amber from Hti Lin

Tay Thye Sun, Arūnas Kleišmantas, Thet Tin Nyunt, Zheng Minrui, Murali Krishnaswamy and Loke Hui Ying

The main source of Burmese amber is located near Tanai village, Hukawng Valley, Kachin State, northern Myanmar. In 2010–2011, another amber deposit was found about 700 km south of Hukawng Valley near Hti Lin (or Tilin) in Magway Region, central Myanmar. The gemmological properties of material from Hti Lin are consistent with those of amber. Microscopic observation revealed flow marks, flattened gas bubbles, reflective thin-film inclusions, various debris (probably organic material) and included pyrite masses. Hti Lin amber fluoresces a very strong chalky blue to long-wave UV radiation and a weak blue to short-wave UV. FTIR spectroscopy confirmed that the samples were amber (and not copal), whereas no useful Raman data could be collected due to the amber's strong photoluminescence to the 785 nm laser.

The Journal of Gemmology, 34(7), 2015, pp. 606–615, http://dx.doi.org/10.15506/JoG.2015.34.7.606

Introduction

Burmese amber or *Burmite* has been commercially exploited for at least two millennia, mainly by the Chinese (Grimaldi, 1996). The history of the use of Burmese amber was reviewed by Webster (1994), Zherikhin and Ross (2000), Grimaldi et al. (2002) and Ross et al. (2010). The main amber-producing area is Hukawng Valley (or Hukawng Basin), Tanai village, Kachin State, northern Myanmar, particularly at Nojie Bum, a hill that rises some 250 m above a broad alluvial plain that lies between two rivers, Idi Hka and Nambyu Hku (Noetling, 1892; Chhibber, 1934; Cruickshank and Ko, 2003; Shi et al., 2012).

A new locality for Burmese amber (e.g. Figure 1) was discovered in 2010–2011 near Hti Lin (or Tilin) township, Gangaw District, Magway Region, central Myanmar (Figure 2). One of the authors (TTS) visited the area in mid-March 2015 with the help of several local contacts. Following an initial report by Tay et al. (2015), this article gives further information on the geology of the area and gemmological properties of the amber.

Geology of the Hti Lin Area

The Hti Lin area lies within the eastern margin of the Indo-Burman Ranges in western Myanmar that extend from the eastern Himalayan syntaxis southward along the eastern side of the Bay of Bengal to the Andaman Sea (Bannert et al., 2011; Figure 3). This mountainous region is composed almost entirely of deep-marine, mostly non-fossiliferous distal turbidite flysch strata—particularly the southern portion, believed to have been deposited into a subducting trench between the Indian and Sunda Plates (Bannert et al., 2011; Win Swe, 2012).

Figure 1: This piece of polished amber from Hti Lin, Myanmar, is partially transparent and contains fractures with dark brown organic matter. The sample measures 72.46 × 45.31 × 24.19 mm and weighs 189.23 ct. Photo by Tay Thye Sun.

The Hti Lin area is underlain by mudstone, shale with coal-bearing layers, some fine-to-medium-grained calcareous sandstone, coarse-grained sandstone with quartz pebbles and conglomerate (Aung Kyi, pers. comm., 2015). These sedimentary layers, which mainly consist of shale intercalated with occasional fine-grained turbidite sandstones, form part of the Late Cretaceous Kabaw Formation (Than Htut, 2015). They strike ~30° and dip ~50° north-east, and are unconformably overlain by the Paunggyi Formation (Win Swe, 2012; Dr A. H. G. Mitchell, pers. comm., 2015). This geological setting is similar to the amber deposits in Hukawng Valley (Noetling, 1892; Chhibber, 1934; Cruickshank and Ko, 2003; Shi et al., 2012).

The specific locality for the Hti Lin amber deposit is known as Kyakhe ('tiger bite' in English), at coordinates N21°41′44.6″, E94°5′47″. At the mines, author TTS saw mostly shale in the tailings piles, occasionally with broken pieces of sub-bituminous coal together with ball-like masses of pyrite and blocks of white calcite. At one of the mining sites were two small vents emitting hot sulphurous fumes, indicative of volcanic activity.

The botanical origin of the amber from Hti Lin has not been studied, but the Cretaceous amber from Hukawng Valley is known to have come from the Araucariaceae family (especially from the genus *Agathis*) and also the Taxodiaceae family (e.g. Poinar and Milki, 2001; Grimaldi et al., 2002). Genera from both families were confirmed by a study of the palynomorphs (i.e. pollen grains, spores, etc.; see Davies, 2001). While it is possible that Hti Lin amber could have a similar botanical origin, further research is needed.

Mining and Production

At the time of author TTS's visit, there were about 100 miners (mostly local farmers) working in an area covering approximately 10 km^2. According to the miners, the amber is hosted by shale layers with a thickness of 30–40 cm. The miners usually look for thin coal seams within the shale, and follow them until they find pieces of amber, typically lying flat along the shale bedding planes. To reach the amber-bearing shale, the miners dig square pits (~1 × 1 m) to a depth of about 15–20 m (Figure 4). Each pit is worked by three to six miners. Author TTS visited two locations that were 1 km apart; one area had about 25 pits while the other had 15 pits. The production of amber from each pit was variable, ranging from a few grams to 1 kg or more after one to two weeks of digging. The pieces ranged from a few grams to a few kilograms each, and nearly all were covered with an opaque black 'skin' that had to be polished off to reveal the quality of the underlying amber.

Materials and Methods

Twenty samples of amber from Hti Lin (e.g. Figure 5) were examined using basic gemmological

Figure 2: The main source of Burmese amber comes from Hukawng Valley in northern Myanmar. The recently discovered deposit in the Hti Lin area is located in eastern-central Myanmar, about 700 km south-east of Hukawng Valley. The different coloured regions refer to the boundaries of Myanmar's states.

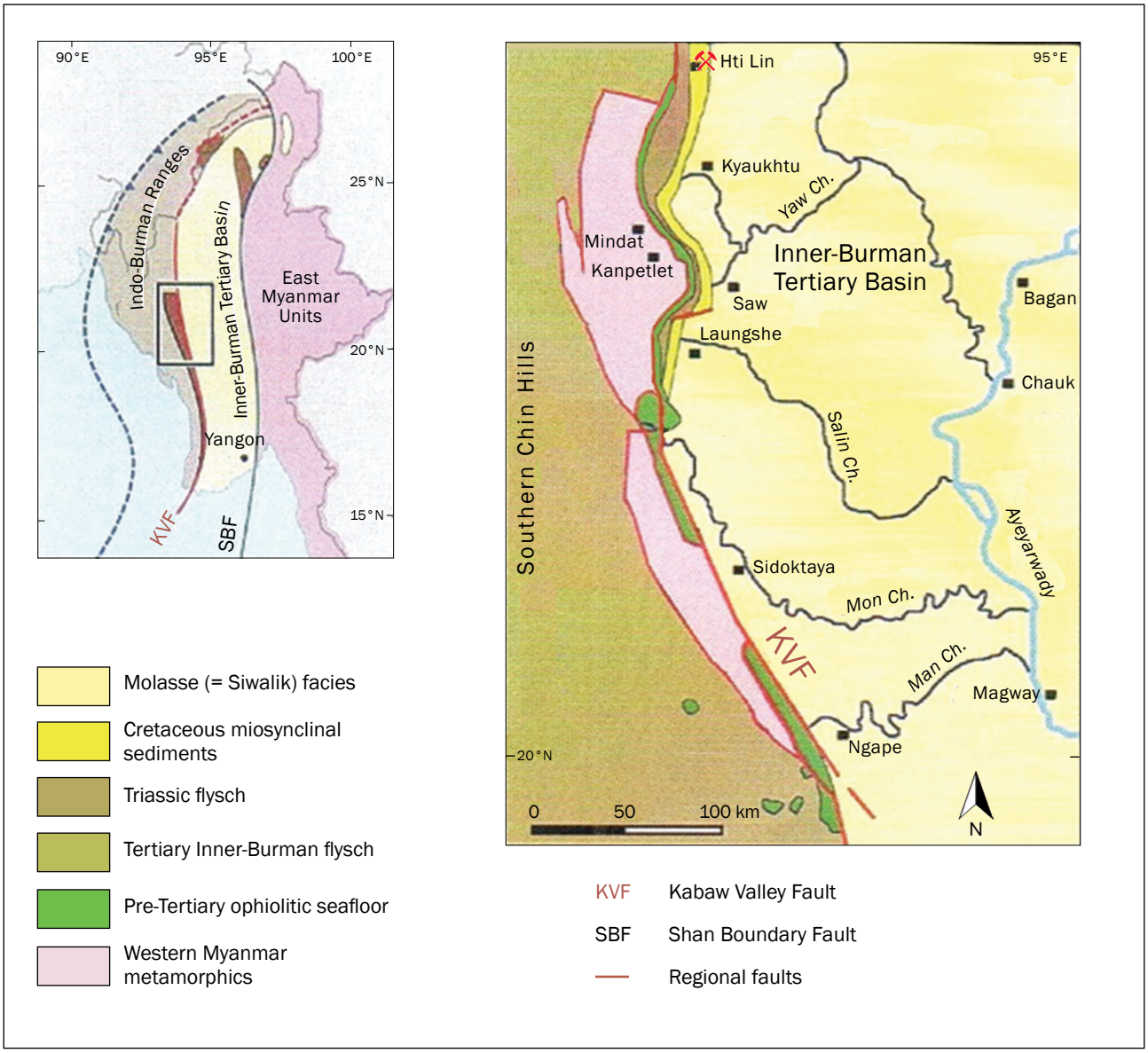

Figure 3: The geological setting of the Hti Lin region is shown here (after Bannert et al., 2011). The amber-mining area is located at the northern edge of the main map.

Figure 4: Pits in the Hti Lin area are typically worked by groups of three to six miners (left). The pit walls are reinforced by timber and bamboo to hold back the soil (right). Photo by Tay Thye Sun.

Figure 5: Some of the rough and polished samples of Hti Lin amber studied for this report are shown here. The disc-like rough piece weighs 45.87 g and measures 87.79 × 88.30 × 14.11 mm, and the large polished sample on the upper right weighs 138.49 ct and measures 88.69 × 59.66 × 12.14 mm. Photo by Tay Thye Sun.

methods. UV fluorescence was observed with a Mineralight UVSL-25 multiband UV 254/365 nm lamp. In addition, five rough amber samples from Hti Lin (0.90, 1.27, 1.66, 2.01 and 5.89 ct) and another five partially polished samples from Hukawng Valley (0.37, 0.40, 0.47, 0.98 and 1.13 ct) were analysed by Fourier-transform infrared (FTIR) and Raman spectroscopy. FTIR data were recorded in transmission mode with a Shimadzu IRPrestige-21 spectrometer in the range of 4000–400 cm^{-1}, with a resolution of 4.0 cm^{-1} and 45 scans. A few milligrams were taken from each sample, crushed into powder, and mixed with KBr to make pellets for analysis. This is a standard method for characterizing amber and its origin and treatments (e.g. Beck et al., 1964; Poinar and Poinar, 1999; Abduriyim et al., 2009; Wolfe et al., 2009) and also for differentiating genuine amber from imitations or forgeries (e.g. Golloch, 1997; Kosmowska-Ceranowicz, 2001). Raman spectroscopy was performed with a Renishaw InVia Raman microscope, using a 785 nm laser in the range of 1768–1400 cm^{-1}. No sample preparation was needed, and this method is also useful for differentiating amber from its imitations (Tay et al., 1998; Shashoua et al., 2006) and determining the country of origin of some ambers (Leelawatanasuk et al., 2013).

Results

Gemmological Data

The colour of the Hti Lin amber ranged from white, yellow and yellowish or reddish brown to dark brown. The diaphaneity was transparent to opaque. The spot RI ranged from 1.54 to 1.55, and the hydrostatic SG was 1.03–1.05. The slightly heavier SG values of the range were probably due to the presence of pyrite inclusions. Most samples fluoresced a very strong chalky blue with white veins to long-wave UV radiation, and a weak chalky blue to short-wave UV. Some of the amber displayed dull green daylight fluorescence.

Viewed with magnification, the samples revealed flattened gas bubbles and groups of thin-film inclusions that were reflective or iridescent under

Figure 6: Flattened gas bubbles and reflective thin-film inclusions are quite common in amber from Hti Lin. Some of them show iridescence when viewed obliquely with fibre-optic lighting (a,b). Groups of these inclusions were folded in some samples (b). The right-hand photo (c) shows masses of reflective thin-film inclusions (right side) and pyrite grains (left side). Photomicrographs by Tay Thye Sun; magnified 15×.

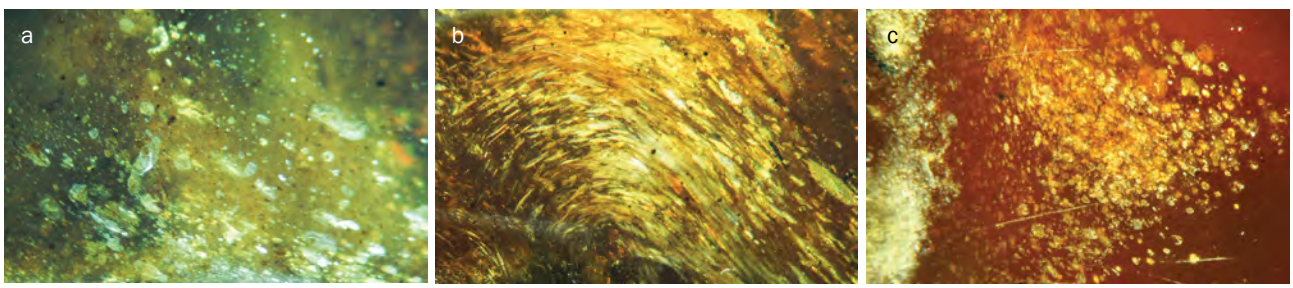

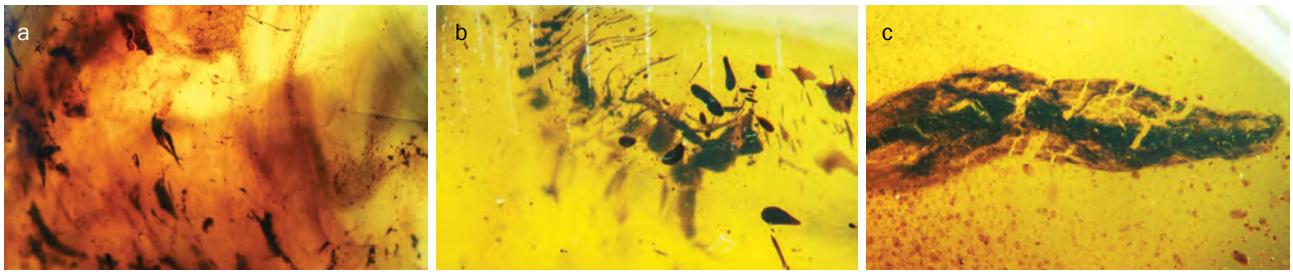

Figure 7: Various types of unidentified debris (probably organic matter) are present in the Hti Lin amber. Some are aligned in the direction of flow marks (a and b, magnified 10× and 15×, respectively). Strange shapes are exhibited by some of these inclusions (c, magnified 10×). Photomicrographs by Tay Thye Sun.

oblique fibre-optic lighting (Figure 6). In addition, various types of unidentifiable (probably organic) debris were noted (Figure 7), sometimes following the direction of flow marks in the amber. Also seen were masses of pyrite (Figures 6c and 8) in some samples that produced gold-like reflections. No insects were present in the pieces examined.

FTIR and Raman Spectroscopy

FTIR spectroscopy of amber from both Hti Lin and Hukawng Valley showed significant bands at approximately 2924, 1724, 1459 and 1376 cm^{-1}, with additional features between 1300 and 1000 cm^{-1} and a weak pair of bands at about 853 and 813 cm^{-1} (Figure 9).

Figure 8: Some of the amber from Hti Lin contains masses of pyrite, as exposed on the surface of this polished sample. Photomicrograph by Tay Thye Sun; magnified 15×.

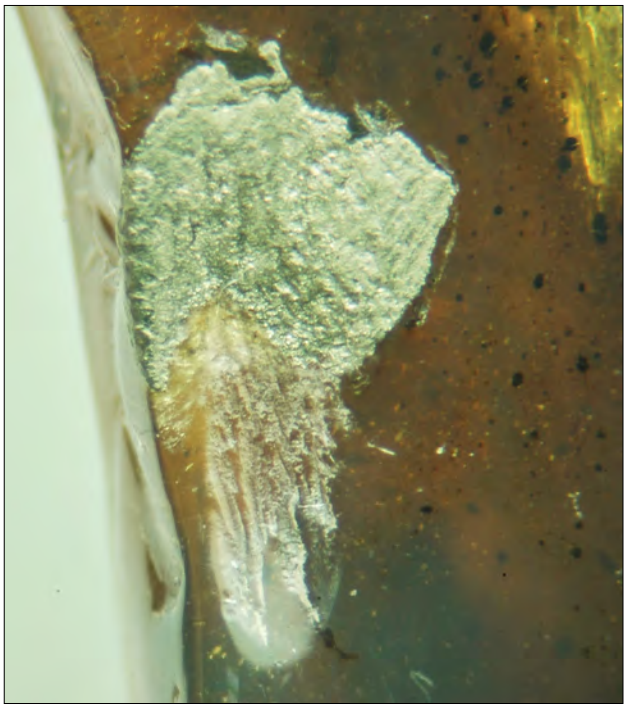

In amber from both localities, the absorption in the C-H stretching region is at wavenumbers below 3000 cm^{-1}, which implies the absence of unsaturated or aromatic compounds. The bands from 3000 to 2850 cm^{-1} are attributed to C-H stretching of sp^3-hybridized C-H bonds of methyl and methylene groups. These are supported by the methylene (CH_2)–bending absorption at ~1458 cm^{-1} and the methyl (CH_3)–bending absorption at ~1375 cm^{-1} (Pavia et al., 2009). The strong band at ~1724 cm^{-1} corresponds to C=O stretching of a carbonyl group. The presence of a second band close to this value in some of the samples could indicate more than one type of carbonyl compound in the amber. The lack of a broad O-H absorption suggests the absence of acid. The complex features between 1300 and 1000 cm^{-1} could be attributed to C-O stretching, and may indicate the presence of an ester (Poulin and Helwig, 2015). Notable is the absence of a 'Baltic shoulder' (i.e. a flat shoulder in the area between 1259 and 1184 cm^{-1}) and an associated feature at 1159 cm^{-1} that has been noted as characteristic of Baltic amber (Beck et al., 1964; Langenheim, 1969). There was no band discerned at 887 cm^{-1} that is characteristic of copal (Guiliano et al., 2007).

No useful Raman spectroscopic data could be collected from samples from either Burmese location because of their strong photoluminescence to the 785 nm laser.

Discussion

Gemmological Data

Amber from Hti Lin is hosted by coal seams within Late Cretaceous shale, in a geological setting that is quite similar to that of Hukawng Valley deposits.

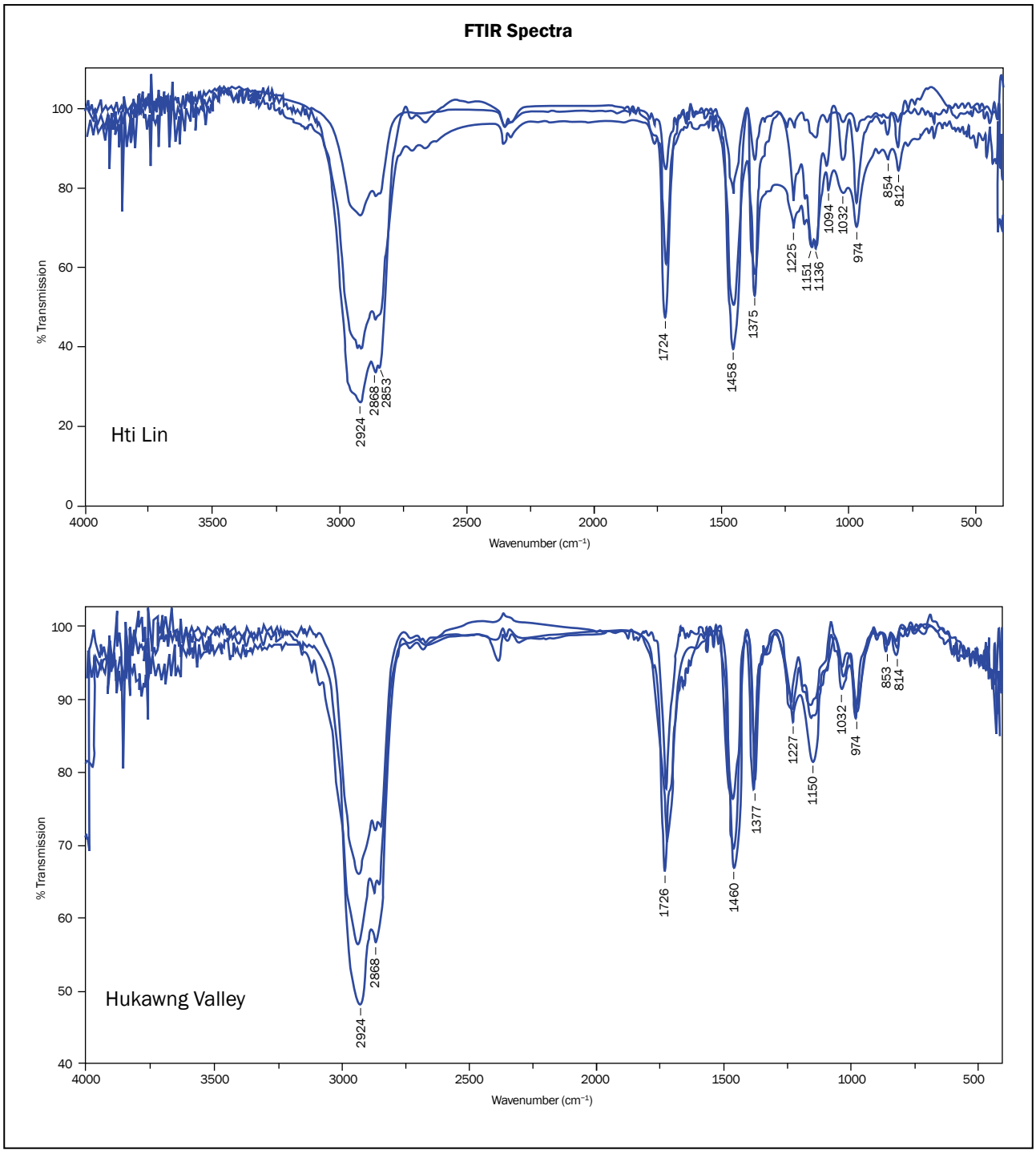

Figure 9: Representative infrared spectra are shown for three amber samples each from Hti Lin and Hukawng Valley.

The gemmological properties of our samples from Hti Lin are typical of amber from other world localities (i.e. RI of 1.54–1.55, SG of 1.03–1.05 and the presence of flow marks, included pyrite masses, and some unidentified [probably organic] debris). Included pyrite masses have been documented in amber from other localities (e.g. from the Baltic area and from New Jersey, USA; Grimaldi, 1996). While Burmese amber from Hukawng Valley is famous for its abundant insect inclusions, the material from Hti Lin had no insects in the limited number of samples examined. The various above-mentioned inclusions are common among amber from other localities around the world, but the flattened and reflective gas bubbles are distinctive for material from Hti Lin.

Considering Hti Lin amber's strong chalky blue fluorescence to long-wave UV radiation, the observed weak chalky blue short-wave UV fluorescence may be due to a 'wavelength bleed' effect that occurs with some dual-wavelength lamps (Williams, 2007).

In daylight, some of the more brownish and reddish brown Hti Lin amber appeared dull green on the surface. Similar colour behaviour has been observed in amber from the Dominican Republic, in which the body colour is yellow and there is a greenish blue surface colour. In addition, amber from Indonesia with a red body colour may show a bluish surface colour. Such colour behaviour has been attributed to UV-stimulated fluorescence together with a variation in colour appearance according to the path length of light through a sample (i.e. the Usambara effect; Liu et al., 2014).

FTIR and Raman Spectroscopy

The IR absorption spectra of the various amber samples from Hukawng Valley and Hti Lin show several common features. The presence of the carbonyl band (1724 cm^{-1}) and the absence of aromatics in the spectra indicate these are likely Class I ambers derived from higher plant resins based primarily on polymers of labdatriene diterpenes (Anderson et al., 1992). The lack of the 'OH' absorption (Pavia et al., 2009), the absence of the 'Baltic shoulder' (Beck et al., 1964; Langenheim, 1969) and a carbonyl stretching vibration at 1724 cm^{-1} that is lower than that of aliphatic esters (Pavia et al., 2009) indicate that this is unlikely to be a Class Ia amber. The classification of the amber into Class Ib or Ic would depend on whether the amber is based on *regular* labdanoids (communic acid, communol and biformenes) or *enantio* labdanoids (ozic acid, ozol and enantio biformene; Anderson, 2001). However, differentiating Class Ib from Ic cannot be ascertained using FTIR spectroscopy alone, and would require further investigation using pyrolysis/gas chromatography/mass spectroscopy. The absence of the 'OH' absorption (Pavia et al., 2009) as well as the lower carbonyl stretching vibration could probably indicate esterification between the labdane alcohol (communol or ozol) and the labdane acid (communic acid or ozic acid) moieties (Poulin and Helwig, 2015).

Previous studies of amber from the Dominican Republic and the Baltic area have attributed bands at 3048, 1642 and 887 cm^{-1} to exocyclic methylene groups of labdanoids, and have drawn conclusions on the maturity of the amber by observing these bands, especially the one at 887 cm^{-1} (Guiliano et al., 2007; Clifford and Hatcher, 1995). The absence of these bands in the Burmese samples indicates a relatively high maturity of the amber (Jehlička, 2012), and confirms that Hukawng Valley and Hti Lin samples are amber and not copal.

Previously, Raman spectroscopy in the 1800–1400 cm^{-1} region was successfully used to differentiate amber from polymer imitations, but this was not possible with the 785 nm laser used in this study due to strong fluorescence from the amber. This photoluminescence is apparently correlative with the very strong blue long-wave UV fluorescence exhibited by the Hti Lin amber. Further investigations using FT-Raman spectroscopy should be undertaken.

Conclusion

Burmese amber from Hti Lin is relatively new to the amber market. Its gemmological properties (i.e. RI, SG and microscopic features) are consistent with those of amber in general. However, it fluoresces a very strong chalky blue to long-wave UV radiation and weak chalky blue to short-wave UV. In daylight, some of the Hti Lin amber exhibits a dull green fluorescence, similar to (but not as strong as) 'blue' amber from the Dominican Republic and Indonesia. Mid-IR spectra of Hti Lin amber show characteristic bands at about 2924, 1724, 1459 and 1376 cm^{-1}, and also between 1300 and 1000 cm^{-1} as well as a weak pair of absorptions at 853 and 813 cm^{-1}. Raman spectroscopy of Hti Lin amber using a 785 nm laser was not effective due to strong photoluminescence, and FT-Raman spectroscopy should be attempted in the future.

In the future, amber mining at Hti Lin is expected to continue, as the amber has become a source of income for the villagers in an otherwise impoverished area. In the opinion of author TTS, it is likely that amber production from Hti Lin will increase in the future with growing demand from the Chinese market.

References

Abduriyim A., Kimura H., Yokoyama Y., Nakazono H., Wakatsuki M., Shimizu T., Tansho M. and Ohki S., 2009. Characterisation of "green amber" with infrared and nuclear magnetic resonance spectroscopy. *Gems & Gemology*, **45**(3), 158–177, http://dx.doi.org/10.5741/gems.45.3.158.

Anderson K.B., 2001. The nature and fate of natural resins in the geosphere Part XI. Ruthenium tetroxide oxidation of a mature class Ib amber polymer. *Geochemical Transactions*, **3**, 4 pp.

Anderson K.B., Winans R.E. and Botto R.E., 1992. The nature and fate of natural resins in the geosphere – II. Identification, classification and nomenclature of resinites. *Organic Geochemistry*, **18**(6), 829–841, http://dx.doi.org/10.1016/0146-6380(92)90051-x.

Bannert D., Lyen A.S. and Htay T., 2011. The Geology of the Indoburman Ranges in Myanmar. *Geologisches Jahrbuch*, *Reihe B*, **101**, 101 pp.

Beck C., Wilbur E. and Meret S., 1964. Infra-red spectra and the origin of amber. *Nature*, **201**(4916), 256–257, http://dx.doi.org/10.1038/201256a0.

Chhibber H.L., 1934. *The Mineral Resources of Burma*. Macmillan & Co., London.

Clifford D.J. and Hatcher P.G., 1995. Chapter 5: Maturation of Class Ib (polylabdanoid) resinites. In K.B. Anderson and J.C. Crelling, Eds., *Amber, Resinite and Fossil Resins*, American Chemical Society Symposium Series, **617**, Washington D.C., 92–104, http://dx.doi.org/10.1021/bk-1995-0617.ch005.

Cruickshank R.D. and Ko Ko, 2003. Geology of an amber locality in Hukawng Valley, northern Myanmar. *Journal of Asian Earth Sciences*, **21**(5), 441–455, http://dx.doi.org/10.1016/s1367-9120(02)00044-5.

Davies E.H., 2001. Palynological analysis and age assignments of two Burmese amber sample sets. Unpublished report by Branta Biostratigaphy Ltd. for Leeward Capital Corp., 4 pp.

Golloch A., 1997. The identification of amber and imitation (forgeries) – An analytical problem. In B. Kosmowska-Ceranowicz and W. Gierłowski, Eds., *Amber – Views, Opinions*, Scientific seminars AMBERIF – International Fair of Amber, Jewellery and Gemstones 1994–2005, The International Amber Association, The Museum of the Earth of the Polish Academy of Sciences and Gdańsk International Fair Co., Gdańsk-Warszawa, Poland, 2006, 81–85.

Grimaldi D.A., 1996. *Amber: Window to the Past*. Harry N. Abrams Inc. and the American Museum of Natural History, New York, New York, USA, 216 pp.

Grimaldi D., Engel M.S. and Nascimbene P., 2002. Fossiliferous Cretaceous amber from Myanmar (Burma): Its rediscovery, biotic diversity, and paleontological significance. *American Museum Novitates*, **3361**, 72 pp., http://dx.doi.org/10.1206/0003-0082(2002)361<0001:fcafmb>2.0.co;2.

Guiliano M., Asia L., Onoratini G. and Mille G., 2007. Applications of diamond crystal ATR FTIR spectroscopy to the characterization of ambers. *Spectrochimica Acta Part A: Molecular and Biomolecular Spectroscopy*, **67**(5), 1407–1411, http://dx.doi.org/10.1016/j.saa.2006.10.033.

Jehlička J., 2012. Chapter 15: Resins and fossil resins. In G.M.H. Edwards and P. Vandenabeele, Eds., *Analytical Archaeometry: Selected Topics*, Royal Society of Chemistry, London, 426–448, http://dx.doi.org/10.1039/9781849732741-00426.

Kosmowska-Ceranowicz B., 2001. Amber forgeries – copal and artificial resins. In B. Kosmowska-Ceranowicz and W. Gierłowski, Eds., *Amber – Views, Opinions*, Scientific seminars AMBERIF – International Fair of Amber, Jewellery and Gemstones 1994–2005, The International Amber Association, The Museum of the Earth of the Polish Academy of Sciences and Gdańsk International Fair Co., Gdańsk-Warszawa, Poland, 2006, 86–92.

Langenheim J., 1969. Amber: A botanical inquiry. *Science*, **163**(3872), 1157–1169, http://dx.doi.org/10.1126/science.163.3872.1157.

Leelawatanasuk T., Wathanakul P., Paramita S., Sutthirat C., Sriprasert B. and Bupparenoo P., 2013. The characteristics of amber from Indonesia. *Australian Gemmologist*, **25**(4), 142–145.

Liu Y., Shi G.H., and Wang S., 2014. Colour phenomena of blue amber. *Gems & Gemology*, **50**(2), 2–8, http://dx.doi.org/10.5741/gems.50.2.134.

Noetling F., 1892. Preliminary report on the economic resources of the amber and jade mines area in Upper Burma. *Records of the Geological Survey of India*, **25**, 130–135.

Pavia D.L., Lampman G.M., Kriz G.S. and Vyvyan J.R., 2009. *Introduction to Spectroscopy*, 4th ed. Cengage Learning, Belmont, California, USA.

Poinar G.O. and Poinar R., 1999. *The Amber Forest*. Princeton University Press, New Jersey, USA, 270 pp.

Poinar G.O. and Milki R., 2001. *Lebanese Amber: The Oldest Insect Ecosystem in Fossilized Resin*. Oregon State University Press, Corvallis, Oregon, USA, 96 pp.

Poulin J. and Helwig K., 2015. Inside amber: New insights into the macromolecular structure of Class Ib resinite. *Organic Geochemistry*, **86**, 94–106, http://dx.doi.org/10.1016/j.orggeochem.2015.05.009.

Ross A., Mellish C., York P. and Crighton B., 2010. Burmese amber. In D. Penney, Ed., *Biodiversity of Fossils in Amber from the Major World Deposits*. Siri Scientific Press, Manchester, 192–207.

Shashoua Y., Berthelsen M.-B.L.D. and Nielsen O.F., 2006. Raman and ATR-FTIR spectroscopies applied to the conservation of archaeological Baltic amber. *Journal of Raman Spectroscopy*,

37(10), 1221–1227, http://dx.doi.org/10.1002/jrs.1586.

Shi G.S., Grimaldi D.A., Harlow G.E., Wang J., Wang J., Yang M., Lei W., Li Q. and Li X., 2012. Age constraint on Burmese amber based on U-Pb dating zircons. *Cretaceous Research*, **37**, 155–163, http://dx.doi.org/10.1016/j.cretres.2012.03.014.

Tay T.S., Shen Z.X. and Yee S.I., 1998. On the identification of amber and its imitations using Raman spectroscopy – Preliminary results. *Australian Gemmologist*, **20**(3), 114–123.

Tay T.S., Kleismantas A., Nyunt T.T., Minrui Z., Krishnaswamy M. and Loke H.Y., 2015. Burmese amber from Hti Lin. *International Gemmological Conference Proceedings*, Vilnius, Lithuania, 26–30 August, 26–29.

Than Htut, 2015. The shale gas prospect in Myanmar. *Journal of the Myanmar Geosciences Society*, **6**(1), 99–130.

Webster R., 1994. *Gems: Their Sources, Descriptions and Identification*, 5th edn., revised by P.G. Read. Butterworth-Heinemann, Oxford, p. 573.

Williams B., 2007. Technology update—Ultraviolet light. *GemGuide*, January/February, 8–11.

Win Swe, 2012. *Outline Geology and Economic Mineral Occurrences of the Union of Myanmar*. Journal of the Myanmar Geosciences Society, Special Publication No. 1, 215 pp.

Wolfe A., Tappert P., Muehlenbachs R., Boudreau K., McKellar M., Basinger R.C. and Garrett J.F., 2009. A new proposal concerning the botanical origin of Baltic amber. *Proceedings of the Royal Society B: Biological Sciences*, **276**(1672), 3403–3412, http://dx.doi.org/10.1098/rspb.2009.0806.

Zherikhin V.V. and Ross A.J., 2000. A review of the history, geology and age of Burmese amber (Burmite). *Bulletin of the Natural History Museum, London (Geology)*, **56**, 3–10.

The Authors

Tay Thye Sun and Loke Hui Ying
Far East Gemological Laboratory
12 Arumugam Road
#04-02, Lion Building B
Singapore 409958
Email: tay@gem.com.sg

Arūnas Kleišmantas
University of Vilnius, Department of Geology and Mineralogy, Vilnius, Lithuania

Thet Tin Nyunt
University of Yangon, Department of Geology, Yangon, Myanmar

Zheng Minrui
National University of Singapore, Physics Department, Kent Ridge, Singapore

Murali Krishnaswamy
NUS High School of Mathematics and Science, Department of Chemistry, 20 Clementi Ave 1, Singapore

Acknowledgements

Author TTS thanks Ma Gjam, Mr Aung Naing, Mr Nyi Nyi Aung, Mr Kyaw Kyaw and Mr Kyaw Min for their assistance with his visit to the Hti Lin amber mining area. Also, thanks to Ms Pek Lay Pheng (Senior Laboratory Technologist, NUS High School of Mathematics and Science, Singapore) for the preparation of samples for FTIR spectroscopy, and Prof. Shen Zexiang and Ms. Yin Ting Ting for Raman microscopy at the Centre for Disruptive Photonic Technologies, Nanyang Technology University, Singapore. Many thanks also to Mr Tin Kyaw Than (former lecturer at the geology department, University of Yangon, Myanmar), Mr Aung Kyi (Department of Geological Survey and Mineral Exploration, Ministry of Mines, Naypyidaw, Myanmar), Dr Andrew H. G. Mitchell (PhD from University of Oxford, and former United Nations adviser to Myanmar on mineral exploration and also former director of the Myanmar Ivanhoe Copper Co. Ltd.) and Prof. Dr Khin Zaw (CODES Centre of Excellence in Ore Deposits, University of Tasmania, Australia) for discussions on the geology of Myanmar, especially the Hti Lin area, and to Mr Thanong Leelawatanasuk (Gem & Jewelry Institute of Thailand, Bangkok) for valuable discussions.

The Application of Differential Interference Contrast Microscopy to Gemmology

Nathan Renfro

Episcopic (reflected light) differential interference contrast (DIC) microscopy can reveal information about rough or cut gems that would otherwise be difficult to obtain using standard gemmological optical microscope illumination techniques. Although not widely used in gemmology due to the current expense of the specialized equipment and its limited applications, this type of contrast-enhancing optical microscopy is particularly useful for observing surface features that may help with such tasks as identifying rough gem materials, detecting heat treatment (in stones that have not been repolished) and assessing whether a gemstone was damaged after it was polished. DIC microscopy is valuable for yielding technical information about a gem, as well as for producing informative and often striking images.

The Journal of Gemmology, 34(7), 2015, pp. 616–620, http://dx.doi.org/10.15506/JoG.2015.34.7.616

Introduction

The microscope is the gemmologist's most powerful instrument, and in many cases its usefulness is limited only by the experience and knowledge of the user. Several illumination techniques are commonly employed for gemmological observations, and each may reveal particular information about a sample that would otherwise go unnoticed. To obtain the greatest amount of information about a stone, it is important to observe it using as many different lighting conditions as possible.

Differential interference contrast (DIC) microscopy was invented in the 1950s by Georges Nomarski (Nomarski, 1960). It was originally developed for diascopic (transmitted light) illumination, but proved to be quite useful for episcopic (reflected light) applications. This type of illumination has been used occasionally in studies of gem materials (e.g. Sunagawa, 1964; Koivula, 1988, 2000, 2009; Takahashi and Sunagawa, 1998; Horikawa, 2001; Evans et al., 2005). DIC microscopy offers a useful perspective on surface structures that may give clues to a gem's identity and whether or not it has been subjected to heat treatment. Also, this lighting environment can be used to assess whether damage occurred to a gem after it was polished. As an added benefit, the images produced often merge the science and art of gemmology because of the striking results that are possible (e.g. Figure 1).

What is Episcopic Differential Interference Contrast?

Episcopic DIC is an optical microscopy method in which a modified Wollaston prism, also known as a Nomarski prism, is incorporated into the light path of a microscope to significantly enhance contrast, revealing very fine detail that would

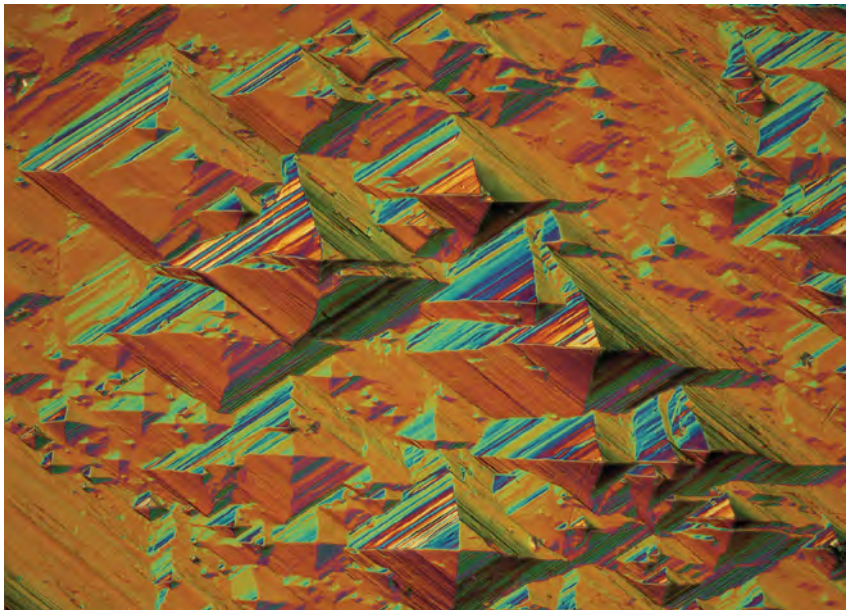

Figure 1: The naturally etched surface of an andradite from Val Malenco, Italy, reveals its isometric morphology in a vibrant display of colour. Photomicrograph by N. Renfro; image width 0.61 mm.

otherwise go unseen. Specimens must be reflective in nature, making polished gemstones and shiny crystals ideal for this type of microscopy. Typically, a compound-type microscope (e.g. Figure 2) is outfitted with a single Nomarski prism located at the rear focal plane of the objective lens. A polarizer and analyser in the optical path are also required components (Brandmaier et al., 2013).

To produce episcopic DIC conditions, an illumination source is polarized by a rotatable filter and directed through the Nomarski prism, where the light is separated into two orthogonally polarized beams. The light then travels through the objective lens where it is focused onto the surface of a sample and reflected back through the objective. The light is then directed back through the Nomarski prism, where the rays are recombined. After exiting the prism, the light travels through an analyser where the orthogonal beams interfere with one another according to variations in path length to produce the interference image that is projected through the oculars. These types of images often display high-order interference colours that can be controlled by the position of the prism in the optical path (Pluta, 1989). This 'optical staining' is not related to the actual coloration of the specimen, but results from the modification of the light used to examine the sample. Even though these types of images may look like they have been artificially produced because of the unnatural-appearing vibrant colour palate, this appearance is what is actually observed in the oculars.

Exploring Surface Features of Rough Gems

Etched gem minerals with their geometric topography provide excellent study subjects for a DIC microscope. Subtle variations of relief can be revealed in a dazzling display of colour and geometry. These etch features can provide clues to a rough gem's identity by revealing symmetry information that corresponds to the crystal system in which the specimen belongs (e.g. Figures 1 and 3). In addition, the surface of a crystal can reveal further information. For example, twin planes that are often seen internally in diamonds are easily observed on the surface of some rough specimens, as evidenced by linear arrangements of trigons (triangular etch features) on octahedral

Figure 2: This Nikon Eclipse LV100 polarizing microscope is equipped with DIC components, and was used to take the photomicrographs in this article. Photo by Kevin Schumacher.

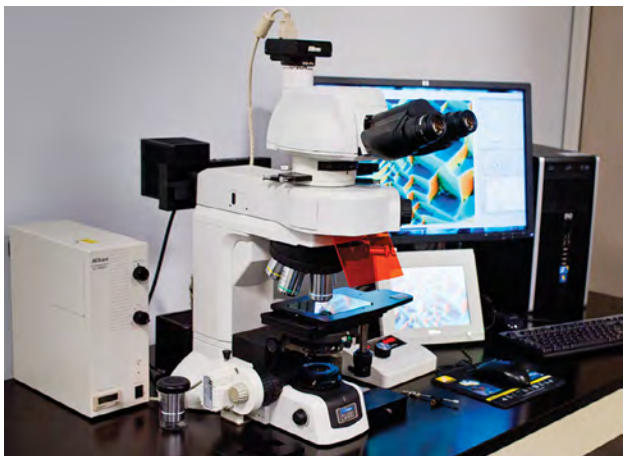

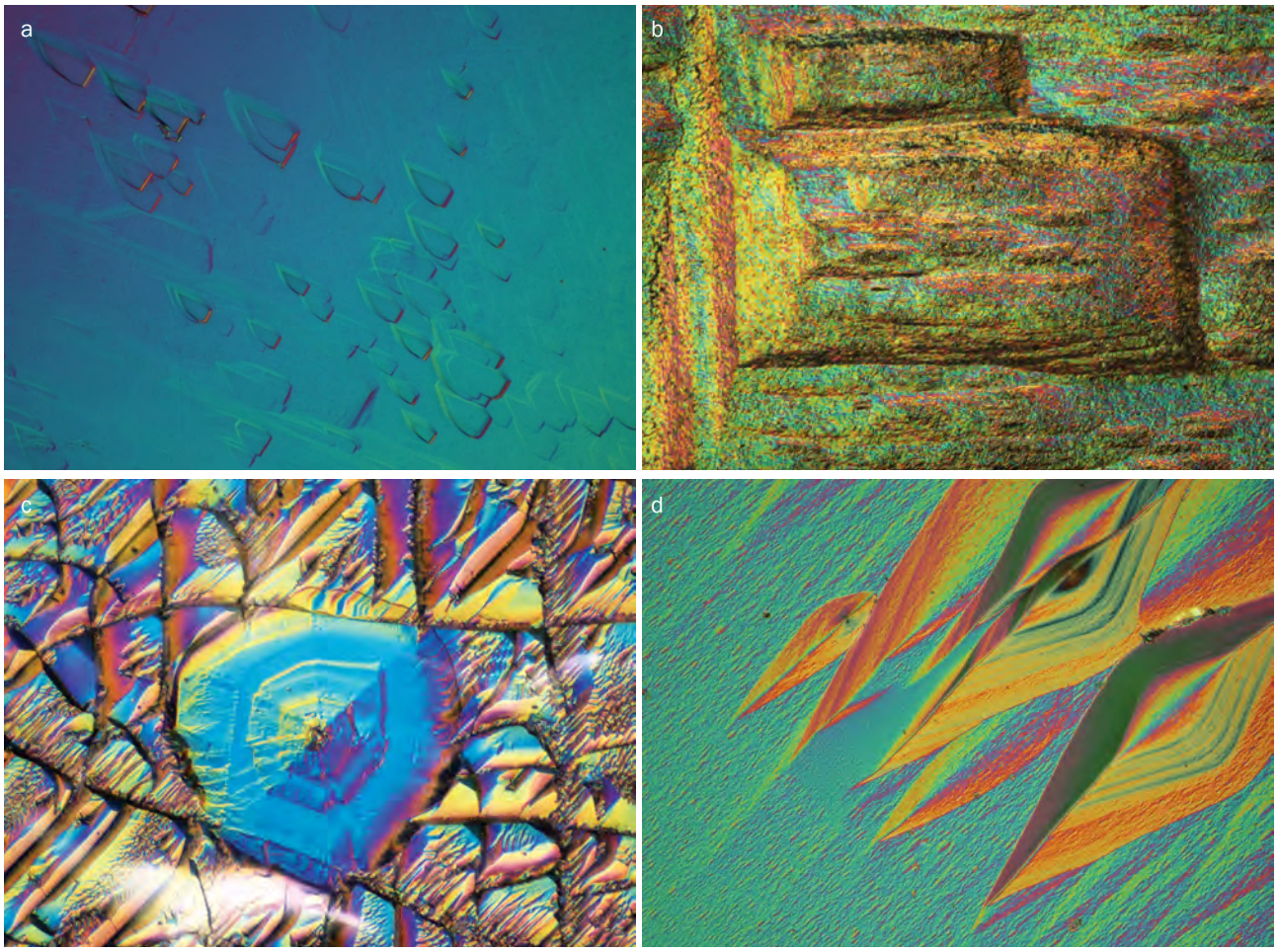

Figure 3: Surface features of gem minerals may provide clues to their identity and crystal structure. (a) These sail-shaped etch features are characteristic of spodumene (image width 0.25 mm). (b) Rectangular etch features are present on the prism faces of a beryl crystal (image width 0.62 mm). (c) The trigonal symmetry of tourmaline is clearly seen in surface etching viewed parallel to the c-axis (image width 0.61 mm). (d) Rhomb-shaped, orthorhombic etching with two-fold symmetry is distinct when looking parallel to the c-axis of this topaz (image width 0.61 mm). Photomicrographs by N. Renfro.

Figure 4: This diamond shows localized areas of higher solubility, as evidenced by the linear arrangement of dissolution trigons along the twin planes. Photomicrograph by N. Renfro; image width 1.24 mm.

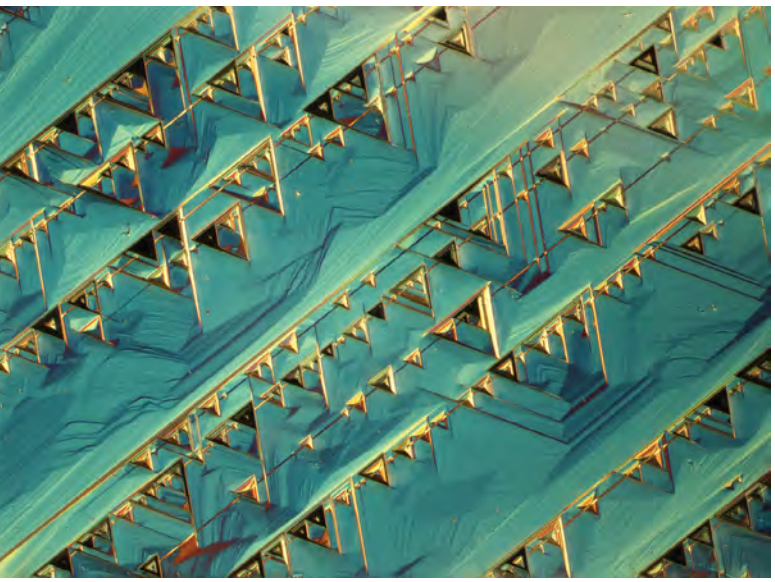

faces (Figure 4). The twinning produces localized areas of high defect concentration that are much more susceptible to etching than areas of pristine structure. As the crystal undergoes dissolution during transport to the earth's surface, the domains with high defect concentration dissolve much faster than the surrounding areas.

Some etch features are also characteristic of certain minerals. For example, sail-shaped, modified triangular etch pits are typical of spodumene (Figure 3a).

Surface features may also give the observer clues about a mineral's genetic environment. Spinel is often hosted by marble, a rock composed of carbonate minerals. The surface morphology of some spinel crystals reveals evidence for carbonate grains in the host rock that interface with the spinel in interesting stepped patterns as the

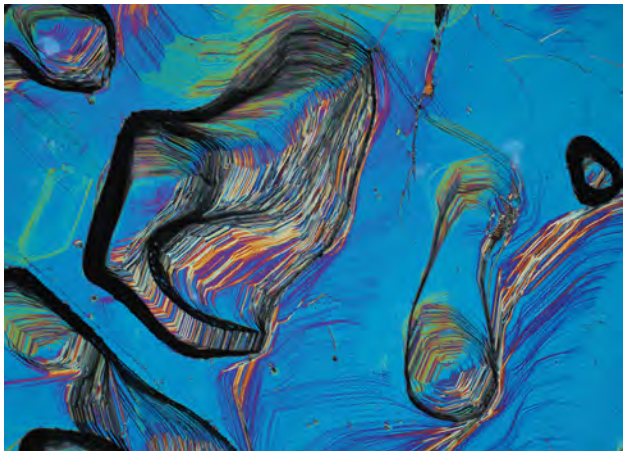

Figure 5: The surface of this Burmese spinel shows stepped patterns corresponding to the interface with carbonate grains in its marble host rock. Photomicrograph by N. Renfro; image width 4.92 mm.

two minerals competed for space in their growth environment (Figure 5).

Heat Treatment Detection

Gems are often treated in ways that leave microscopic evidence. Sometimes this evidence is so subtle that it is difficult to resolve using traditional microscopic illumination. DIC microscopy can help reveal these hidden clues to the observant gemmologist. In particular, heat treatment can cause subtle melt damage on the surface of gems (Gübelin and Koivula, 2008; Koivula, 2009). If a stone does not appear obviously damaged after treatment, then there will be no reason to repolish it, and such evidence may be visible with DIC microscopy.

At the GIA Laboratory in Carlsbad, California, USA, a blue sapphire was recently examined that showed no internal or spectroscopic evidence that it had been heated. However, upon closer inspection using episcopic DIC microscopy, melt damage on the facets of the stone was revealed, proving the sample had been subjected to heating (Figure 6, left). Additionally, when gem corundum is heated, tiny glassy melt droplets are occasionally fused to the surface of the stone. If the gem's surface was not noticeably damaged during the treatment, and therefore not repolished after heating, then viewing these glassy melt droplets with DIC microscopy also provides evidence that the stone has been heated (Figure 6, centre and right).

Damage Assessment

Although diamonds are among the hardest materials known, they are still susceptible to cracking along cleavage planes, should they sustain an impact from certain directions. If a cleavage fracture is observed in a diamond, it can be important to know if the damage was pre-existing or if perhaps it was introduced after polishing. This can help in determining, for example, if a jeweller may be liable for damaging a stone.

Drag lines are polish features that originate from surface imperfections such as graining, pits and cleavage fractures. Their association with a crack proves that the fracture must have existed prior to polishing. However, such drag lines can be extremely difficult, if not impossible, to observe using traditional reflected-light microscopic examination on diamonds that have an excellent or very good polish. Using episcopic DIC, these subtle polish lines can be resolved in high contrast, enabling the microscopist to determine whether a crack existed before the stone was polished (Figure 7, left), or if the gem was damaged after it was cut (Figure 7, right).

Figure 6: Melt damage on the surface of a faceted sapphire (left) is clearly seen using episcopic DIC microscopy, which proves that it was heated after the cutting process. Glassy droplets fused to the surface of a polished sapphire also confirm heat treatment (centre and right). The sharp straight lines are facet junctions. Also apparent in the right-hand image are polish lines that were plastically deformed during heat treatment, taking on an irregular, wavy appearance. Photomicrographs by N. Renfro; image width 1.24 mm (left and right) and 0.62 mm (centre).

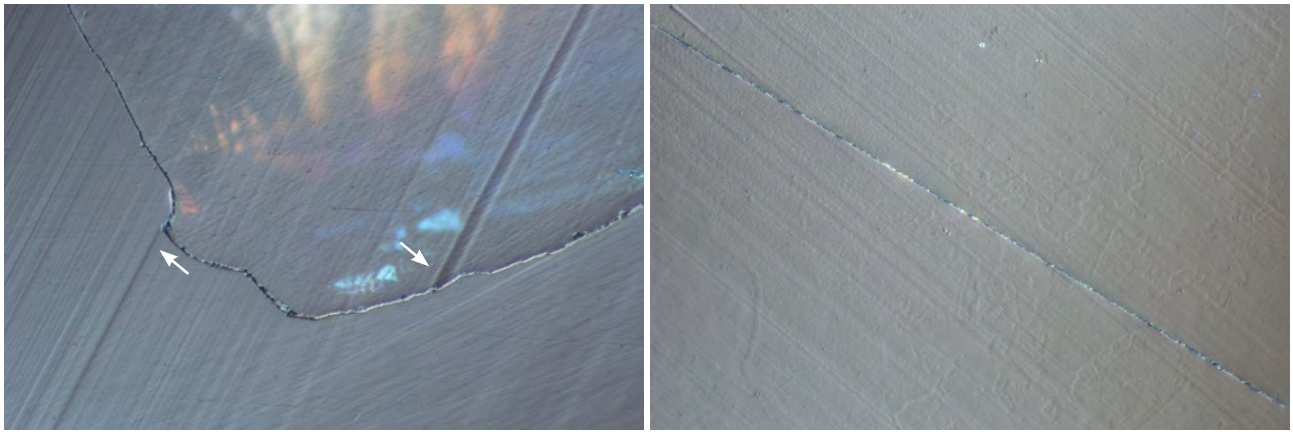

Figure 7: Polish lines that originate from a crack or surface defect can be difficult to see without episcopic DIC microscopy. The left image shows polish lines that stop or start along a fracture in a diamond, proving that the crack was present at the time the stone was polished. By contrast, polish lines that continue across a crack uninterrupted (right) indicate that the diamond was damaged after polishing. Also visible in the right-hand image are subtle irregular surface features known as 'burn marks' that were created from the heat generated while polishing the diamond. Photomicrographs by N. Renfro; image width 0.25 mm.

Conclusion

Episcopic DIC can reveal otherwise unobservable characteristics and information about a gem and is quite useful for certain applications, such as viewing surface features on rough gems, detecting heat treatment in stones that have not been repolished and assessing the timing of damage (fractures) relative to when a diamond was polished. Because of the sharp contrast and spectacular colour palette that is possible, DIC imaging often produces striking artistic photomicrographs where science and art are merged into a single image (Renfro, 2015).

References

Brandmaier C., Spring K.R. and Davidson M.W., 2013. Reflected light DIC microscopy. http://microscopyu.com/articles/dic/reflecteddic.html.

Evans D.J.F., Fisher D. and Kelly C.J., 2005. Coated pink diamond—A cautionary tale. *Gems & Gemology*, **41**(1), 36–41, http://dx.doi.org/10.5741/gems.41.1.36.

Gübelin E.J. and Koivula J.I., 2008. *Photoatlas of Inclusions in Gemstones*, Vol. 3. Opinio, Basel, Switzerland, p. 332.

Horikawa Y., 2001. Identification of a new type of laser treatment (KM treatment) of diamonds. *Journal of Gemmology*, **27**(5), 259–263, http://dx.doi.org/10.15506/jog.2001.27.5.259.

Koivula J.I., 1988. Etch figures on beryl. *Journal of Gemmology*, **21**(3), 142–143, http://dx.doi.org/10.15506/jog.1988.21.3.142.

Koivula J.I., 2000. *Microworld of Diamonds*. Gemworld International, Northbrook, Illinois, USA.

Koivula J.I., 2009. Micro-magma chambers in natural rubies and sapphires: The behavior of some mineral inclusions in corundum at high temperatures. www.gia.edu/ongoing-research/micro-magma-chambers-in-natural-rubies-and-sapphires.

Nomarski G., 1960. Interferential Polarizing Device for Study of Phase Objects. US Patent No. 2,924,142 A, issued 9 February.

Pluta M., 1989. *Advanced Light Microscopy: Specialized Methods*, Vol. 2. Elsevier, Amsterdam, The Netherlands.

Renfro N., 2015. Digital photomicrography for gemologists. *Gems & Gemology*, **51**(2), 144–159, http://dx.doi.org/10.5741/gems.51.2.144.

Sunagawa I., 1964. A distinction between natural and synthetic emeralds. *American Mineralogist*, **49**(5–6), 785–792.

Takahashi Y. and Sunagawa I., 1998. Tourmaline: Morphological and compositional variations during the growth history of uvite single crystals. *Journal of Gemmology*, **26**(4), 226–237, http://dx.doi.org/10.15506/jog.1998.26.4.226.

The Author

Nathan Renfro FGA

Gemological Institute of America, Carlsbad, California, USA. Email: nrenfro@gia.edu

Acknowledgement

The author thanks John Koivula (GIA, Carlsbad) for his constructive advice pertaining to the applications of DIC microscopy and for introducing the author to this technique.

YOUR GLOBAL PARTNER

Gem Identification Report and Gemstone Memo

GIT, The utmost advanced Gem and Precious Metal Testing Laboratory in Thailand, is recognized by CIBJO (The World Jewellery Confederation) and also a member of LMHC and ICA, we are well equipped with the world's most advanced instruments operated by highly experienced gemologists.

LABORATORY SERVICES

ensuring the authenticity of your valuable gems & jewelry

The Gem and Jewelry Institute of Thailand (Public Organization)
140 ITF Tower, Silom Rd., Bangkok 10500,Thailand
TEL : +66 2634 4999 FAX : +66 2634 4970
http://www.git.or.th E-mail: jewelry@git.or.th

Conferences

34th International Gemmological Conference

The 34th biennial IGC took place in Vilnius, Lithuania, on 26–30 August 2015. The conference was organized by **Dr Arūnas Kleišmantas** (Vilnius University, Lithuania), **Vilma Misiukonienė** (Infobalt Lithuania, Vilnius) and **Dr Jayshree Panjikar** (PANGEMTECH, Pune, India) in collaboration with Vilnius University and duSafyrai gem laboratory and museum in Vilnius. Approximately 75 delegates, observers and guests gathered for the event (Figure 1), and some of them attended pre- and post-conference field trips. Individual abstracts of the oral and poster presentations, as well as the entire proceedings volume, can be downloaded at www.igc-gemmology.net/proceedings.

Lithuania is a source of Baltic amber, and several presentations focused on amber from this region and elsewhere. **Dr Sigitas Podenas** (Vilnius University, Lithuania) reviewed the broad diversity of crane flies preserved as inclusions in Baltic amber. A total of 160 species representing five genera have been identified, and these lived during the latter part of the Eocene epoch, approximately 54 to 44 million years ago. **Dr Albertas Bitinas** (Klaipeda University, Lithuania) covered the geological origin of amber in the south-east Baltic Sea region. The deposits originated from resin of a *Pinus succinifera* forest and were transported by rivers and then deposited in deltas. Today, amber is known to exist in a 2-m-thick layer of silty sands on the Sambia Peninsula in the Kaliningrad area of Russia, at a depth of 10 m below the present sea level. Erosion of this layer during periods of lower sea level (approximately six million years ago) released some of the amber into the Baltic Sea, where it was

Figure 1: Delegates, observers and guests of the 34th International Gemmological Conference gathered at Trakai Castle in Lithuania for a group photo. Courtesy of B. M. Laurs.

eventually redeposited in offshore spits and lagoons. **Dr Jonas Satkūnas** (Lithuanian Geological Survey, Vilnius) discussed amber production in Lithuania, beginning with the 1858 establishment of Stantien & Becker for gathering amber from the northern part of the Curonian Lagoon. More recently, in 1992–1994, exploration by the Lithuanian Geological Survey near the town of Klaipeda identified an inferred resource of 227 tonnes that could produce an estimated 20–30 tonnes/year of amber, but mining in this area is currently restricted so it is unlikely that the deposits will be exploited. **Willow Wight** (Canadian Museum of Nature, Ottawa) reviewed Canadian amber localities. Although not commercially important, deposits are known at Cedar Lake in Manitoba (Late Cretaceous) and from three sites in the Canadian Arctic (Eocene). **Dr Lore Kiefert** (Gübelin Gem Lab, Lucerne, Switzerland) discussed natural-colour green amber from central Ethiopia, which was discovered in 2010 in Cretaceous sediments that are overlain by Tertiary basalt. It is hypothesized that heat from the basalt flow caused the green coloration of the amber. **Tay Thye Sun** (Far East Gemological Laboratory, Singapore) and co-authors characterized Burmese amber from a relatively new locality near Hti Lin (see article on pp. 606–615 of this issue of *The Journal*).

In diamond presentations, **Dr Thomas Hainschwang** (GGTL Laboratories, Balzers, Liechtenstein) and co-authors examined unusual black diamonds containing inclusions of lonsdaleite (the hexagonal polymorph of diamond) and CO_2. Although such diamonds may be mistakenly identified as synthetic based on the one-phonon region of their infrared spectra, they actually consist of polycrystalline aggregates of natural diamond that are heavily included by non-diamond carbon. **Dr Hiroshi Kitawaki** (Central Gem Laboratory, Tokyo, Japan) and co-authors described type Ib yellow to brownish yellow CVD synthetic diamonds (see article on pp. 594–604 of this issue of *The Journal*). **Dr Joe C. C. Yuan** (Taiwan Gemmological Institute, Taipei; and Solstar Diamond Co. and Taidiam Technology, Zhengzhou, China) predicted that high pressure, high temperature (HPHT)–grown synthetic diamonds produced under even (not gradient) temperature conditions will likely become the most important type of gem-quality synthetic diamonds in the future.

In presentations on gem corundum, **Anette Juul-Nielsen** (Ministry of Mineral Resources, Nuuk, Greenland) provided an update on small-scale mining of rubies and pink sapphires near Fiskenaesset, Greenland. She reported a significant increase in the number of small-scale licences issued, although most activities are focusing on prospecting rather than production at this early stage. **Dr Jayshree Panjikar** and **Aatish Panjikar** investigated the cause of asterism in star ruby from Neriya, Karnataka, India. They attributed the asterism to the presence of rutile needles in addition to micro-inclusions of tialite (Al_2TiO_5, identified by Raman spectroscopy in hazy areas of the gems). **Kentaro Emori** and **Dr Hiroshi Kitawaki** (Central Gem Laboratory, Tokyo, Japan) reported on the geographic origin determination of ruby and blue sapphire based on trace-element analysis using laser ablation–inductively coupled plasma–mass spectrometry (LA-ICP-MS) data in three-dimensional plots. Due to some overlap between localities, they found that such data can help with origin determination but that more analyses are needed from samples of known provenance. **Dr Stefanos Karampelas** (Gübelin Gem Lab, Lucerne, Switzerland) discussed recent research on zircon inclusions in blue sapphires done by **Emilie Elmaleh** (University of Geneva, Switzerland) and their co-authors. Potentially locality-specific characteristics of the zircon inclusions consist of cathodoluminescence zoning features and U-Pb age data, but more research is needed before they can be applied to the origin determination of sapphire. **Dr J. C. (Hanco) Zwaan** (Netherlands Gemmological Laboratory, Leiden) and co-authors performed inclusion and LA-ICP-MS trace-element studies of alluvial sapphires from Montana, USA. Both the inclusion suite and a plot of Fe vs. Ga/Mg supported a metasomatic origin for these sapphires. **E. Gamini Zoysa** (Institute of Gemmological Sciences, Colombo, Sri Lanka) reviewed sapphire deposits of Sri Lanka. He described recent mining at Wellawaya for in-situ corundum, at Getahetta for sapphire 'geodes', at Bogawantalawa for large opaque corundum crystals, and overall gem production from Hasalaka, Elahara and Kolonna. **Dr Karl Schmetzer** (Petershausen, Germany) and co-authors reported on dual-colour double stars in corundum and quartz; these results were recently published in *Gems & Gemology* (Vol. 51, No. 2, 2015, pp. 112–143). **Dr Visut Pisutha-Arnond** and co-authors (Gem and Jewelry Institute of Thailand, Bangkok) performed Be-diffusion experiments on sapphires under reducing and oxidizing conditions. Trapped-hole centres that formed during oxidative heating were inactivated by heating in a reducing atmosphere, and therefore the resulting colour was solely controlled by the Mg/Ti ratio in the sapphires. Further heating under oxidizing conditions reactivated the Be-induced trapped-hole centres. **Dr Walter A.**

Balmer (Swiss Gemmological Institute SSEF, Basel, and Chulalongkorn University, Bangkok, Thailand) and **Dr Michael S. Krzemnicki** provided preliminary results of using Fourier-transform infrared (FTIR) spectroscopy to detect Be diffusion in corundum. The presence of a weak band at 2490 cm^{-1} appears to indicate that a sample was Be diffused, but the absence of this peak is inconclusive. **Dr Pornsawat Wathanakul** (Gem and Jewelry Institute of Thailand, Bangkok) presented the results of an investigation by Thanong Leelawatanasuk and other co-authors on 'surface de-leaded' glass-filled ruby. Lead was reportedly removed from the glass filling near the surface of these stones so that the treatment would be more resistant to the heat of a jeweller's torch. The examined samples showed features consistent with typical glass-filled rubies. Energy-dispersive X-ray fluorescence (EDXRF) spectroscopy of the stones' surfaces appeared to show less Pb than typical glass-filled rubies, but more data is needed since the Pb content recorded by this technique is dependent on the overall amount of glass-filled fractures in the area analysed, as well as on the amount of Pb in the glass. Using photoluminescence spectroscopy, **Dr Ahmadjan Abduriyim** (Gemological Institute of America [GIA], Tokyo Laboratory, Japan) examined the residual pressure distribution of mineral inclusions in sapphires from New England, New South Wales, Australia. The pressure surrounding the inclusions was visualized and quantified, but the technique is only applicable to unheated sapphires and inferring the original crystallization conditions is not possible due to annealing that occurred during magmatic transport of the sapphires to the earth's surface. **This author** reported on mining methods for ruby and other gems in primary and secondary deposits near Mogok, Myanmar (see Gem Notes on pp. 387–390 of *The Journal* Vol. 34, No. 5, 2015).

In other coloured stone topics, **Dr Edward Liu** (Gemmological Association of Hong Kong) and co-authors used variable pressure–scanning electron microscopy–energy dispersive spectroscopy and backscattered electron imaging coupled with a Raman spectroscopy system to perform non-destructive in-situ chemical and structural analyses of jadeite (*fei cui*). The technique was useful for differentiating areas of jadeite and omphacite within compositionally and texturally zoned samples. **Prof. Mimi C. M. Ou Yang** (Hong Kong Institute of Gemmology) and co-authors described the texture of jadeite (*fei cui*). Using cathodoluminescence and microscopic observation of petrographic thin sections, various jadeite varieties could be correlated to different textures according to their grain size and the granoblastic or porphyroblastic size distribution of their mineral constituents. **Shane F. McClure** (GIA Laboratory, Carlsbad, California, USA) described the mining, cutting and gemmological properties of emeralds from the Belmont mine in Brazil. He witnessed the faceting of an unusually large piece of rough (29.8 g) into a fine rectangular step-cut gem weighing 18.17 ct (together with numerous small stones) that was set into a custom diamond ring. **Masaki Furuya** (Japan Germany Gemmological Laboratory, Kofu, Japan) and **Scott Davies** studied the gemmological features of pallasitic peridot from six different meteorites (Admire, Brahin, Esquel, Fukang, Jepara and Seymchan). Peridot from two of the meteorites, Jepara and Seymchan, contained inclusions that were distinctive enough to identify their host bodies. Using a combination of trace-element analysis and FTIR and ultraviolet-visible–near infrared (UV-Vis-NIR) spectroscopy, the meteoritic origin of the various samples could be determined in some cases. Peridot from Esquel and Fukang were the most difficult to separate, and those meteorites may have come from the same origin in space. **Roman Serov** and co-authors (all from the Gemological Center, Lomonosov Moscow State University, Russia) examined the colour origin of Russian demantoid using heating experiments. The optimal heating conditions (up to 650°C in reducing conditions) modified the intensity of the 430 nm cutoff in the UV-Vis spectra, resulting in a less brown and more green coloration; this suggested that the colour was caused by intervalence charge transfer between Fe^{2+} and Ti^{4+} or involving Fe^{3+}. **Dr Andy H. Shen** and co-authors (all from China University of Geosciences, Wuhan) reported on the country-of-origin determination of nephrite jade from East Asia. They developed a statistical method (iterative binary linear discriminant analysis) to process large amounts of trace-element data generated by LA-ICP-MS analyses. Using 22 elements, they were successful in separating samples from eight localities to a high degree of confidence. **Karen E. Fox** (Waterloo, Ontario, Canada) reported on recent visits to Australian opal deposits at Lightening Ridge, Yowah and Coober Pedy, and also discussed opal's stability to crazing. **Dr Emmanuel Fritsch** (Institut des Matériaux Jean Rouxel and University of Nantes, France) and co-authors described green-luminescing hyalite opal from Zacatecas, Mexico (see article on pp. 490–508 of *The Journal* Vol. 34, No. 6, 2015). **Dr Ulrich Henn** (German Gemmological Association, Idar-Oberstein) reported the properties of some rare

gem materials: wurtzite from Merelani, Tanzania; mosandrite from the Kola Peninsula, Russia (see Gem Note on pp. 565–566 of this issue of *The Journal*); and buchite from Eifel, Germany (see Gem Note on pp. 562–563 of this issue of *The Journal*). **Dr Claudio C. Milisenda** (German Gemmological Association, Idar-Oberstein) and co-authors examined some gemstones with photochromism: hackmanite, tugtupite and scapolite. The interesting colour behaviour of these gems is due to S_2^- ions. **Dr Dietmar Schwarz** (Asian Institute of Gemological Sciences Lab Co. Ltd., Bangkok, Thailand) gave an overview of mines and markets for coloured gemstones. He indicated that East Africa is the most promising area for coloured stone production, and some recent trends in the industry include involvement by large mining companies and the importance of ethical mining and marketing.

Several talks focused on pearls. **Prof. Dr Henry A. Hänni** gave a presentation for **Dr Michael S. Krzemnicki** (both from the Swiss Gemmological Institute SSEF, Basel) and co-authors on the imaging of pearls using X-ray phase contrast and X-ray scattering. X-ray analysis with a grating interferometer allows for simultaneous measurement of conventional X-ray absorption, refraction (phase contrast) and scattering, with improved sensitivity to light materials such as soft tissue. The procedure is fast (seconds to minutes) and may be used to analyse an entire necklace at once. Using known natural and non-bead-cultured *Pinctada maxima* pearls, **Nick Sturman** (GIA Laboratory, Bangkok, Thailand) and co-authors illustrated several examples showing the challenges of correctly interpreting structures seen using X-ray computed microtomography. **Sutas Singbamroong** (Dubai Central Laboratory, United Arab Emirates) and co-authors presented observations of natural non-nacreous pearls reportedly from various *Tridacna* clam species. Observations of a large collection of these pearls showed that they were mostly white (some had yellow areas) and semi-translucent to opaque with chalky blue long-wave UV fluorescence. Many had well-developed flame structures that sometimes showed iridescence. SG values typically ranged from 2.81 to 2.85, although some had significantly lower values of 2.63–2.67. X-radiography commonly revealed no internal features, or only dark areas (probably organic material) in the core of those that had the lower SG values. **Dr Jayshree Panjikar** gave a presentation for **Elisabeth Strack** (Gemmologisches Institut Hamburg, Germany) on freshwater pearls from Wisconsin, USA. These pearls were gathered from the 1930s until 1996 (when pearl fishing was banned) and are found in local museums and private collections, in addition to being available from a few local dealers. They are typically white (less commonly pink, purple, blue or green) and range up to 15+ mm, with baroque shapes being most common.

There were two presentations related to instrumentation. **Dr Lutz Nasdala** (University of Vienna, Austria) and co-authors described the search for appropriate gem zircon samples to use as an analytical reference material for age dating using ion microprobes. Large cut gemstones from Ratnapura, Sri Lanka, have shown good potential for such reference material. **Manfred Eickhorst** (System Eickhorst, Hamburg, Germany) recounted technical progress on the use of light-emitting diodes (LEDs) in gemmological instruments. The main benefits of LED lighting are that it is cool to the touch and has versatility with regards to spot vs. diffused beam types and colour temperature/wavelength (from daylight to long-wave UV).

Poster presentations covered diverse topics. **Gagan Choudhary** (Gem Testing Laboratory, Jaipur, India) described emeralds from Jharkhand State, India, which are unusual for being free of any fluid inclusions. **Helmut Pristacz** (University of Vienna, Austria, and University of Tokyo, Japan) and co-authors studied synthetic turquoise from the Natural History Museum in Vienna, Austria, and found that it had an oolitic microstructure composed of a fibrous amorphous phase (related to the high-pressure berlinite structure) together with natural turquoise (presumably used as a starting material) and synthetic turquoise. **Antonello Donini** and co-authors (all from CISGEM Laboratory – Fondazione Gemmologica Italiana, Milan) described some unusual gemmological materials seen in their laboratory, including several ornamental objects made from rhinoceros horn and a necklace composed of ambergris (an intestinal secretion produced by sperm whales). **Dr Emmanuel Fritsch** and **Joel Ivey** characterized 'Mustard Jasper' or 'Bumble Bee Stone' from western Java, Indonesia, which consists of calcite that is coloured yellow to orange by inclusions of pararealgar and realgar (both polymorphs of As_4S_4) and black by pyrite impurities. **Dr John M. Saul** (Oryx, Paris, France) examined the historical use of the word *electrum* for both amber and for the naturally occurring alloy of gold and silver. **Dr Guanghai Shi** (China University of Geoscience, Beijing) and co-authors examined the infrared spectral characteristics of amber from three sources: the Baltic Sea, Dominican Republic and Myanmar. Transmission spectra were obtained by specular reflection using the KBr pellet method, and could be correlated with the ambers' age, plant provenance and geological environment. **Elizabeth Su** (Gemsu Rona, Shanghai,

China) described jadeite markets in China, including wholesale outlets in Guangdong Province (Yangmei, Guangzhou, Pingzhou and Sihui) and Yunnan Province (Ruili, Tengchong and Kunming), as well as retail markets in Beijing and Shanghai. **Thanong Leelawatanasuk** and co-authors (all from The Gem and Jewelry Institute of Thailand, Bangkok) provided an update on their studies of treated 'black' sapphires that appeared in late 2013 and mid-2014. The very dark blue body colour of these gems resulted from the Ti-diffusion treatment of heavily fractured starting material of metamorphic origin. **Supparat Promwongnan** and co-authors (all from The Gem and Jewelry Institute of Thailand, Bangkok) described a synthetic ruby overgrowth on natural corundum encountered in early January 2015. Such material was circulated in the market in the early 2000s and sold under the misleading name 'diffusion ruby'. It can be identified by a sharp contact boundary between the core and the overgrowth seen under immersion, as well as contrasting fluorescence behaviour shown with the DiamondView.

This author also attended the post-conference field trip, which visited amber museums (e.g. Figure 2) and an amber-processing facility in Lithuania (to be reported in the next issue of *The Journal*).

Brendan M. Laurs

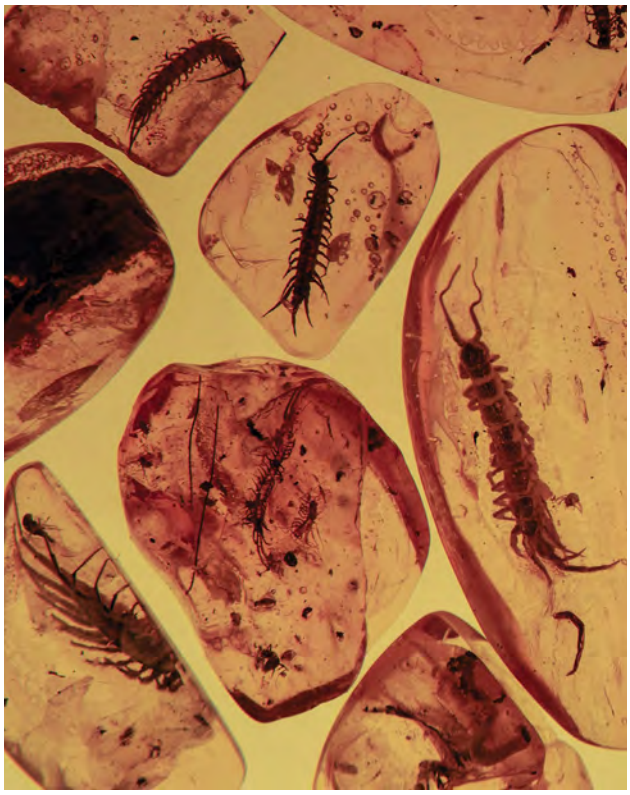

Figure 2: Polished pieces of Baltic amber containing various inclusions (here, millipedes, ~1–2 cm long) were on display at the Amber Queen Museum in Klaipeda, Lithuania. Photo by B. M. Laurs.

1st Mediterranean Gemmological and Jewellery Conference

On 27–28 June 2015, Athens (Greece) was host to the first of a new series of conferences—the Mediterranean Gemmological and Jewellery Conference, organized by the Independent Gemological Laboratory (IGL, Athens, Greece) and CGL-GRS Swiss-Canadian Gemlab (Vancouver, British Columbia, Canada). The event featured an international line-up of speakers and covered a range of topics, including synthetic diamonds, pink diamonds, pearls, rubies and gem treatments. A conference proceedings volume is available from IGL for €10 before 1 February 2016 by emailing iglcert@yahoo.com.

Growing synthetic diamonds using both gradient and even-temperature HPHT methods was addressed by **Dr Joe Yuan** (Taiwan Gemmological Institute, Taipei; and Solstar Diamond Co. and Taidiam Technology, Zhengzhou, China). The latter method produces small octahedral crystals suitable for cutting melee. Samples of colourless rough and cut synthetic diamonds were available for inspection and purchase, along with CVD-grown samples. Dr Yuan described microscopic and spectroscopic characteristics useful for detecting synthetic diamonds, a theme that was continued in detail by **Dr Thomas Hainschwang** from GGTL Laboratories (Balzers, Liechtenstein), who has screened thousands of colourless melee diamonds and to date found only one that was a CVD synthetic. In contrast, his lab has found that all parcels of yellow melee diamonds examined since 2011 were contaminated with synthetics, usually at levels of 1–2% but in one instance as high as 35%. To aid in the detection of synthetic diamonds, instruments have been produced by De Beers, which **Dr Brad Cann** (De Beers Technologies, Maidenhead) described, with special focus on identifying CVD synthetics. A recent optical modification to the DiamondView instrument enhances the visibility of red fluorescence from NV and Si-V centres, indicative of synthetic origin. A late programme change accommodated a talk by **Andre Katrusha**, research adviser for New Diamond Technology (St Petersburg, Russia), on the global synthetic diamond industry and in particular on recent achievements that include producing the world's largest colourless synthetic diamond. The

rough specimen weighed 32 ct, and was polished into a 10.02 ct (E colour, VS_1 clarity) emerald-cut gem that was inspected by many of the conference participants at the end of the day, along with other synthetic diamonds of various colours displayed by Voldstat Diamonds (Seddiner See, Germany). **Heiner Voldstat** from the company presented two posters on growth methods and equipment, including toroid presses.

While much technology has been aimed at colourless diamonds, **Branko Deljanin** (CGL-GRS Swiss-Canadian Gemlab) has directed his research on pink and blue colours. He shared his findings on the birefringence, fluorescence and spectroscopic features that can distinguish Argyle pink and blue diamonds from CVD-grown treated pink and blue synthetics coming from new producers in Asia and USA. His talk was complemented by a presentation by **this author** on pink diamonds from the Argyle mine, covering their history, production, grading and pricing, as well as their colour-change behaviour.

In other presentations, **Dr Thomas Hainschwang** discussed cultured pearls and practices used to disguise their detection, particularly initiating growth with plastic beads or natural pearls, both of which are difficult to detect in X-radiographs. **Wolf Kuehn** (Gemlab Research and Technology, Vancouver, Canada) introduced participants to portable spectrometers and light sources for making absorption, Raman and luminescence spectral measurements, and how the spectra can be used to identify gems. **Andre Huber** (GRS, Switzerland) surprised delegates with price comparisons between Burmese and Mozambican rubies, both of which have enjoyed 300–400% price increases since 2011 and have risen 25% in the past six months. To appreciate the difficulty of mining rubies, a 3D movie was shown of a mine visit in Mogok, Myanmar by **Dr Adolf Peretti** from GRS. The challenges of valuing antique jewellery were highlighted by **Gail Brett Levine** (National Association of Jewelry Appraisers, Rego Park, New York, USA), who stressed the importance of using comparable items, both to help recognize modifications and to understand factors that affect value.

Figure 3: Nikolai Khikhinashvili shows synthetic diamonds to workshop attendees at the Mediterranean Gemmological and Jewellery Conference. Photo by J. G. Chapman.

The day concluded with a 'roundtable' discussion moderated by **this author**, with panellists representing various producers and laboratories. An audience of 65 asked questions about the market for synthetic diamonds, production technologies and melee screening (for details, see https://gemconference.com/round-table-synthetics). Special guest **Nikolai Khikhinashvili** of New Diamond Technology also shared information about the three largest HPHT-grown synthetic diamonds that they produced in the past six months.

The second day of the conference featured a workshop conducted by **Branko Deljanin** that provided hands-on instruction in the detection of synthetic and treated diamonds (Figure 3). The 40 samples that were provided were studied by 30 participants using polariscopes, microscopes and a UV lamp.

The success of the conference has ensured that next year a second Mediterranean Gemmological and Jewellery Conference will take place, and it is scheduled for 7–8 May 2016, in Valencia, Spain. Further details will be available at www.gemconference.com.

John G. Chapman (john@gemetrix.com.au)
Gemetrix Pty. Ltd., Perth, Western Australia

13th Society of Geology Applied to Mineral Deposits Meeting

The Society of Geology Applied to Mineral Deposits (SGA) was founded in 1965 in Heidelberg, Germany, and the 2015 SGA meeting celebrated the 50th anniversary of the Society. The 13th SGA biennial meeting was held in Nancy, France, from 24 to 27 August. The conference theme was Mineral Resources in a Sustainable World, and the meeting included 15 sessions and five symposia. Session 12 was dedicated to Gems and Industrial Materials, and was chaired by Prof. Lee Groat (University of British Columbia, Vancouver, Canada), Dr Daniel Ohnenstetter (Centre de Recherches Pétrographiques et Géochimiques [CRPG], Nancy, France), this author and

Prof. François Martin (University of Toulouse, France). Gem topics were covered in four oral presentations and two posters. Extended abstracts are published in André-Mayer et al. (2015).

Dr Yannick Branquet (University of Orléans, France) discussed the tectono-stratigraphic significance of a regional emerald-bearing evaporitic breccia horizon in the Gachalá-Chivor-Macanal area of Colombia. This horizon contains evidence of sabkha-like evaporitic sediment reworking and destabilization on active sedimentary slopes. Detailed field, petrographic and structural evidence highlighting the role of evaporites in the formation of Colombia's eastern emerald belt were presented. The emerald deposits formed 65 million years ago in local extensional structures related to the initiation of a foreland bulge and associated flexure, via the migration of hot, saline and overpressurized fluids at depths of 5–6 km.

This author investigated the oxygen and hydrogen isotopic compositions of emeralds from the Ianapera deposit at Madagascar. The isotopic data indicate a magmatic-hydrothermal origin for these emeralds. The oxygen isotopic composition of water in equilibrium with emerald coupled with the hydrogen isotopic composition of water in the emerald channels fit with the isotopic water values defined for S-type granitic magmatism.

This author also delivered a presentation for **Dr Jean-Emmanuel Martelat** (University of Lyon 1, France) on the U-Pb ages of zircon and monazite from tsavorite-bearing Neoproterozoic rocks of south-eastern Kenya and the significance of static crystallization of the tsavorite. Detailed field investigations, geochemical studies and U-Pb radiometric dating of various geological formations in the Kasigau and Kurase areas showed that the formation of tsavorite in the Voi region was the result of a metasedimentary sequence preserved from strain but heated by surrounding granulitic rocks between approximately 600 and 595 million years ago.

Albert Gilg (Technische Universität München, Germany) used a variety of non-destructive methods (Raman and UV-Vis spectroscopy, and portable EDXRF analysis) to characterize more than 90 rough and 25 faceted gem-quality pyropes from various localities in Bohemia, and compared their properties to pyrope samples from other significant locations worldwide as well as red Cr-poor magmatic pyropes. This resulted in criteria used for determining the provenance of Cr pyropes in archaeological and historical jewellery (i.e. Merovingian cloisonné jewellery from Bavaria, religious objects of the St Vitus treasure in Prague and Bohemian costume jewellery from the 19th century in Sudetendeutsche Museum in Munich).

Dr Daniel Ohnenstetter delivered a poster on the boron isotopic composition of tourmaline from tsavorite deposits in the Neoproterozoic Mozambique Metamorphic Belt, with a special focus on the mining districts in Kenya. Dravitic tourmalines associated with different types of rock from tsavorite-bearing metasedimentary sequences in Kenya, Tanzania and Madagascar show two ranges of isotopic compositions. The first range is for dravites associated with tsavorite in nodules, which clearly involve continental evaporitic boron material. The second concerns dravites from clastic metasediments, metapegmatite and marbles intercalated in the metasedimentary sequence containing tsavorite nodules, which reflect a magmatic source for clastic dravite and probably an evaporitic one for dravite in marble.

Dr Juan Manuel Garcia presented a poster on the first known occurrence of green quartz related to a polymetallic Cu-Au-Mo porphyry-type deposit in Argentina. The quartz is hosted by a vein-related shear zone and is associated with sulphide, sulphosalt, carbonate and manganese oxide minerals. Preliminary data suggest that the shear-zone-related deformation in the deposit, along with the circulation of hydrothermal fluids and reprecipitation of silica due to pressure dissolution mechanisms, led to the generation of green quartz from the deformation and dissolution of previous smoky quartz. A genesis from a radioactive source is discounted since rocks with high potassium content were not found in the study area.

Reference

André-Mayer A.S., Cathelineau M., Muchez P., Pirard E. and Sindern E., Eds., 2015. *Mineral Resources in a Sustainable World—Proceedings of the 13th Biennial SGA Meeting,* Nancy, France, 24–27 August, six volumes, 2,134 pages (see Vol. 4 for gem-related abstracts).

Dr Gaston Giuliani (giuliani@crpg.cnrs-nancy.fr)
Institute of Research for Development at CRPG and University of Lorraine, France

Gem-A Notices

GIFTS TO THE ASSOCIATION

The Association is most grateful to the following for their gifts for research and teaching purposes:

Mattias Haag, Lothar Haag, Idar-Oberstein, Germany, for three emeralds (0.84–0.97 ct) from Brazil, Zambia and Colombia.

I**an Mercer FGA**, Chelmsford, Essex, for a copy of *Chinese Jade* by Yu Ming.

Roy Rimington, Bristol, for a rough sample and a polished sphere of plastic imitation ivory.

Antonio Silva, London, for copies of *Jules Sauer – O Caminho Das Pedras* by Mariucha Monero and *The Eras of the Diamond* by Jules Roger Sauer, as well as samples of dendritic agate, howlite, kyanite, opal and various ornamental stones.

Tay Thye Sun FGA, Far East Gemological Laboratory, Singapore, for seven pieces of tumbled amber from Tanai, Hukawng Valley, Myanmar.

ANNUAL GENERAL MEETING

The Gem-A Annual General Meeting was held on 29 July 2015 at The Crypt, 14 Ely Place, London EC1N 8SJ. The meeting was chaired by Nigel Israel, the Chairman of the Council. The Annual Report and Accounts were approved. Hazlems Fenton were re-appointed as auditors for the year.

The AGM was adjourned on the Agenda item 'Election of the Council' until 26 August, when the AGM was reconvened in the Bruton Room at Gem-A, 21 Ely Place, London EC1N 8TD. Jessica Cadzow-Collins and Alan Hart had been appointed to the Council since the previous AGM, and Paul Greer and Richard Slater who retired in rotation, sought re-election to the Council; Paul Greer, Alan Hart and Richard Slater were re-elected. Kathryn Bonanno, Justine Carmody, Kerry Gregory, Alan Hodgkinson, Jack Ogden and Christopher Smith were elected to serve on the Council.

CHIEF EXECUTIVE OFFICER

In July the Association parted company with James Riley, its Chief Executive Officer (CEO), and we thank him for the many good things he did for the Association during his tenure.

MEMBERSHIP

On 23 July 2015, the Council elected the following to membership:

Fellowship and Diamond Membership (FGA DGA)

Smith, Jennifer, *Stourport-on-Severn, Worcestershire*

Fellowship (FGA)

Zerhouni, Yousra, *Montreal, Quebec, Canada*
Zhu Yuenan, *Hangzhou, Zhejiang, P.R. China*
Zuo Tenglong, *Zhengzhou City, P.R. China*

Diamond Membership (DGA)

Li Wenzhuo, *Wuhan, Hubei, P.R. China*
Yeung Yuen Man, *Shatin, Hong Kong*

Associate Membership

King, Rosanna, *Athy, Co. Kildare, Rep. of Ireland*
Lewis, Owen, *Winchester, Hampshire*
McAlister, Diana, *Reading, Berkshire*
Wiser, Fernand, *Luxembourg*

Fellowship of the Gemmological Association of Australia (FGAA) to FGAA FGA

ten Hoedt, Yma, *Beaconsfield, New South Wales, Australia*

At a meeting of the Council held on 11 September 2015, the following were elected to membership:

Fellowship and Diamond Membership (FGA DGA)
Timms, Andrew, *Lancaster, Lancashire*

Fellowship (FGA)
Caya, Elie-Anne, *Quebec, Quebec, Canada*
Fang Xiang, *Shanghai, P.R. China*
Ouahed, Daniel, *Montreal, Quebec, Canada*
Zhou Wei, *Basel, Switzerland*

Diamond Membership (DGA)
Struthers, Rebecca, *Birmingham, West Midlands*

Associate Membership
Alhaider, Ali, *London*
Buckland, John, *Bedlington, Northumberland*
Choudrie, Karina, *London*
Maddock, Jay, *Warrington, Cheshire*
Rodriquez Aguilar, Itzel Montserrat, *Woodinville, Washington, USA*
Szynkier, Diane, *Paris, France*
Walker, Gloria, *Southall, Middlesex*

Fellowship of the Gemmological Association of Australia (FGAA) to FGAA FGA
Murray, Peter, *West Hobart, Tasmania, Australia*

Corporate Membership
Jewellery Quarter Bullion, *Birmingham, West Midlands*

OBITUARIES

Ian Campbell
1931–2015

The gemmological communities in Southern Africa and Europe were devastated at the end of July this year by the loss of one of our stalwarts, Ian Campbell.

An engineering draughtsman by trade, Ian's true passion was gemmology. In 1970 he became a Fellow of the Gemmological Association of Great Britain. He received a Diamond Grading and Evaluation Certificate in 1979, and went on to achieve certification as a Certified Valuator for the Gemmological Association of South Africa in 1988.

But Ian's achievements went far further than this. He enjoyed a lengthy stint in the Northern and Southern Rhodesian Government in the early 1950s, and continued to work in civil service even after he had launched his own gemmology business in 1965. His passion for the craft, his attention to detail and his ongoing commitment to learning saw him become a gemmology consultant in the early to mid-1970s.

Ian founded and managed the Coloured Stones Laboratory for the Jewellery Council of South Africa from 1980 until 1982, when he formed his own business, ICSL (Independent Coloured Stones Laboratory), which he operated until 2000. Ian's reputation for industry excellence spread far and wide, and his gemmological laboratory was recognized by both the Accredited Gemmologists Association in the USA and the International Coloured Gemstone Association. Ian also consulted to the European Gemological Laboratory, before finally retiring in 2010.

Ian was a prolific writer and was always ready to share his wisdom and experience with eager gemmologists, young and old. He published many reports and publications on his area of expertise, and eventually became the editor-in-chief of the *Great South African Gemmologist*, at one time South Africa's foremost gemmology publication.

Ever committed to ethical and accurate gemmology, Ian served as the founder and chairman of the Gemmological Association of Rhodesia and the Matabeleland Gem and Mineral Society. He was also a member of the International Society of Appraisers in the USA, the Accredited Gemmologists of South Africa, and the Micro-mount Society of South Africa.

Ian married Betty Keal at Umzinto, KwaZulu Natal, South Africa, on 11 December 1958. Between them they had three sons and a daughter, and our thoughts are with them at this time of loss. Ian's career and hobbies, which included a passion for fishing, led the family on a life of adventure as they travelled from Livingstone in Northern Rhodesia to Bulawayo in Southern Rhodesia. Ian also loved prospecting, going all over Matabeleland Province in Rhodesia in pursuit of amethyst, rose quartz and agate. When he was 49 years

old, Ian took up karate. Here, as in every aspect of his life, he was dedicated and committed. He achieved his black belt in the early 1990s at the age of 60.

I met Ian in 1985 at a karate training farm in Stilbaai, South Africa. Little did I know then that my life was about to change forever. I was fascinated by his compulsive pebble gathering, and when he explained that he was analysing the iron and minerals in the stones he collected, I was hooked. I sold the photographic equipment I had been collecting for my photography career, and spent every weekend for the next two years at Ian's laboratory. He became a mentor and friend, and set me on the path I walk today.

I owe Ian an enormous debt, as does the gemmological world at large. We are poorer for his passing.

…the river sliding along its banks, darker now than the sky descending a last time to scatter its diamonds into these black waters that contain the day that passed, the night to come.

— Excerpt from the poem
'The Mercy' by Philip Levine

Jeremy Rothon FGA
Kenilworth, Cape Town, South Africa

Tino Hammid

1952–2015

Internationally renowned gem and jewellery photographer Tino Hammid passed away too soon from cancer at the age of 63. His portfolio of work uniquely communicated the beauty of the gem world, in publications ranging from *The Journal of Gemmology* to *Gems & Gemology, Modern Jeweler,* Christie's auction catalogues and numerous trade publications and books including *Coloured Diamonds* (on the Aurora Collection) and *The Handbook of Gemmology*. Tino is survived by his wife Petra, young twins Antonia and Tobias, and adult daughter Evelyn.

The son of Academy Award–winning filmmaker Alexander Hammid, Tino began his career in gem photography at the Gemological Institute of America, where he worked as a staff photographer from 1980 to 1982. Robert Weldon, manager of photography and visual communications for GIA, told *JCK* he "always admired" Tino's work. Of Hammid's photographs, Weldon continued, "They are beautiful because of the attention he paid to detail—the attention he paid to the lighting, the positioning of the stone. His photos are all about the gem. His photography of gemstones has become the definition of excellence in what a gem photograph should be" (www.jckonline.com/2015/07/13/celebrated-gem-photographer-tino-hammid-dies).

In 1983 Tino started his freelance career in gem and jewellery photography, and this began a 25-year association with David Federman in providing images for *Modern Jeweler*'s monthly Gem Profile column. During this period they jointly won two Jesse H. Neal awards. "I always felt Tino was the Richard Avedon of gem photography," Federman told *JCK*. "He didn't take pictures, he took portraits. Colored stones 'sat' for him the way celebrities sat for Avedon." New York gem dealer Alan Bronstein, who worked with

The family: Tino between daughter Evelyn and wife Petra, with twins Antonia and Tobias.

Tino digitally placed these three D-Flawless diamonds (up to ~10 ct) on a background of stars that was taken by the Hubble telescope. Photo © Tino Hammid.

The beauty of the 90.38 ct Briolette of India diamond is captured in this impressive photograph. Courtesy of Christie's; photo © Tino Hammid.

Hammid on two books and on photographing the Aurora Collection, told *JCK* that Tino was "one of the greatest living gem photographers of our time". He continued, "Tino always strived for the purest, cleanest, and most honest photographs of the true color of cut and uncut gemstones. His integrity was unparalleled in his life and his work."

Most recently, in collaboration with author Geoff Dominy, Tino was delighted to contribute a large body of his work to *The Handbook of Gemmology* eBook, where he was able to render his images more accurately and beautifully in this digital medium (using RGB colour) than was possible in print. Of Tino, Dominy says "quite simply he was a genius and had the unique ability to coax the natural beauty out of a stone. He was more than a gem photographer, he was an artist who used the lens to paint the most beautiful pictures".

This author was fortunate to spend 15 years collaborating with and learning from Tino on all aspects of gem photography and digital processing, areas where Tino was always 'ahead of the curve' technically and artistically. He was enthusiastic and giving of his time and knowledge to anyone who asked. Tino had an avid interest in science and its application to his photographic imaging. Most appreciated by this author was his genius in capturing the beauty of colourless diamonds, one of the most challenging of gemstones to photograph well. That beauty, and his interest in astronomy, is apparent in his rendering of three diamonds against a starburst background taken from a Hubble telescope photograph. Equally stunning is his rendering for Christie's of the 90.38 ct Briolette of India, an historically important D-colour, type IIa diamond.

Tino will be missed by all who knew him, but fortunately his work lives on in his photographs.

Michael Cowing
ACA Gemological Laboratory
Crownsville, Maryland, USA

ERRATUM

In the Literature of Interest section of *The Journal* Vol. 34, No. 6, 2015, p. 556, the publication year for two of the articles listed from *Superhard Material Engineering* should have been given as 2014 rather than 2015. The titles of these articles are 'Distinction character of synthetic diamond in jewelry (1)' and 'Distinction character of synthetic diamond in jewelry (2)'.

Learning Opportunities

CONFERENCES AND SEMINARS

1st International Emerald Symposium
Bogotá, Colombia
13–15 October 2015
www.worldemeraldsymposium.com

Canadian Gemmological Association Gem Conference 2015
16–18 October 2015
Vancouver, British Columbia, Canada
www.gemconference2015.com

American Society of Appraisers International Appraisers Conference
18–21 October 2015
Las Vegas, Nevada, USA
www.appraisers.org/Education/conferences/asa-conference

2015 Geological Society of America Annual Meeting
1–4 November 2015
Baltimore, Maryland, USA
www.geosociety.org/meetings/2015
Session of interest: Gemological Research in the 21st Century – Exploration, Geology and Characterization of Diamonds and other Gem Minerals

Jewelry Virtual Expo
10–11 November 2015
Online conference
www.jewelriesexpo.com

36th Annual New Mexico Mineral Symposium
14–15 November 2015
Socorro, New Mexico, USA
www.geoinfo.nmt.edu/museum/minsymp/home.cfml

Gem-A Conference, hosting the 18th FEEG Symposium
21–22 November 2015
London
www.gem-a.com/news--events/events/gem-a-conference-2015.aspx
Note: Register soon for workshops and museum visits.

3rd Annual Jewelry History Series
26–27 January 2016
Miami Beach, Florida, USA
www.originalmiamibeachantiqueshow.com/show/jewelry-series

Compiled by Georgina Brown and Brendan Laurs

45th ACE IT Annual Winter Education Conference
31 January–1 February 2016
Tucson, Arizona, USA
www.najaappraisers.com/html/conferences.html

AGTA Tucson GemFair 2016
2–7 February 2016
Tucson, Arizona, USA
www.agta.org/tradeshows/gemfair-tucson.html
Note: Includes a seminar programme.

Accredited Gemologists Association Conference
3 February 2016
Tucson, Arizona, USA
http://accreditedgemologists.org/currevent.php

PDAC International Convention, Trade Show & Investors Exchange
6–9 March 2016
Toronto, Ontario, Canada
www.pdac.ca/convention
Session of interest: Diamonds

Hasselt Diamond Workshop 2016
9–11 March 2016
Hasselt, Belgium
www.uhasselt.be/UH/SBDD/SBDD-XXI

The Open Forum on Sustainability & Responsible Sourcing in the Jewelry Industry
10–13 March 2016
New York, New York, USA
www.jewelryindustrysummit.com

Amberif—International Fair of Amber, Jewellery and Gemstones
16–19 March 2016
Gdańsk, Poland
www.amberif.amberexpo.pl/title,SEMINAR,pid,1284.html
Note: Includes a seminar programme.

2nd Mediterranean Gem and Jewellery Conference
5–7 May 2016
Valencia, Spain
www.gemconference.com

Society of North American Goldsmiths SNAG^{neXt}
19–21 May 2016
Asheville, North Carolina, USA
www.snagmetalsmith.org/events/snagnext

10th International Conference on New Diamond and Nano Carbons
22–26 May 2016
Xi'an, China
http://ndnc2016.xjtu.edu.cn

12th International GeoRaman Conference
9–15 June 2016
Novosibirsk, Russia
http://georaman2016.igm.nsc.ru

EXHIBITS

Asia

The Art of Bulgari: 130 Years of Italian Masterpieces
Until 29 November 2015
Tokyo National Museum, Tokyo, Japan
www.tnm.jp/modules/r_free_page/index.php?id=1733

Europe

The Munich Show--Mineralientage München
30 October–1 November 2015
Munich, Germany
Note: Includes a seminar programme and special gem-related exhibitions
http://munichshow.com/en/the-munich-show/public-days/highlights-2014/special-exhibitions

The Feel of the City—Jewellery from Centres of this World
Until 1 November 2015
Schmuckmuseum, Pforzheim, Germany
www.schmuckmuseum.de/flash/SMP_en.html

Mademoiselle Privé [Chanel jewellery]
Until 1 November 2015
Saatchi Gallery, London
www.saatchigallery.com/current/mademoiselle_prive.php

Rooted: Swedish Art Jewellery
Until 8 November 2015
Kath Libbert Jewellery Gallery, Bradford, West Yorkshire
www.kathlibbertjewellery.co.uk/rooted/rooted_exhibition.html

Emaux de Bresse…et aujourd'hui?
Until 15 November 2015
Museum of Bresse, Domain Planon, Saint-Cyr-sur-Menthon, France
www.ain.fr/jcms/cd_7944/exposition-temporaire-et-animations-2014-au-musee-departemental-de-la-bresse

A Sense of Jewellery
Until 19 November 2015
The Goldsmiths' Centre, London
www.goldsmiths-centre.org/whats-on/exhibitions/a-sense-of-jewellery

The Art of Beauty—Jewelry Creations by Gianmaria Buccellati
Until 29 November 2015
Palace of Venaria, Turin, Italy
www.lavenaria.it/web/en/calendar/mostre/details/247-larte-della-bellezza.html

Colourful World of Quartz Materials Around Us
Until 2016
Moravian Museum, Brno, Czech Republic
www.mzm.cz/en/dietrichstein-palace-exhibitions/colourful-world-of-quartz-materials-around-us

Urartian Jewellery Collection
Until 31 January 2016
Rezan Has Museum, Istanbul, Turkey
www.rhm.org.tr/en/event/rezan-has-museum-urartian-jewellery-collection

The Silversmith's Art: Made in Britain Today
Until 4 January 2016
National Museum of Scotland, Edinburgh
www.nms.ac.uk/national-museum-of-scotland/whats-on/the-silversmiths-art/

Celts: Art and Identity
Until 31 January 2016
British Museum, London
www.britishmuseum.org/whats_on/exhibitions/celts.aspx

Brilliant! – Jewellery – Photograph – Sound
Until 2 February 2016
The National Museum of Finland, Helsinki, Finland
www.kansallismuseo.fi/en/nationalmuseum/exhibitions/temporary#brilliant_jewelry

Elements: From Actinium to Zirconium
Until 28 February 2016
Ulster Museum, Belfast, Northern Ireland
http://nmni.com/um/What-s-on/Current-Exhibitions/Elements---From-Actinium-to-Zirconium

Take it Personally
Until 1 June 2016
Museum of Cultural History, Oslo, Norway
www.khm.uio.no/english/visit-us/historical-museum/temporary-exhibitions/2015/this-is-personal.html

130 Ans de Création Joaillière à Bastia: l'Atelier Filippi
Until 19 July 2016
Musée Municipal d'Art et d'Histoire, Bastia, Corsica
www.musee-bastia.com/musee-bastia/musee.php?nav=16&lang=en

Fitting and Befitting—Fibulae and Brooches
20 November 2015–21 February 2016
Schmuckmuseum, Pforzheim, Germany
www.schmuckmuseum.de/flash/SMP_en.html

Bejewelled Treasures: The Al Thani Collection
21 November 2015–28 March 2016
Victoria and Albert Museum, London
www.vam.ac.uk/content/exhibitions/exhibition-bejewelled-treasures-the-al-thani-collection
Note: Gem-A is hosting a trip to the see this exhibition as part of the Gem-A Conference 2015. Visit www.gem-a.com/news--events/gem-a-conference-2015.aspx to book your place.

A Motley Crew—New Pieces from the Collection
18 March–12 June 2016
Schmuckmuseum, Pforzheim, Germany
www.schmuckmuseum.de/flash/SMP_en.html

Heavenly Bodies—The Sun, Moon and Stars in Jewellery
8 July–30 October 2016
Schmuckmuseum, Pforzheim, Germany
www.schmuckmuseum.de/flash/SMP_en.html

Smycken: Jewellery. From Decorative to Practical
Ongoing
Nordiska Museet, Stockholm, Sweden
www.nordiskamuseet.se/en/utstallningar/jewellery

North America

Haystack Components: Metals and Jewelry
Until 1 November 2015
Fuller Craft Museum, Brockton, Massachusetts, USA
http://fullercraft.org/event/haystack-components-metals-and-jewelry

Beneath the Surface: Life, Death, and Gold in Ancient Panama
Until 1 November 2015
Penn Museum, Philadelphia, Pennsylvania, USA
www.penn.museum/exhibitions/special-exhibitions/beneath-the-surface

Bent, Cast and Forged: The Jewelry of Harry Bertoia
Until 29 November 2015
Cranbrook Art Museum, Bloomfield Hills, Michigan, USA
www.cranbrookart.edu/museum/CAMec3.html

Fabergé: From A Snowflake to an Iceberg
Until 31 December 2015
Houston Museum of Natural Science, Texas, USA
www.hmns.org/index.php?option=com_content&view=article&id=594&Itemid=621

Maker and Muse: Women and Early 20th Century Art Jewelry
Until 3 January 2016
Driehaus Museum, Chicago, Illinois, USA
www.driehausmuseum.org/maker-and-muse

Out of this World! Jewelry in the Space Age
Until 4 January 2016
Carnegie Museum of Natural History, Pittsburgh, Pennsylvania, USA
www.carnegiemnh.org/exhibitions/event.aspx?id=25727

Glittering World: Navajo Jewelry of the Yazzie Family
Until 10 January 2016
The National Museum of the American Indian, New York, New York, USA
http://nmai.si.edu/explore/exhibitions/item/?id=890

Arts of Islamic Lands: Selections from The al-Sabah Collection, Kuwait
Until 30 January 2016
Museum of Fine Arts, Houston, Texas, USA
www.mfah.org/exhibitions/arts-islamic-lands-selections-al-sabah-collection-

The Glassell Collections of African, Indonesian and Pre-Columbian Gold
Until 30 January 2016
Museum of Fine Arts, Houston, Texas, USA
www.mfah.org/art/collections/Glassell-Gold-Collections

Turquoise, Water, Sky: The Stone and Its Meaning
Until 2 May 2016
Museum of Indian Arts & Culture, Santa Fe, New Mexico, USA
www.indianartsandculture.org/current?&eventID=1989

Variations on a Theme: 25 Years of Design from the AJDC
Until June 2016
Gemological Institute of America, Carlsbad, California
www.gia.edu/gia-museum-variations-theme-25-years-design-AJDC

A Passion for Jade: The Heber Bishop Collection
Until 19 June 2016
The Metropolitan Museum of Art, New York, New York, USA
www.metmuseum.org/exhibitions/listings/2015/passion-for-jade

Thunderbirds: Jewelry of the Santo Domingo Pueblo
Until 5 September 2016
Abby Aldrich Rockefeller Folk Art Museum, Williamsburg, Virginia, USA
www.colonialwilliamsburg.com/do/art-museums/rockefeller-museum/thunderbirds-jewelry

Generations of Mastery: Gemstone Carvings by Dreher
Until mid-November 2015
Gemological Institute of America, Carlsbad, California, USA
www.gia.edu/gia-museum-generations-mastery-gemstone-carvings-dreher

Fabergé from the Matilda Geddings Gray Foundation Collection
Until 27 November 2016
The Metropolitan Museum of Art, New York, New York, USA
www.metmuseum.org/exhibitions/listings/2011/faberge

Glitterati. Portraits & Jewelry from Colonial Latin America
Until 27 November 2016
Denver Art Museum, Denver, Colorado, USA
www.denverartmuseum.org/exhibitions/glitterati

Gold and the Gods: Jewels of Ancient Nubia
Until 14 May 2017
Museum of Fine Arts, Boston, Massachusetts, USA
www.mfa.org/exhibitions/gold-and-gods

Douglas Harling: Residence of the Heart
6 December 2015–6 March 2016
Metal Museum, Memphis, Tennessee, USA
www.metalmuseum.org/upcoming_exhibitions

City of Silver and Gold: From Tiffany to Cartier
Ongoing
Newark Museum, New Jersey, USA
www.newarkmuseum.org/SilverAndGold.html

Crystals Transformed Through Vision & Skill
Ongoing
Houston Museum of Natural Science, Texas, USA
www.hmns.org/index.php?option=com_content&view=article&id=481&Itemid=502

Gilded New York
Ongoing
Museum of the City of New York, New York, USA
www.mcny.org/content/gilded-new-york

Jewelry, from Pearls to Platinum to Plastic
Ongoing
Newark Museum, New Jersey, USA
www.newarkmuseum.org/jewelry

Mightier than the Sword: The Allure, Beauty and Enduring Power of Beads
Ongoing
Yale Peabody Museum of Natural History, Yale University, New Haven, Connecticut, USA
http://peabody.yale.edu/exhibits/mightier-sword-allure-beauty-and-enduring-power-beads

Australia and New Zealand

Wunderrūma: New Zealand Jewellery
Until 1 November 2015
Auckland Art Gallery, Auckland, New Zealand
www.aucklandartgallery.com/whats-on/events/2015/july/wunderruma-new-zealand-jewellery

Opals
Until 14 February 2016
South Australian Museum, Adelaide, South Australia, Australia
www.samuseum.sa.gov.au/explore/exhibitions/opals

A Fine Possession: Jewellery and Identity
Until 22 May 2016
Powerhouse Museum, Sydney, New South Wales, Australia
www.powerhousemuseum.com/exhibitions/jewellery

OTHER EDUCATIONAL OPPORTUNITIES

Gem-A Workshops and Courses
Gem-A, London
www.gem-a.com/education/course-prices-and-dates.aspx

Lectures with The Society of Jewellery Historians
Burlington House, London, UK
www.societyofjewelleryhistorians.ac.uk/current_lectures

27 October—'Beauty and Belief: Techniques and Traditions of Omani Jewellery' by Aude Mongiatti and Fahmida Suleman

24 November—'Digital Tools and New Technologies in Contemporary Jewellery' by Dauvit Alexander

New Media

Gem Testing Techniques

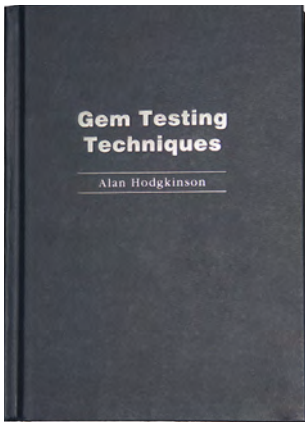

Alan Hodgkinson, 2015. Valerie Hodgkinson, Scotland, 541 pages, illus., hardcover, no ISBN, www.gemtesting techniques.co.uk. £128.00 United Kingdom, £165.00 Europe, £210.00 Canada, or £185.00 elsewhere.

Gem Testing Techniques is an impressive tome, the culmination of over 40 years of gemmological interest, experimentation, research, and general life-long passion. From his humble beginning as a gemmology student, to working with such visionaries as Eric Bruton and Bill Hanneman, the author has risen through the ranks to become a world-renowned gemmologist, not least in the field of visual optics, an area that he has effectively made his own.

Now, that vast wealth of gemmological knowledge has come together in this much-anticipated book, spanning 15 chapters and 541 pages. Extensively illustrated throughout, the chapters include:

1. Magnification: from the loupe to microscope, includes alternate techniques and filters
2. Polariscope/Conoscope: also describes various mineral accessory plates
3. Refractometer: details different models and methods, with in-depth analysis for proper interpretation of results
4. Spectroscope: comprehensive instruction, with numerous examples of spectra
5. Specific Gravity: examples of and instruction on various methods available
6. Visual Optics: the author's specialty, and one that is overlooked in a great many texts
7. Acid Testing: for opal and resins
8. Electro-conductivity: concise information, mainly in conjunction with diamond
9. Filters: the full range are covered, including those produced by Hanneman and Hanneman/ Hodgkinson
10. Hardness: not an often recommended test, this is given due consideration
11. Magnetism: covers diamagnetism, paramagnetism and general magnetic responses
12. Pleochroism: given a new twist with the addition of 'anomalous dichroism'
13. Radiation: brief but useful guide to radioactivity and the needed safety precautions
14. Thermal Testing: not only thermal probes; includes opal, jet, and their simulants
15. Ultraviolet: detailed introduction to UV reactions and how they are useful for gem identification

Within each of these main chapters are various subheadings, which cover the main points of each gemmological aspect in a straightforward and easy-to-follow way. Images and diagrams are sequentially numbered, including reference to the chapter numbers, and are cross-referenced throughout the text. Colour coding of the various chapters provides a useful way of keeping track of important parts of the text.

Some specific aspects worth mentioning include the Spectroscope chapter, which gives detailed instruction on the use of this tool, in all its variants, before providing the reader with 422 full-colour reference spectra, a catalogue that this reviewer believes is unsurpassed in any available standard gemmological text on the market. It is in areas like this that the book comes into its own, providing a unique reference for students and practising gemmologists alike. In addition, the chapter on Visual Optics gives this subject thorough consideration, from both the theoretical side (e.g. how features such as 'primaries' and 'secondaries' occur) and the practical side (e.g. how to view them using very basic gemmological equipment, and in many cases, nothing more advanced than the human eye). Within this section, that author also explains how the concept was used in the creation of the Hodgkinson Refractometer, a large desktop setup that can be created by anyone, and which, with careful practice, can be used to give good results.

Following the extensive main text are equally informative appendices. These provide the usual gemmological constants, but also some welcome additions such as a glossary of gemmological terms and special sections on chrome spinel, feldspar, garnet and ivory. In the appendix on garnet, the author explains the difficulty in identifying the various varieties. By showing a comparison of the constants supplied by various gemmological authorities (Gem-A, GIA, GAA and more), he demonstrates that there is no universally accepted framework for identifying borderline garnet species, and that the situation has

become further complicated by the introduction of varietal names such as rhodolite. Using ternary diagrams, he highlights areas that are still currently not recognized with species names, before going on to include colour and magnetic characteristics in an effort to show the reader the complexities of this mineral group. In the appendix on ivory, the author covers not only elephant and mammoth, but also narwhal, warthog, walrus, hippopotamus and sperm whale ivories, providing a comprehensive breakdown on their uses and identification.

This book offers an easy-to-read, yet informative insight into the world of gemmology, approaching it as Alan Hodgkinson always does, from a light-hearted but accurate viewpoint. This reviewer believes that this book will become a standard text for many future gemmological students.

Andrew Fellows FGA DGA

Ivory

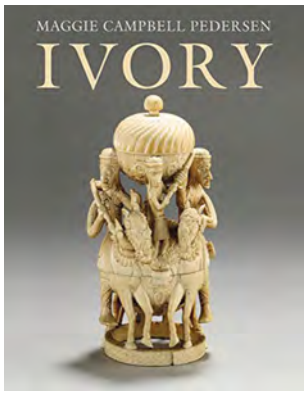

Maggie Campbell Pedersen, 2015. Robert Hale Ltd., London, 240 pages, illus., hardcover, ISBN 978-0719800535, www.maggiecp.co.uk/book.html. £45.00.

Maggie Campbell Pedersen FGA is a well-known organics expert, with ivory being her main area of expertise. This new book provides invaluable information on ivory—its history, sources, composition, imitations, environmental and ethical issues (and resulting legislation) and trade routes.

The book is divided into three chapters. The first one, titled What and Where, covers the occurrence of ivory in nature, beyond the elephant and mammoth varieties, including walrus, hippopotamus, orca (killer whale) and even wild boar. A section for each ivory-bearing animal is included with their facts and features, as well as lore. The ethical and legal aspects and place within our society of this beautiful—but controversial—material is examined and put into context. Differing views exist from country to country, and these have evolved through time. Campbell Pedersen touches on the topic of ivory legislation to prevent elephant poaching, how countries comply with the law, and the consequences for the gem trade. Updated information on banned ivory and the threats to various animals are a must for anyone in the field wanting to understand the ins and outs of the ivory trade.

The second chapter, titled How and What, explores the composition and characterization of ivory. The reader learns how the structure of the dentine can be used to distinguish different types of ivory, and how, according to their structure, each variety is suitable for certain uses such as carvings or beads. Of course, with ivory being such a desirable material, imitations are inevitable. Bone, 'vegetable ivory' and more are presented in detail with their characteristics, localities, principal uses and identification. Also covered are man-made ivory substitutes such as celluloid, casein, elforyn (created specifically to simulate ivory) and others. Visual observation of a sample's structure is most important for proper identification, and UV fluorescence (especially long-wave) is probably the next most helpful non-destructive test; burning (combustion testing) is a useful last resort, but destructive. FTIR and Raman spectroscopy are useful for separating ivory from simulants, and Raman analysis can further distinguish between different types of ivory. Additional (destructive) testing that may be useful for ivory identification includes trace-element and isotopic analyses. Also, carbon-14 dating can be used to establish when the host animal died, although the time that a piece was actually carved cannot be determined. DNA testing can determine species, but sufficient usable material must be extracted and compared to known reference material. The chapter closes with information on the fashioning of ivory and how the general age of a piece can sometimes be established through the carving style. Also explained are carving processes and the final treatments used to finish a piece (e.g. dyeing), as well as methods used to 'age' ivory—possibly in an attempt to circumvent restrictions on some modern varieties.

In the third and final chapter, called Where and When, Campbell Pedersen elaborates on ivory trade routes, and how for thousands of years ivory has been prized by various cultures. Information is provided on the use of mammoth ivory as a tool in prehistoric times, and Campbell Pedersen then progresses through the different types of ivory used in various periods and regions, such as the use of narwhal, sperm whale, orca and walrus ivory in the Arctic. She explains the cultural traditions of the Inuit people and how they relate to ivory, even in the manufacture of toys.

An appendix and glossary are included at the end of this very informative book. *Ivory* is an essential guide for anyone interested in studying this fascinating organic gem material.

Amandine Rongy FGA

Jewelry Appraisal Handbook, 8th edn.

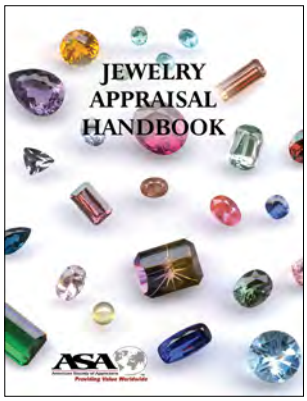

American Society of Appraisers (ASA), 2015. ASA, Reston, Virginia, USA, 50 pages, illus., www.appraisers.org/marketplace. US$112.00 three-ring binder, US$80.00 PDF file or US$152.00 for both.

This 8th edition of the *Jewelry Appraisal Handbook,* a collaborative effort of members of the American Society of Appraisers—Gems and Jewelry (ASA-GJ) discipline, is an essential reference for all who work in the jewellery industry. As one of the most complete resources for the professional jewellery valuer, it contains more than just lists of gemmological properties, useful weight tables and volumetric formulae for common shapes of gemstones. 'Useful', in fact, is the operative word for this publication, which bills itself as a wiki-handbook, in that it is constantly being updated by the ASA-GJ committee.

The first chapter begins with page after page of tables to estimate the weight of mounted diamonds using their measurements, including round, baguette and tapered baguette, marquise, princess, pear and triangle shapes. Accompanying the tables are the formulae upon which they are based, cut-grade parameters for round-cut diamonds and plotting symbols, all courtesy of the Gemological Institute of America (GIA). Following is a coloured stones section with more of the same useful tables and formulae, including GIA nomenclature for the description of colour and clarity types.

Separate informative sections follow for diamonds, coloured stones, pearls, jade, watches, jewellery in general, carvings, beads, phenomenal gems and organic materials. These comprehensively outline descriptive terms and value factors for each of these categories. One page is devoted to a system to estimate the 'condition' of jewellery and watches. There are also more limited sections on unit conversions, jewellery hallmarks and common gold coins.

From Jewelers of America is a page referencing their 2013 Cost of Doing Business report, with data from a survey of retail gross profit margins. Heavy in statistical terminology, the valuer must run the data through several computations to arrive at retail mark-ups. Hopefully in future editions this section will be easier to understand and apply.

Potentially the most useful part of this publication is its Research and Business Web Links Project. This is a compendium of nearly 500 links (and growing) to websites useful to valuers, encompassing topics such as auction houses, suppliers, metals, estate jewellery, diamonds, coloured stones, pearls, watches, coins, hallmarks and trademarks, flatware and hollowware, marketing, appraisers (valuers), laboratories, technical information, insurance, legal and statistical information. This is where the 'wiki' function occurs, as the broader valuation and jewellery communities are encouraged to add to this formidable collection of stored knowledge. For those with the digital (PDF) version, any updates or additions are instantaneous.

The *Jewelry Appraisal Handbook* is a legacy of the late Kirk Root, GG ASG ASA MGA, who began creating and compiling its contents in 1997. The ASA-GJ discipline continues to build the *Handbook* to be as complete a general reference as possible for the jewellery valuation profession.

Charles I. Carmona

OTHER BOOK TITLES*

Gem Localities

Rockbound: An Experience of the North
By Michael Gordon, 2015. Self-published (www.lulu.com), 168 pages, ISBN 978-1312992979. US$56.49 softcover.

Rockhounding Oregon: A Guide to the State's Best Rockhounding Sites
By Lars Johnson, 2014. Falcon Guides, Guilford, Connecticut, USA, 288 pages, ISBN 978-0762783663. US$19.95 softcover.

General Reference

The Collector and his Legacy: Irénée du Pont and the Mineralogical Collection of the University of Delaware
By Sharon Fitzgerald, 2015. Mineralogical Record, Tucson, Arizona, USA, 84 pages. US$15.00 softcover.

Guide to Selling Jewelry in the 21st Century: Legal Compliance for Designers, Independent Jewelers
By Jewelers Vigilance Committee, 2014. Jewelers Vigilance Committee, New York, New York, USA, 32 pages, ISBN 978-0692370025. US$25.00 staple bound.

* Compiled by Georgina Brown and Brendan Laurs

Miller's Antiques Handbook & Price Guide 2016–2017
By Judith Miller, 2015. Mitchell Beazley, Epping, 648 pages, ISBN 978-1784720292. £30.00 hardcover.

Mineral Collections in the American Midwest
Ed. by Terry Huizing and Wendell Wilson, 2015. Mineralogical Record, Tucson, Arizona, USA, 240 pages. US$25.00 softcover.

Jewellery and *Objets d'Art*

Art in Industry: The Work of Paul Storr
By Christopher Hartop, 2015. John Adamson, Cambridge, 168 pages, ISBN 978-1898565147. £49.52 softcover.

Arts of the Hellenized East: Precious Metalwork and Gems of the Pre-Islamic Era
By Martha L. Carter and Prudence O. Harper, 2015. Thames and Hudson, London, 424 pages, ISBN 978-0500970690. £45.00 hardcover.

Cartier Panthère
By Bérénice Geoffroy-Schneiter, Vivienne Becker and Joanna Hardy, 2015. Assouline, London, 300 pages, ISBN 978-2759407453. £104.50 hardcover (in French).

Egyptian Gold Jewellery
By Marielle Bulsink, 2015. Brepols Publishers, Turnhout, Belgium, 208 pages, ISBN 978-2503553672. US$83.00 softcover.

Gold Struck: A Life Shaped by Jewellery
By Stephen Webster, 2015. Salma Editions, London, 400 pages, ISBN 978-0956873842, £50.00 hardcover.

Graff
By Vivienne Becker, Maria Doulton and Nina Hald, 2015. Rizzoli, New York, New York, USA, 272 pages, ISBN 978-0847844814. US$95.00 hardcover.

Jewellery by Suzanne Belperron
By Patricia Corbett, Ward Landrigan and Nico Landrigan, 2015. Thames and Hudson, London, 240 pages, ISBN 978-0500517901. £50.00 hardcover.

Jewels of the Renaissance
By Yvonne Hackenbroch and Gonzague Saint Bris, 2015. Assouline, London, 200 pages, ISBN 978-1614282037. £120.00 hardcover.

A Rothschild Renaissance: Treasures from the Waddesdon Bequest
By Dora Thornton, 2015. British Museum Press, London, 352 pages, ISBN 978-0714123455. £30.00 hardcover.

Swarovski: Celebrating a History of Collaborations in Fashion, Jewelry, Performance, and Design
By Nadja Swarovski, 2015. Rizzoli International Publications, New York, NewYork, USA, 352 pages, ISBN 978-0847844180. US$85.00 hardcover.

The Traditional Jewelry of Egypt
By Azza Fahmy, 2015. The American University in Cairo Press, Cairo, Egypt, 272 pages, ISBN 978-9774167201, US$49.50 hardcover.

The Treasures of the Buccellati Foundation: From Mario to Gianmaria, 100 Years of Goldsmith Art History
By Riccardo Gennaioli, 2015. Skira Editore, Milan, Italy, 368 pages, ISBN 978-8857227573. US$55.00 hardcover.

Treasures of the Goldsmith's Art: The Michael Wellby Bequest to the Ashmolean Museum
By Timothy Wilson and Matthew Winterbottom, 2015. Ashmolean Museum Publications, Oxford, 160 pages, ISBN 978-1910807019, £15.00 softcover.

Vintage Jewellery
By Caroline Cox, 2015. Carlton Books Ltd., London, 224 pages, ISBN 978-1780977089. £15.90 softcover.

Vogue—The Jewellery
By Carol Woolton, 2015. Conran Octopus, London, 304 pages, ISBN 978-1840916577. £75.00 hardcover.

Women Jewellery Designers
By Juliet Weir–De Rouchefoucauld, 2015. Antique Collector's Club, Suffolk, 176 pages, ISBN 978-1851497416. £55.00 hardcover.

Literature of Interest

Coloured Stones

Application of Raman spectroscopic technique to investigation of nephrite color. X.Y. Feng, T. Lu, H. Zhang, Y. Zhang and J. Zhang, *Journal of Mineralogy and Petrology*, **35**(1), 2015, 1–6 (in Chinese with English abstract).

Canalicules et fractures roses dans une tourmaline de type "Paraíba". S. Leblan, E. Fritsch, A. Droux and O. Segura, *Revue de Gemmologie*, **192**, 2015, 9–10.

Color measurement and analysis of yellow jadeite. M. An and E. Zu, *Superhard Material Engineering*, **26**(4), 2014, 55–58 (in Chinese with English abstract).

Color mechanisms in spinel: Cobalt and iron interplay for the blue color. V. D'Ippolito, G.B. Andreozzi, U. Halenius, H. Skogby, K. Hametner and D. Gunther, *Physics and Chemistry of Minerals*, **42**, 2015, 431–439, http://dx.doi.org/10.1007/s00269-015-0734-0.

Dual-color double stars in ruby, sapphire, and quartz: Cause and historical account. K. Schmetzer, M.P. Steinbach, H.A. Gilg and A.R. Blake, *Gems & Gemology*, **51**(2), 2015, 112–143, http://dx.doi.org/10.5741/gems.51.2.112.

Fluid inclusions in the Myanmar jadeitites. M. Qi, K. Shen and H. Xiang, *Acta Petrologica et Mineralogica*, **34**(3), 2015, 405–417 (in Chinese with English abstract).

Gemmological and spectroscopic characteristics of chrome tourmaline appeared on the market recently. L. Sun, M.X. Yang and G. Wu, *Journal of Gems & Gemmology*, **17**(1), 2015, 31–37 (in Chinese with English abstract).

Les gisements de rubis et de spinelle rouge de la Ceinture Métamorphique Néoprotérozoique Mozambicaine. G. Giuliani, J.-E. Martelat, D. Ohnenstetter, J. Feneyrol, A.E. Fallick and A. Boyce, *Revue de Gemmologie*, **192**, 2015, 11–18.

The impacts of the variation of Myanmar jade component on its infrared spectroscopy. Y. Wang, B. Shi, X. Yuan, L. Pei, T. Chen and X. Xie, *Spectroscopy and Spectral Analysis*, **35**(8), 2015, 2094–2098 (in Chinese with English abstract).

The main structural characteristics of omphacite jade and its influence on transparence. Y. Shao and X. Yang, *Acta Petrologica et Mineralogica*, **33**(2), 2014, 69–73 (in Chinese with English abstract).

Microstructures of opal related to gemological characteristics. S. Toaree, B. Wanthanachaisaeng and C. Sutthirat, *Australian Gemmologist*, **25**(9), 2015, 326–329.

Mineralogical characteristics of copper pectolite [larimar]. L. Peng and S. Qin, *Acta Petrologica et Mineralogica*, **33**, Suppl. 2, 2014, 55–60 (in Chinese with English abstract).

Mineralogy and coloration of oil-green jadeite jade. K. Yin, J. Tian, Y. Ma, Y. Wu and Y. Wang, *Spectroscopy and Spectral Analysis*, **34**(12), 2014, 3323–3326 (in Chinese with English abstract).

Olivine – peridot. H.A. Hänni, *Journal of the Gemmological Association of Hong Kong*, **36**, 2015, 35–37, www.gahk.org/journal/GAHK_Journal_2015_v5.pdf.*

Variety and identification of garnet. Y. Luo, Q. Zhen and C. Wang, *Journal of Gems & Gemmology*, **17**(3), 2015, 36–42 (in Chinese with English abstract).

Cultural Heritage

The Brremangurey pearl: A 2000 year old archaeological find from the coastal Kimberley, Western Australia. K. Szabo, B. Koppel, M.W. Moore, I. Young, M. Tighe and M.J. Morwood, *Australian Archaeology*, **80**, 2015, 112–115.*

Case study on an emerald bead: Is it from the ancient mines in Egypt or not? M.S. Krzemnicki and L.E. Cartier, *Journal of the Gemmological Association of Hong Kong*, **36**, 2015, 46–49, www.gahk.org/journal/GAHK_Journal_2015_v5.pdf.*

Du Turkestan à la Birmanie: La quête du jade dans les sources chinoises, 3ème et dernière partie. L. Long, *Revue de Gemmologie*, **192**, 2015, 19–20.

Diamonds

The basal conglomerate of the Capacete Formation (Mata da Corda Group) and its relation to diamond distributions in Coromandel, Minas Gerais State, Brazil. A.F. Fernandes, J. Karfunkel, D.B. Hoover, P.B. de A. Sgarbi, G.N.C. Sgarbi, G.D. Oliveira, J.C. de S.P. Gomes and K. Kambrock, *Brazilian Journal of Geology*, **44**(1), 2014, 91–103, http://dx.doi.org/10.5327/z2317-4889201400010008.*

The buffering capacity of lithospheric mantle: Implications for diamond formation. R.W. Luth

Compiled by Brendan Laurs

* Article freely available for download, as of press time

and T. Stachel, *Contributions to Mineralogy and Petrology*, **168**(5), 2014, article 1083, 12 pp., http://dx.doi.org/10.1007/s00410-014-1083-6.

Conditions of diamond crystallization in kimberlite melt: Experimental data. Y.N. Palyanov, A.G. Sokol, A.F. Khokhryakov and A.N. Kruk, *Russian Geology and Geophysics*, **56**(1–2), 2015, 196–210, http://dx.doi.org/10.1016/j.rgg.2015.01.013.

Defects in cubic diamonds from the placers in the northeastern Siberian platform: Results of IR microspectrometry. S.V. Titkov, A.A. Shiryaev, N.N. Zudina, N.G. Zudin and Y.P. Solodova, *Russian Geology and Geophysics*, **56**(1–2), 2015, 354–362, http://dx.doi.org/10.1016/j.rgg.2015.01.026.

Le diamant noir polycristallin rencontré en joaillerie [Polycrystalline black diamond used in jewellery]. J. Masselot, Diplome d'Universite de Gemmologie, University of Nantes, France, 2014, 55 pp., www.gemnantes.fr/documents/pdf/DUGs/Masselot_DUG.pdf (in French).*

Diamond-bearing gravels along the lower Kwango River DRC. M.C.J. De Wit and E. Thorose, in M.J. de Wit et al., Eds., *Geology and Resource Potential of the Congo Basin*, Springer, Berlin, Germany, 2015, 341–360, http://dx.doi.org/10.1007/978-3-642-29482-2_16.

Diamond formation—Where, when and how? T. Stachel and R.W. Luth, *Lithos*, **220–223**, 2015, 200–220, http://dx.doi.org/10.1016/j.lithos.2015.01.028.*

Diamond thermoelastic properties and implications for determining the pressure of formation of diamond-inclusion systems. R.J. Angel, M. Alvaro, F. Nestola and M.L. Mazzucchelli, *Russian Geology and Geophysics*, **56**(1–2), 2015, 211–220, http://dx.doi.org/10.1016/j.rgg.2015.01.014.

Diamonds from the Coromandel area, west Minas Gerais State, Brazil: An update and new data on surface sources and origin. J. Karfunkel, D. Hoover, A.F. Fernandes, G.N.C. Sgarbi, K. Kambrock and G.D. Oliveira, *Brazilian Journal of Geology*, **44**(2), 2014, 325–338, http://dx.doi.org/10.5327/z2317-4889201400020011.*

Evolution of diamond resorption in a silicic aqueous fluid at 1-3GPA: Application to kimberlite emplacement and mantle metasomatism. Z. Zhang, Y. Fedortchouk and J.J. Hanley, *Lithos*, **227**, 179–193, http://dx.doi.org/10.1016/j.lithos.2015.04.003.*

Isotope fractionation of carbon during diamond crystallization in model systems. V.N. Reutsky, Y.N. Palyanov, Y.M. Borzdov and A.G. Sokol, *Russian Geology and Geophysics*, **56**(1–2), 2015, 239–244, http://dx.doi.org/10.1016/j.rgg.2015.01.017.

The luminescent nature of orange coloration in natural diamond: Optical and EPR study. S.V. Titkov, R.M. Mineeva, N.N. Zudina, A.M. Sergeev, I.D. Ryabchikov, A.A. Shiryaev, A.V. Speransky and V.P. Zhikhareva, *Physics and Chemistry of Minerals*, **42**, 2015, 131–141, http://dx.doi.org/10.1007/s00269-014-0705-x.

Multiple growth events in diamonds with cloudy microinclusions from the Mir kimberlite pipe: Evidence from the systematics of optically active defects. S.Y. Skuzovatov, D.A. Zedgenizov, A.L. Rakevich, V.S. Shatsky and E.F. Martynovich, *Russian Geology and Geophysics*, **56**(1–2), 2015, 330–343, http://dx.doi.org/10.1016/j.rgg.2015.01.024.

Olivine with diamond-imposed morphology included in diamonds. Syngenesis or protogenesis? F. Nestola, P. Nimis, R.J. Angel, S. Milani, M. Bruno, M. Prencipe and J.W. Harris, *International Geology Review*, **56**(13), 2014, 1658–1667, http://dx.doi.org/10.1080/00206814.2014.956153.

Peculiarities of nitrogen impurity aggregation in diamonds from the Sytykanskaya pipe, Yakutia. M.I. Rakhmanova, V.A. Nadolinny, O.P. Yuryeva, N.P. Pokhilenko and A.M. Logvinova, *European Journal of Mineralogy*, **27**(1), 2015, 51–56, http://dx.doi.org/10.1127/ejm/2014/0026-2413.

A review of diamonds in Zimbabwe – A century on. V. Stocklmayer and S. Stocklmayer, *Australian Gemmologist*, **25**(9), 2015, 316–325.

A review of the kimberlites of the Democratic Republic of Congo. M.C.J. De Wit and H.A. Jelsma, in M.J. de Wit et al., Eds., *Geology and Resource Potential of the Congo Basin*, Springer, Berlin, Germany, 2015, 361–369, http://dx.doi.org/10.1007/978-3-642-29482-2_17.

Review of lithospheric diamonds and their mineral inclusions. X. Zhao, G. Shi and J. Zhang, *Advances in Earth Science*, **30**(3), 2015, 310–322 (in Chinese with English abstract).

The secondary origin of diamonds: Multi-modal radiation tomography of diamondiferous mantle eclogites. G.H. Howarth, N.V. Sobolev, J.F. Pernet-Fisher, P.H. Barry, D. Penumadu, S. Puplampu, R.A. Ketcham, J.A. Maisano, D. Taylor and L.A. Taylor, *International Geology Review*, **56**(9), 2014, 1172–1180, http://dx.doi.org/10.1080/00206814.2014.926784.

3-D X-ray tomography of diamondiferous mantle eclogite xenoliths, Siberia: A review. G.H. Howarth, N.V. Sobolev, J.F. Pernet-Fisher, R.A. Ketcham, J.A. Maisano, L.N. Pokhilenko, D. Taylor and L.A. Taylor, *Journal of Asian Earth Sciences*, **101**, 2015, 39–67, http://dx.doi.org/10.1016/j.jseaes.2014.10.039.

Typomorphic features of graphite inclusions in diamond: Experimental data. A.F. Khokhryakov and D.V. Nechaev, *Russian Geology and Geophysics*, **56**(1–2), 2015, 232–238, http://dx.doi.org/10.1016/j.rgg.2015.01.016.

Gem Localities

Age and origin of charoitite, Malyy Murun Massif, Siberia, Russia. Y. Wang, H. He, A.V. Ivanov, R. Zhu and C. Lo, *International Geology Review*, **56**(8), 2014, 1007–1019, http://dx.doi.org/10.1080/00206814.2014.914860.

Brief report of a visit to emerald mines in Colombia. Chan Chi Keung, *Journal of the Gemmological Association of Hong Kong*, **36**, 2015, 16–28, www.gahk.org/journal/GAHK_Journal_2015_v5.pdf (in Chinese with English abstract).*

Diagnostic characteristics of precious opals from the Raduzhnoe deposit (Primorsky Region, Russia). V.B. Tishkina, V.A. Pakhomova and D.G. Fedoseev, *Journal of the Gemmological Association of Hong Kong*, **36**, 2015, 80–82, www.gahk.org/journal/GAHK_Journal_2015_v5.pdf.*

Gemmological characteristics of jadeite and its crust from Muna mine. Y. Yan, D. Ye and J. Weng, *Journal of Gems & Gemmology*, **17**(1), 2015, 10–16 (in Chinese with English abstract).

The gemmological characteristics of "Mixian County Jade" from Henan, PRC. Pan Yu and He Xue-mei, *Journal of the Gemmological Association of Hong Kong*, **36**, 2015, 69–71, www.gahk.org/journal/GAHK_Journal_2015_v5.pdf (in Chinese with English abstract).*

The gemological and mineral characteristics of variscite from Ma'anshan of Anhui Province. Y. Zhou, L. Qi, H. Dai, Q. Zhang and X. Jiang, *Rock and Mineral Analysis*, **33**(5), 2014, 690–697 (in Chinese with English abstract).

Gemological and mineralogical characteristics of the Sleeping Beauty turquoise from the USA. X. Bai and Y. Liu, *Acta Petrologica et Mineralogica*, **33**(2), 2014, 61–68 (in Chinese with English abstract).

Geochemical and oxygen isotope signatures of mantle corundum megacrysts from the Mbuji-Mayi kimberlite, Democratic Republic of Congo, and the Changle alkali basalt, China. G. Giuliani, M. Pivin, A.E. Fallick, D. Ohnenstetter, Y. Song and D. Demaiffe, *Comptes Rendus Geoscience*, **347**(1), 2015, 24–34, http://dx.doi.org/10.1016/j.crte.2014.12.003.

Mineralogical characteristics of emerald from Malipo, Yunnan Province. W. Huang, P. Ni, T. Shui and P. Yang, *Acta Petrologica et Mineralogica*, **34**(1), 2015, 103–109 (in Chinese with English abstract).

Photoluminescence response from the Turkish dentritic [*sic*] agates. M. Hatipoğlu, Y. Kibici, G. Yanık, C. Özkul and M. Demirbilek, *Spectroscopy Letters*, **48**(5), 2015, 386–392, http://dx.doi.org/10.1080/00387010.2014.891627.*

Red rain • Mozambique ruby pours into the market. R.W. Hughes, *Journal of the Gemmological Association of Hong Kong*, **36**, 2015, 39–43, www.gahk.org/journal/GAHK_Journal_2015_v5.pdf.*

Rubies and sapphires from Snezhnoe, Tajikistan. E.S. Sorokina, A.K. Litvinenko, W. Hofmeister, T. Hager, D.E. Jacob and Z.Z. Nasriddinov, *Gems & Gemology*, **51**(2), 2015, 160–175, http://dx.doi.org/10.5741/gems.51.2.160.*

Searching for sapphires in Sri Lanka. C. Unninayar, *JNA*, **371**, 2015, 56–58.

Sri Lanka. S. Turner, *GemGuide*, **34**(4), 2015, 2–7.

Zircons from the Nezametninskoe deposit (the Russian Far East). D.G. Fedoseev, V.A. Pakhomova, N.V. Zarubina, D.S. Ostapenko and K.N. Nikolaeva, *Journal of the Gemmological Association of Hong Kong*, **36**, 2015, 30–32, www.gahk.org/journal/GAHK_Journal_2015_v5.pdf.*

Instruments and Techniques

The application of X-ray absorption spectroscopy to gemology. J. Gao, X. Wu and S. Qin, *Acta Petrologica et Mineralogica*, **33**, Suppl. 2, 2014, 155–160 (in Chinese with English abstract).

AVASPEC 2048: An innovative spectroscopic methodology to differentiate the natural emeralds from the synthetic ones. A. Leone, F. Caucia, A. Leone and L. Marinoni, *Periodico di Mineralogia*, **84**(2), 2015, 247–261, http://dx.doi.org/10.2451/2015PM0012.*

Digital photomicrography for gemologists. N. Renfro, *Gems & Gemology*, **51**(2), 2015, 144–159, http://dx.doi.org/10.5741/gems.51.2.144.*

Luminescence studies of gemstones and diamonds. M.D. Sastry, S. Mane, M. Gaonkar, M.K. Bhide, S.N. Desai and K.T. Ramachandran, *International Journal of Luminescence and Applications*, **5**(3), 2015, 293–297, http://ijlaindia.org/wp-content/uploads/2015/07/Volume5/Issue3/112.pdf.*

Raman-in-SEM, a multimodal and multiscale analytical tool: Performance for materials and expertise. G. Wille, X. Bourrat, N. Maubec and A. Lahfid, *Micron*, **67**, 2014, 50–64, http://dx.doi.org/10.1016/j.micron.2014.06.008.

Miscellaneous

Australian Opal Centre: A glittering palace for the queen of gems. J. Brammall, *Australian Gemmologist*, **25**(9), 2015, 304–315.

Elevating the quality of staffs at jewelry boutique stores: Implementing chinkless teaching concept for course training and planning. Chiao-Ping Bao, Nai-Chieh Wei and Shu-Chuan Chen, *The International Journal of Organizational Innovation*, **8**(1), 2015, www.ijoi-online.org/attachments/article/45/FINAL%20ISSUE%20VOL%208%20NUM%201%20JULY%202015.pdf.*

The iconic blue box: A semiotic analysis of Tiffany & Company advertisements. L. Drewniany, BA thesis, California Polytechnic State University – San Luis Obispo, USA, 2015, 27 pp., http://digitalcommons.calpoly.edu.*

News Press

Ancient pearl dated as 2,000 years old in WA's Kimberley region. N. Jones, *ABC News*, 3 June 2015, www.abc.net.au/news/2015-06-03/ancient-pearl-thousands-years-old-in-kimberley/6519650.*

This artist will craft your loved one's ashes into beads. K. Sola, *Huffington Post*, 1 April 2015, www.huffingtonpost.com/2015/04/01/merry-coor-ash-beads_n_6980078.html.*

The dangerous search for emeralds in Colombia. G. Miller, *Washington Post*, 9 August 2015, www.washingtonpost.com/sf/world/2015/08/09/the-dangerous-search-for-emeralds-in-colombia.*

At jewelry auctions, color is king. G.B. Mitic, *New York Times*, 13 May 2015, www.nytimes.com/2015/05/14/fashion/at-jewelry-auctions-color-is-king.html.*

The photographer and the jade mine: Documenting extractive governance challenges in Myanmar's Kachin State. M.Z. Oo, Natural Resources Governance Institute, 29 October 2014, www.resourcegovernance.org/news/blog/photographer-and-jade-mine-documenting-extractive-governance-challenges-myanmars-kachin-st.*

Ruby sets record, pink diamond and pearls shine at Sotheby's sale. S. Nebehay, Reuters, 12 May 2015, www.reuters.com/article/2015/05/12/art-auction-jewels-idUSL5N0Y35D520150512.*

Stone bracelet is oldest ever found in the world. A. Liesowska, *Siberian Times*, 7 May 2015, http://siberiantimes.com/science/casestudy/features/f0100-stone-bracelet-is-oldest-ever-found-in-the-world.*

Organic Gems

Amber from México: Coahuilite, Simojovelite and Bacalite. F. Riquelme, J.L. Ruvalcaba-Sil, J. Alvarado-Ortega, E. Estrada-Ruiz, M. Galicia-Chávez, H. Porras-Múzquiz, V. Stojanoff, D.P. Siddons and L. Miller, *Materials Research Society Symposium Proceedings*, **1618**, 2014, 12 pages, http://dx.doi.org/10.1557/opl.2014.466.

Blue-fluorescing amber from Cenozoic lignite, eastern Sikhote-Alin, Far East Russia: Preliminary results. I.Yu. Chekryzhov, V.P. Nechaev and V.V. Kononov, *International Journal of Coal Geology*, **132**(1), 2014, 6–12, http://dx.doi.org/10.1016/j.coal.2014.07.013.

FTIR and ^{13}C spectrum characterization and significance of amber from different origins. Y.Y. Xing, L.J. Qi, Y.C. Mai and M.H. Xie, *Journal of Gems & Gemmology*, **17**(2), 2015, 8–16 (in Chinese with English abstract).

Identification of tortoise shell and its two imitations. C. Tang, Z. Zhou and Z. Liao, *Journal of Gems & Gemmology*, **16**(6), 2014, 6–13 (in Chinese with English abstract).

Infrared spectral characteristics of ambers from three main sources (Baltic, Dominica and Myanmar). Y. Wang, G. Shi, W. Shi and R. Wu, *Spectroscopy and Spectral Analysis*, **35**(8), 2015, 2164–2169 (in Chinese with English abstract).

Inside amber: New insights into the macromolecular structure of class Ib resinite. J. Poulin and K. Helwig, *Organic Geochemistry*, **86**, 2015, 94-106, http://dx.doi.org/10.1016/j.orggeochem.2015.05.009.

Organic elements and spectroscopic characteristics of ambers from different producing areas. X. Fang and Y. Chen, *Acta Petrologica et Mineralogica*, **33**(2), 2014, 107–110 (in Chinese with English abstract).

Tracing the most ancient amber: The origin and evolution of resin-producing plants. P. Zong, J. Xue and B. Tang, *Acta Petrologica et Mineralogica*, **33**, Suppl. 2, 2014, 111–116 (in Chinese with English abstract).

Pearls

Historical geography of pearl harvesting and current status of populations of freshwater pearl mussel *Margaritifera margaritifera* (L.) in the western part of northern European Russia. A. Makhrov, J. Bespalaya, I. Bolotov, I. Vikhrev, M. Gofarov, Y. Alekseeva and A. Zotin, *Hydrobiologia*, **735**(1), 2014, 149–159, http://dx.doi.org/10.1007/s10750-013-1546-1.

Spectroscopy characteristic comparative study of golden seawater cultured pearl from South Sea and dyed seawater cultured pearl. D. Zhou, L. Li, B. Luo and C. Zhou, *Journal of Gems & Gemmology*, **17**(3), 2015, 1–9 (in Chinese with English abstract).

The use of probabilistic neural network and UV reflectance spectroscopy as an objective cultured pearl quality grading method. S. Agatonovic, *Modern Chemistry & Applications*, **3**(2), article 1000152, 2015, 6 pp., http://dx.doi.org/10.4172/2329-6798.1000152.*

Yes, it turns: Experimental evidence of pearl rotation during its formation. Y. Gueguen, Y. Czorlich, M. Mastail, B. Le Tohic, D. Defay, P. Lyonnard, D. Marigliano, J.-P. Gauthier, H. Bari, C. Lo, S. Chabrier and G. Le Moullac, *Royal Society Open Science*, **2**, article 150144, 2015, 8 pp., http://dx.doi.org/10.1098/rsos.150144.*

Synthetics and Simulants

Comparison of synthetic colourless sapphire and natural light-coloured sapphire. S. Song, G. Shi, X. Li and Y. Li, *Journal of Gems & Gemmology*, **17**(2), 2015, 25–30 (in Chinese with English abstract).

Design of a novel large volume cubic high pressure apparatus for raising the yield and quality of synthetic diamond. Q.-G. Han, Q.-C. Ban and P.-W. Zhu, *Journal of Crystal Growth*, **422**, 2015, 29–35, http://dx.doi.org/10.1016/j.jcrysgro.2015.04.028.

Dyed and filled sillimanite as ruby imitation. X. Lu and X. Wu, *Journal of Gems & Gemmology*, **16**(6), 2014, 39–42 (in Chinese with English abstract).

FTIR imaging in diffusion studies: CO_2 and H_2O in a synthetic sector-zoned beryl. G. Della Ventura, F. Radica, F. Bellatreccia, A. Cavallo, G. Cinque, L. Tortora and H. Behrens, *Frontiers in Earth Science*, **3**, article 33, 2015, 11 pp., http://dx.doi.org/10.3389/feart.2015.00033.*

Gemmological characteristics of grossular jade as jadeite imitation. J. Liu, R. Li, M. Xie and Z. Xu, *Journal of Gems & Gemmology*, **16**(6), 2014, 47–50 (in Chinese with English abstract).

The identification of a kind of amber-plastic mixture. G. Fan, F. Yu, S. Weng and M. Sun, *Acta Petrologica et Mineralogica*, **33**(2), 2014, 140–146 (in Chinese with English abstract).

Identification of lab-grown diamonds. Kook-Whee Kwak, Young Wook Ju and SeWoom Oh, *Journal of the Gemmological Association of Hong Kong*, **36**, 2015, 53–57, www.gahk.org/journal/GAHK_Journal_2015_v5.pdf.*

A marriage of science and art: Creating quartz specimens in the laboratory. J.H. Clifford and V.A. Klipov, *Rocks & Minerals*, **90**(4), 379–385, http://dx.doi.org/10.1080/00357529.2015.1012958.

NDT breaking the 10 carat barrier: World record faceted and gem-quality synthetic diamonds investigated. B. Deljanin, M. Alessandri, A. Peretti and M. Åström, *Contributions to Gemology*, **15**, 2015, 1–7, www.gemresearch.ch/news/2015-07-21_NDT_Diamonds_HPHT/NDT_Diamonds_HPHT.pdf.*

Synthetic gem quality diamonds: The product, the perception, and the retailer. G.A. Roskin, *GemGuide*, **34**(4), 2015, 8–10.

Treatments

A tentative discussion on Zachery-treated turquoise. L. Sun, A. Ling, F. Yu, Z. He and W. Ma, *Acta Petrologica et Mineralogica*, **33**(2), 2014, 165–171 (in Chinese with English abstract).

Compilations

***G&G* Micro-World.** Amber with mite inclusion • Apatite 'piñata' • Iridescent musgravite • Cat's-eye phenakite • Unusual pink sapphire bead • Bicoloured double-eye tourmaline. *Gems & Gemology*, **51**(2), 2015, 190–197, www.gia.edu/gems-gemology.*

Gem News International. Diamond-bearing eclogite xenoliths • Cat's-eye calcite from Pakistan • Large chatoyant Brazilian emerald • Nonbead-cultured pearls from *Strombus gigas* • Purple scapolite • Synthetic star sapphire with diffusion-induced colour and star • Partially filled blue chalcedony • Presumably oiled ruby • Inclusions in synthetic star sapphire • Diamond slices • Large Namibian demantoid • Nephrite from British Columbia • Baroque cultured pearls • Ruby from Namya, Myanmar • Rock Creek sapphire update • Unusual tourmaline necklace • Conference reports. *Gems & Gemology*, **51**(2), 2015, 198–219, www.gia.edu/gems-gemology.*

Lab Notes. Intense blue diamond with high boron level • Type IIb grey-purple diamond • Fluorite sphere with phosphorescent coating • Assembled and bead-cultured pearls • Strong pinkish purple freshwater bead-cultured pearls • Beryllium-diffused and lead-glass-filled orange sapphire • LPHT-annealed pink CVD synthetic diamonds • Near-colourless melee-sized HPHT synthetic diamonds • Phosphorescence of synthetic sapphire • Chemical analysis of zircon. *Gems & Gemology*, **51**(2), 2015, 176–188, www.gia.edu/gems-gemology.*

Conference Proceedings

AMBERIF 2015—The 22th Seminar on Succinite and Selected Fossil Resins of Europe: Localities, Properties, Archaeology. Gdańsk, Poland, 27 March 2015, www.amberif.amberexpo.pl/mtgsa2010/library/File/AMBERIF/2015/Amberif_2015_en1_EWW.pdf.*

34th International Gemmological Conference. Vilnius, Lithuania, 26–30 August 2015, www.igc-gemmology.net/proceedings.*

FEEG
FEDERATION FOR EUROPEAN EDUCATION IN GEMMOLOGY

Gain a European Certificate in Gemmology

Founded in 1995, The Federation for European Education in Gemmology (FEEG) supports a European gemmology qualification that is recognized by all gem and jewellery bodies and institutions across Europe.

FEEG comprises 11 gemmological organizations from eight European countries. Graduates of these organizations can take the exam (available in five languages) to gain the European Certificate in Gemmology. **Graduates of Gem-A's Gemmology Diploma are eligible to take the exam**. If you are a Gemmology Diploma graduate and want to find out more, contact information@gem-a.com.

Participating organizations:

- **WIFI Oberösterreich**
  Linz, Austria
- **Academie voor Mineralogie**
  Antwerp, Belgium
- **Société Belge de Gemmologie**
  Etterbeek, Belgium
- **Institut National de Gemmologie**
  Paris, France
- **Deutsche Gemmologische Gesellschaft**
  Idar-Oberstein, Germany
- **Istituto Gemmologico Italiano**
  Milan, Italy
- **Netherlands Gemmological Laboratory**
  Leiden, The Netherlands
- **Dutch Gemmological Institute**
  Schoonhoven, The Netherlands
- **Escola de Gemmologia de la Universitat de Barcelona**
  Barcelona, Spain
- **Instituto Gemológico Español**
  Madrid, Spain
- **Gem-A**
  London, United Kingdom

The 18th FEEG Symposium will be held in conjunction with Gem-A's 2015 Conference — email events@gem-a.com to be added to the mailing list

Whenas that ruby which you wear,
Sunk from the tip of your soft ear,
Will last to be a precious stone
When all your world of beauty's gone.

— Robert Herrick, "To Dianeme"

Pala International

Palagems.com / Palaminerals.com
+1 800 854 1598 / +1 760 728 9121

Natural Ruby, Mozambique • 3.59 ct • 7.9 x 7.8 x 6.6 mm
Photo: Orasa Weldon